

Nanomedicine for Diagnosis and Treatment of Atherosclerosis

Jingyun Cheng, Hui Huang,* Yu Chen,* and Rong Wu*

With the changing disease spectrum, atherosclerosis has become increasingly prevalent worldwide and the associated diseases have emerged as the leading cause of death. Due to their fascinating physical, chemical, and biological characteristics, nanomaterials are regarded as a promising tool to tackle enormous challenges in medicine. The emerging discipline of nanomedicine has filled a huge application gap in the atherosclerotic field, ushering a new generation of diagnosis and treatment strategies. Herein, based on the essential pathogenic contributors of atherogenesis, as well as the distinct composition/structural characteristics, synthesis strategies, and surface design of nanoplateforms, the three major application branches (nanodiagnosis, nanotherapy, and nanotheranostic) of nanomedicine in atherosclerosis are elaborated. Then, state-of-art studies containing a sequence of representative and significant achievements are summarized in detail with an emphasis on the intrinsic interaction/relationship between nanomedicines and atherosclerosis. Particularly, attention is paid to the biosafety of nanomedicines, which aims to pave the way for future clinical translation of this burgeoning field. Finally, this comprehensive review is concluded by proposing unresolved key scientific issues and sharing the vision and expectation for the future, fully elucidating the closed loop from atherogenesis to the application paradigm of nanomedicines for advancing the early achievement of clinical applications.

1. Introduction

Cardiovascular and cerebrovascular diseases are sweeping the globe and becoming the primary reason of mortality and morbidity worldwide.^[1] Atherosclerosis, the leading cause of cardiovascular and cerebrovascular diseases, is a chronic, systemic, and inflammatory disease, mainly affecting large and medium-sized arteries.^[2] It is particularly common in arteries with low endothelial shear stress or disturbed blood flow, such as the site of arterial bends or bifurcations.^[3] The adverse consequences usually depend on the site of occurrence, such as the coronary arteries (coronary artery syndrome), carotid or intracranial arteries (stroke, transient ischemic attack), renal arteries (renovascular hypertension or renal dysfunction), and peripheral arteries (cold extremities or claudication).^[4] The common risk factors include hyperlipidemia, hypertension, smoking, diabetes, etc.^[5] Atherosclerosis is characterized by high incidence, disability as well as mortality rates at present, and changes in modern diet and exercise habits have given the disease a trend of getting younger. Therefore,

early detection, diagnosis, and treatment should be the primary focus.^[6]

As for atherosclerotic diagnosis, it mainly relies on ultrasound (US), magnetic resonance (MR), and computed tomography (CT) imaging, but they can merely identify advanced lesions, and the assessment of plaque vulnerability is not accurate enough.^[7] Furthermore, conventional contrast agents are only able to assist in morphological detections. Therefore, additional alternative measures are needed to optimize early diagnosis. Besides general treatment, atherosclerotic treatment mainly includes the best medical therapy (BMT) and surgery.^[8] On the one hand, the BMT refers to lipid-lowering, antiplatelet, and antithrombotic treatments, which should be carefully selected based on the patient's condition. Nowadays, statin is mostly recommended to reduce circulating lipids by upregulating the low-density lipoprotein receptor (LDLr) with the assist of apolipoprotein B (ApoB).^[9] However, long-term drug treatment will cause liver damage, gastrointestinal bleeding, muscle discomfort, and arrhythmia.^[10] On the other hand, if severe stenosis happens, surgical intervention has to be considered, such as endarterectomy, balloon dilation, or stent implantation.^[11] While surgical treatment requires high demands on the patient's vital signs and may

J. Cheng, R. Wu
Department of Ultrasound
Shanghai General Hospital
Shanghai Jiao Tong University School of Medicine
Shanghai 200080, P. R. China
E-mail: wurong7111@sjtu.edu.cn
H. Huang, Y. Chen
Materdicine Lab
School of Life Sciences
Shanghai University
Shanghai 200444, P. R. China
E-mail: huanghuish@shu.edu.cn; chenyu@shu.edu.cn
Y. Chen
Oujiang Laboratory (Zhejiang Lab for Regenerative Medicine, Vision and Brain Health)
Wenzhou Institute of Shanghai University
Wenzhou, Zhejiang 325088, P. R. China



The ORCID identification number(s) for the author(s) of this article can be found under <https://doi.org/10.1002/advs.202304294>

© 2023 The Authors. Advanced Science published by Wiley-VCH GmbH. This is an open access article under the terms of the Creative Commons Attribution License, which permits use, distribution and reproduction in any medium, provided the original work is properly cited.

DOI: 10.1002/advs.202304294

result in postoperative restenosis or bleeding complications.^[12] As a result, there is an urgent need to develop an accurate and efficient therapeutic method to reduce adverse reactions and improve treatment performance, which is more conducive to enhancing patient compliance and improving prognosis.

Nanotechnology integrates knowledge from various interdisciplinary fields including materials science, physics, biology, and chemistry, and is the result of the combination of modern science and technology.^[13] This technology explores the molecular world from a nanoscale perspective and has achieved widespread application in many fields, such as material engineering, biomedical science, environmental protection, electronic devices, and plant science.^[14] To date, the rapid development of nanotechnology and increasing clinical demands have given rise to the emerging interdisciplinary field of nanomedicine, bringing about a profound paradigm shift.^[15] Over the past few decades, a large number of nanomaterials used for disease diagnosis and/or treatment have been proposed, and the advantages of nanomaterials have gradually emerged: I) the ultra-small size of nanomaterials provides a large surface area and more reaction sites;^[16] II) the physical and chemical properties of nanomaterials (e.g., optical, magnetic, mechanical, and electrical properties) can be regulated by the controllable composition and structure of the nanomaterials;^[17] III) the size of nanomaterials is much smaller than that of cells, which makes them easily penetrate through various biological barriers and have favorable biocompatibility;^[18] IV) the enhanced permeability and retention (EPR) effect promotes passive targeting accumulation of nanomaterials in tumors or other pathological sites;^[19] V) the off-target effect of nanomaterials can be significantly reduced by modifying the active targeting ligand.^[20] These characteristics endow nanomaterials with potential value for clinical application.

Based on the continuous development of nanotechnology and the deepening of pathological research, nanomedicine has made breakthrough progress in the field of atherosclerosis, providing opportunities for precise individualized diagnosis and treatment.^[21] In general, atherosclerosis is characterized by excessive inflammatory burden, endothelial injury, neovascularization, and epigenetic abnormalities.^[22] According to these abnormalities, nanomedicine can be rationally designed and developed to differentiate these lesions from healthy tissues for subsequent diagnosis and/or treatment.^[23] In response to the problems existed in traditional imaging methods, the introduction of nanomaterials broadens the timing and scope of disease monitoring, achieving earlier and more comprehensive diagnosis with greater precision.^[24] Regarding adverse reactions associated with drugs or surgery, nanomaterials achieve higher drug utilization rates or further enrich the range of surgical options (such as nanodrug-coated balloons or stents) through elaborated design.^[25] Importantly, nanomaterials provide the ability to integrate diagnosis and treatment for atherosclerosis. In the past, diagnosis and treatment were two separate fields. However, the surfaces or interiors of nanomaterials can easily couple with various components, making it possible to undergo treatment under imaging guidance or real-time monitoring during treatment.^[26] This undoubtedly promotes ever-greater advances and offers unprecedented solutions for disease exploration.

To provide comprehensive information for researchers in this field, this review summarizes the pathological basis, develop-

ment process, and corresponding animal models currently used in preliminary research. We also highlight the inorganic, organic, and biomimetic nanomaterials applied in the diagnosis and/or treatment of atherosclerosis and their physicochemical properties including particle size, shape, and potential. Furthermore, we provide a detailed and comprehensive introduction to the utilization of nanomaterials in the diagnosis (e.g., MR, CT, radionuclide, fluorescence (FL), photoacoustic (PA), optical coherence tomography (OCT), multi-modal imaging and reported clinical trials), therapy (e.g., drug delivery, phototherapy, sonodynamic therapy (SDT), immunotherapy, gas therapy and reported clinical trials), and theranostic of atherosclerosis in recent years (**Figure 1**). Besides, we summarize and conclude the issue on how to establish a biosafety evaluation system for nanomaterials, including but not limited to in vivo distribution and metabolism assessment, biological evaluation, immunological evaluation, and toxicology evaluation. Finally, existing challenges of nanomedicine in the atherosclerotic field are pointed out, and effective approaches and potential development directions for each issue are proposed to boost their entry into clinical practices.

2. Background and Foundation of Nanomaterials in Atherosclerosis

2.1. Pathological Characteristics

The term “atherosclerosis” originates from “atheroma” and “sclerosis,” where “atheroma” represents the atheromatous lesions formed by necrosis of lipid deposits and “sclerosis” refers to collagen fibrous hyperplasia. Macroscopically, the progression of atherosclerosis can be divided into four stages, including fatty streaks, fibrous plaque, atheromatous plaque, and secondary lesions. Besides, microscopic observation demonstrated the presence of endothelial cell damage, infiltration of inflammatory cells, migration of vascular smooth muscle cells (VSMCs), and lipid accumulation within the lesion. In this section, we mainly focus on the pivotal pathological components and progression within atherosclerosis (**Figure 2**).

2.1.1. Endothelium

Endothelium, the first barrier in contact with the blood, is normally in dynamic equilibrium with the various blood components.^[27] A series of irritants such as cholesterol, cigarette ingredients, hyperglycemia, and local hemodynamic disturbances cause endothelial cell dysfunction and impaired anatomical integrity. Increased endothelial permeability provides an opportunity for lipid to flow into subendothelial space, which in turn further activates the endothelium. Endothelial cell adhesion molecule (ECAM) is highly expressed in risk endothelium associated with atherosclerosis. In particular, vascular cell adhesion molecule 1 (VCAM-1) binds to the very late antigen 4 (VLA-4) on the monocytes and T cells, while intracellular adhesion molecule 1 (ICAM-1) binds to lymphocyte function-associated antigen 1 (LFA-1) on neutrophils, which mediates the cellular adhesion.^[28] What is more, the up-regulation of P-selectin and E-selectin also

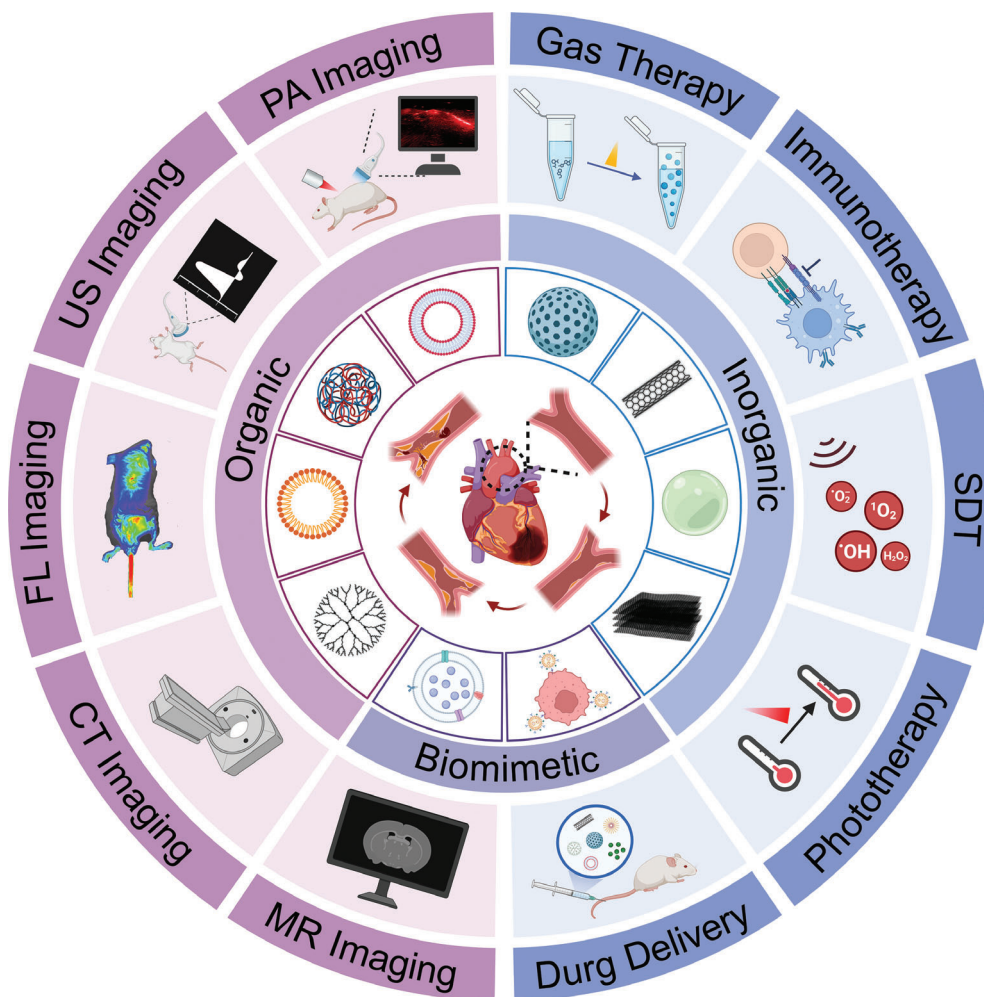


Figure 1. Schematic illustration of the application of nanomaterials in atherosclerosis, including atherogenesis (covering fatty streaks, fibrous plaque, atheromatous plaque, and secondary lesions), the representative classification of reported nanomaterials (including inorganic, organic, and biomimetic nanomaterials), diagnosis (e.g., magnetic resonance (MR), computed tomography (CT), fluorescence (FL), ultrasound (US), and photoacoustic (PA) imaging) and therapy strategies like drug delivery, phototherapy, sonodynamic therapy (SDT), immunotherapy, and gas therapy. Figure was created with BioRender.com.

assists in the adherence of blood cells. Furthermore, activated endothelium secretes chemokines such as monocyte chemoattractant protein 1 (MCP-1), granulocyte-monocyte stimulating factor (GM-CSF), and interleukin 8 (IL-8) to strengthen the association of inflammatory cells with the lesion.^[29]

2.1.2. Lipoproteins

Lipids in the blood are transported in the form of lipoproteins. Briefly, a lipoprotein is made up of a single ApoB as well as the composition of triglycerides and cholesterol in different content. Whatever the content of the lipid, a lipoprotein with a diameter of less than 70 nm can penetrate the compromised endothelial barrier.^[30] Thereby, excess lipoproteins in plasma more easily enter the subendothelial space in the case of dyslipidemia.^[31] Among lipoproteins, the low-density lipoprotein (LDL) has already been confirmed to promote atherogenesis.^[32] They deposit

in the intima, where without plasma antioxidants, are easily oxidized by reactive oxygen species (ROS) produced by endothelial cells, macrophages, and VSMCs to proatherogenic and proinflammatory oxidized low-density lipoprotein (ox-LDL), which has explicit associations with clinical atherosclerotic cardiovascular disease.^[33] Compared to LDL, ox-LDL is a more influential atherogenic lipoprotein throughout atherosclerotic formation and development. It promotes the secretion of various proinflammatory cytokines of endothelial cells,^[34] damages endothelial cells, reduces the gene expression of endothelial nitric oxide synthases (eNOS) and nitric oxide (NO) production,^[35] and weakens the self-protective function of the vessel wall. In addition, it binds to and up-regulates scavenger receptors (SR) on macrophages as auto-antigen, accelerates the foaming process of macrophages and chemokines secretion, thereby, further amplifying the inflammatory cascade response.^[36] What's more, VSMCs are stimulated to proliferate and migrate from the media, phagocytose ox-LDL with oxidized LDL receptor 1 (LOX-1), and produce collagen-

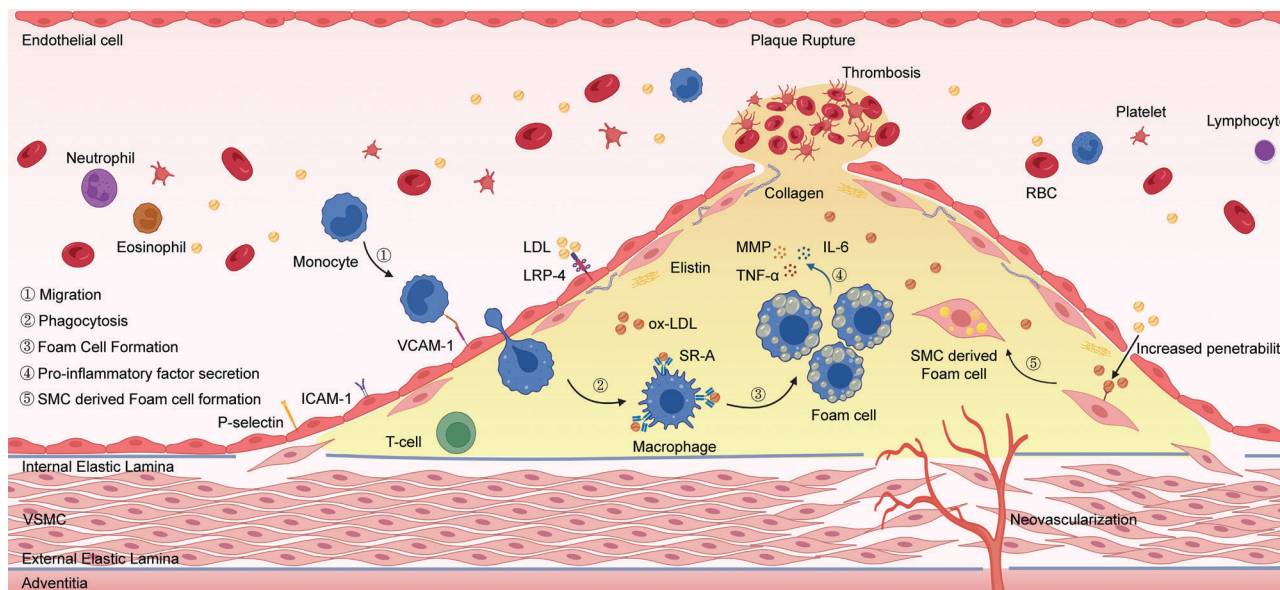


Figure 2. The diagrammatic sketch of the main components and the formation process of the atherosclerotic lesion. Figure was created with BioRender.com.

rich matrix, conferring plaque stability and mediating luminal narrowing.^[37]

2.1.3. Inflammatory Cells

Initially, multiple inflammatory cells respond to the call of the activated endothelium, and especially circulating monocytes will recruit (rolling, activation, and arrest) and differentiate into macrophages in the intima. Monocyte-derived macrophages engulf lipoproteins and switch them to foam cells via the SR, such as CD36 and scavenger receptors A1 (SR-A1).^[38] Subsequently, foamy macrophages within the plaques secrete various cytokines such as MCP-1, chemokine receptor 2 (CCR2), chemokine receptor 5 (CCR5), etc. to further recruit bone marrow cells. While in advanced plaque, macrophage proliferation *in situ* seems to play a crucial role.^[39] It is noteworthy that the number of macrophages in vulnerable plaques is three to five times higher than in stable plaques, hence the enrichment of macrophages becomes an important indicator of plaque vulnerability.^[40] These macrophages attempt to eliminate or efflux cholesterol to high-density lipoprotein (HDL) with cholesterol efflux transporters ATP-binding cassette transporter A1 (ABCA1) and G1 (ABCG1).^[41] Unfortunately, the SR won't down-regulate its expression even though lipoproteins are already overloaded, so less efficient cholesterol efflux is observed compared with lipoproteins uptake. The foamy macrophages keep eating lipoproteins and finally have the inability to withstand undue stress and die.^[42]

Macrophage apoptosis is beneficial in the early lesions because normal efferocytosis (refers to the engulfment of cell corpses by phagocytes) usually clears apoptosis cells in several minutes.^[43] As the disease progresses, macrophage apoptosis and necrosis increase, while efferocytosis-associated proteins such as milk fat globule-EGF factor 8 (Mfge8) and Mer receptor tyrosine kinase (Mertk) are dysfunctional. Massive cell corpses are unable to be

removed by the defective efferocytosis and accumulate within the plaque to gradually establish, and expand a necrotic core, which exacerbates plaque instability.^[44]

Besides, neutrophils, the most abundant white blood cells, are also early contributors to plaque and are associated with poor clinical prognosis.^[45] Neutrophils release metalloproteinases (MMPs) and proteolytic proteins to disrupt the physical barrier of the endothelium, and deposit chemotactic proteins like cathelicidin on the endothelium to promote monocyte recruitment.^[46] After entering subendothelial space, neutrophils further release myeloperoxidase (MPO), MMPs, elastases, cathelicidin, cathepsin G, and ROS, enhancing the oxidative stress levels and plaque vulnerability.

The bone marrow response is accompanied by the infiltration of adaptive immune systemic T cells and B cells. T cells are classified into multitude subtypes, of which CD4⁺ T cells are closely correlated with atherosclerotic progression.^[47] The T helper 1 (Th1) cells differentiated from CD4⁺ T cells are the most abundant T cell subpopulation in the lesion after antigen presentation, while the role of other T cell subtypes requires further confirmation.^[48] The investigation of B cells has lagged behind other cells, and early studies demonstrated that there were significantly fewer B cells in intimal plaques than in the adventitia.^[49]

2.1.4. Vascular Smooth Muscle Cells (VSMCs)

The balance of VSMCs proliferation and death is relevant to atherogenesis.^[50] To repair the injury, VSMCs within the media will migrate into the intima through the internal elastic lamina, proliferate and secrete extracellular matrix including collagen, elastin, and proteoglycan to form a fibrous cap that prevents plaque rupture and intrude into the arterial lumen.^[51] Over time, the senescence and death (especially apoptosis) of

Table 1. The advantages, disadvantages, and representative models of different animal models.

Animal models	Advantages	Disadvantages	Representative models
Mice	I. Easy availability, II. high reproductive capacity, III. controlled conditions, IV. short experimental periodicity V. low price	I. Limited plaque lesions, II. difficult operation because of thin blood vessels, III. abnormal inflammation and immune function.	I. C57BL/6J mice with a Western diet, II. ApoE ^{-/-} mice, III. LDLr ^{-/-} mice, IV. ApoE/LDLr ^{-/-} mice, V. ApoE3-Leiden mice VI. ApoE ^{-/-} Fbn1 ^{C1039G/+} mice
Rats	I. Large volume, II. easy operation	I. No gallbladder, II. difficult lipid absorption III. significant physiological differences to humans	I. Wistar or SD rats with a Western diet, II. I and vitamin D injection III. ApoE and/or LDLr ^{-/-} mice
Rabbits	I. Easy operation, II. similar anatomical structures and lipid metabolism to humans, III. high absorption of cholesterol.	I. High cost, II. inflammatory and hepatotoxicity, III. long duration or surgery required	I. New Zealand rabbits with a Western diet, II. I and balloon injury surgery, III. WHHL rabbits
Large animal models	I. Human-like predilection site, homologous intimal structure,	I. High cost, II. long feeding time, III. small simple size, IV. large individual differences	I. Porcine model II. non-human primates

VSMCs contribute to a thin fibrous cap, large necrotic core, and inflammation activation, which are important features of the vulnerable plaque sites (mainly the shoulder).^[52] In addition, the loss of VSMCs induces medial atrophy, vascular calcification, vessel remodeling, and even the formation of aneurysm.^[53]

With further studies, much plasticity of VSMCs was demonstrated that they can convert to other cell phenotypes from contractile phenotype during atherogenesis.^[54] Recent evidence suggests that they are derived into a transitional cell called “SEM” cells with versatility and such “SEM” cells have the potential to dedifferentiate or differentiate into macrophage-like cells.^[55] To some degree, it explains why some VSMCs possess macrophage markers and can phagocytose lipoproteins to form VSMCs-derived foam cells. Another important message is that judging a certain cell type within plaque barely based on a specific surface marker may be oversimplified.

Although there is no unanimous conclusion about the mechanisms of atherosclerotic formation, it is widely accepted that its internal environment is an intricate inflammation network in which both innate and adaptive immunity are involved. The above-mentioned cells play the role of a double-edged sword as the characteristic components of the atherosclerotic lesions. Therefore, the stage of disease progression, cellular origin, and function should be considered comprehensively when developing therapy strategies.

2.2. Experimental Animal Models

Direct atherosclerotic studies in humans are time-consuming and difficult to obtain ideal specimens with many uncertain risks and confounding factors. Therefore, experimental animal models with similar pathogenesis and clinical manifestations to human atherosclerosis are needed for alternative studies. Currently, animals used to construct atherosclerotic models chiefly include mice, rats, rabbits, pigs, and non-human primates. The modeling

methods cover genetic engineering, high-fat and high-cholesterol feeding, surgical damaging as well as the introduction of risk factors (e.g., diabetes or pneumonia). In this section, we discuss the pros and cons of common experimental animal models and typical experimental modeling methods (Table 1).

2.2.1. Mice

Mice are the most common experimental animals due to their easy availability, docile temperament, high reproductive capacity, and controlled conditions. For example, C57BL/6J mice, the popular strain of atherosclerotic mice, are fed a high-cholesterol and high-fat diet to mimic the hyperlipidemia environment in humans. However, in terms of plaque formation, C57BL/6J mice need a long feeding period and form small plaques, thus genetic editing is introduced to regulate lipid metabolism. Apolipoprotein E knockout (ApoE^{-/-}) mice and LDL-receptor deficient (LDLr^{-/-}) mice are the most widely applied models since the appearance of genetic editing.^[56] Apolipoprotein E (ApoE), an arginine-rich protein, is found in many lipoproteins (e.g., chylomicron, chylomicron remnants, VLDL, LDL, and some HDL) and possesses anti-inflammatory, antioxidant, and anti-atherosclerosis effects.^[57] Generally, ApoE binds to LDLr on hepatocytes to participate in the uptake and degradation of lipoproteins by the liver, clears chylomicron via LDLr-related proteins, engages in reverse cholesterol transport, and activates fat hydrolases.^[58] LDLr is a multifunctional protein widely distributed on the surface of hepatocytes, mediating the entry of plasma LDL into cells, regulating cholesterol levels, and exerting a hypolipidemic effect. Hence, the plasma cholesterol level is significantly elevated in LDLr^{-/-} mice.^[59] Although both are suitable for atherosclerotic experiments, it is noteworthy that ApoE^{-/-} mice can generate plaque with a normal diet, suggesting the difference in atherosclerotic mechanism between the two models. And in fact, when fed with a high cholesterol and high-fat diet, ApoE^{-/-} mice exhibit higher

cholesterol levels in plasma, larger plaque volumes, and greater necrotic cores compared to LDLr^{-/-} mice, making the former more widely used.^[60] Soon after, the ApoE/LDLr double knockout (ApoE/LDLr^{-/-}) experimental mice were proposed by Bontho and co-workers. Faster lesion formation was observed in this model and it promised to investigate atherosclerosis with a normal diet.^[61] Additionally, to get closer to human lipid metabolism, ApoE3-Leiden mice were created with a similar lipoprotein profile to human.^[62] Functional ApoE could be detected in ApoE3-Leiden mice, and the effect of dyslipidemia on disease progression can be explored separately without the disturbance of inflammation compared to ApoE^{-/-} mice.^[63]

The above genetically manipulated mice have generally matured with their own advantages, but still struggle to construct thrombosis, plaque rupture, and other complex complications. To address it, the cuff, artery partial ligation or angiotensin II infusion can be performed to artificially induce further endothelial damage and hemodynamic disturbances, thereby accelerating plaque formation, hemorrhage, and rupture.^[64] Another option is ApoE^{-/-}-Fbn1^{C1039G/+} mice, a mutant heterozygote with a propensity for fibrin breakage, which develops highly unstable plaques that rupture spontaneously or even die suddenly.^[65] Combined with a western diet (21% fat and 0.15% cholesterol), ApoE^{-/-}-Fbn1^{C1039G/+} mice can exhibit characteristic human-like advanced plaques, which provides the opportunity to contribute to the research of vulnerable plaque.

2.2.2. Rats

In general, Wistar or SD rats are also needed to establish the atherosclerotic model. Rats have an absent gallbladder and low lipid uptake, requiring prolonged feeding with a diet containing bile salts, thiouracil, high fat, and high cholesterol.^[66] High-fat and high-cholesterol feeding combined with intraperitoneal vitamin D injection are more popular since it promotes blood calcium absorption to damage the vascular endothelium.^[67] However, no available evidence to support the superiority of rats over mice. Similarly, to induce hyperlipidemia and atherosclerotic formation, ApoE^{-/-},^[68] LDLr^{-/-},^[69] or double knockout rats^[70] were constructed synchronously. Besides, there are significant physiological differences between rats and humans, thereby, conclusions drawn from rats are not necessarily applicable to humans. Notably, invasive manipulation such as balloon injury, electroshock injury, and arterial clamping and ex vivo analysis is more easily achieved in rats due to their volume superiority.

2.2.3. Rabbits

Rabbits, the well-established animal model for atherosclerosis, possess more similar lipid metabolism to humans than mice. At present, rabbit models used to study lipid metabolism and atherosclerosis include rabbits fed with a Western diet, Watanabe heritable hyperlipidemic (WHHL) rabbits, and genetically edited rabbits. First, New Zealand rabbits are usually chosen to develop the atherosclerotic lesions by 12–16 weeks and establish advanced plaque for more than 28 weeks with a high cholesterol diet (0.3%–1%).^[71] It is emphasized that rabbits fed with

high cholesterol for a long time are prone to develop inflammation, hepatotoxicity, and fatty liver, which can incorporate balloon endothelial debridement to shorten the feeding period. Second, WHHL rabbits are characterized by more LDLs and fewer HDLs owing to defective LDLr expression, which is analogous to human familial hypercholesterolemia and atherosclerosis.^[72] Furthermore, genes involved in lipid metabolism could be introduced into or knocked out from rabbits by gene editing, providing new insights into the understanding of atherosclerosis.^[73] Nevertheless, rabbits are not a substitute for rodents as each rabbit requires a separate cage space, longer feeding time, and expense, and they are not inbred and vary widely among individuals. Overall, rabbits are more suitable for the studies of hyperlipidemia, clinical translation of drugs or pre-experiments in large experimental animal models (pigs and monkeys).

2.2.4. Large Animal Models

Small animal models are available for mechanistic exploration as well as preliminary pharmacological and toxicological studies. However, in order to apply previous research to the human body and achieve atherosclerotic diagnosis and treatment, other more appropriate animal models are needed.^[74] The atherosclerotic pig model is a promising bridging tool, and shares many similarities with human progressive atherosclerosis, including human-like predilection site, homologous intimal structure, abundant neovascularization, and internal calcification.^[75] Pigs share similar omnivorous preferences with humans and possess a cardiovascular system of comparable size, making them more susceptible to the heightened fat content in their diets and corresponding vascular responses.^[76] Existing research manifested that nicotine injection combined with balloon injury can rapidly promote intimal hyperplasia, successfully inducing atherosclerotic pigs within one month.^[77] In addition, exerting extra for pigs PCSK9 gene mutation or somatic nuclear transfer aided by a high-fat diet is also a kind of promising technique.^[78] Besides, the conclusions drawn from non-human primates have high applicability in humans because of their comparative physiological similarity to humans.^[79] The development of gene editing tools may provide new approaches and reinforce the similarity between large animal models and human atherosclerosis.^[80] However, working with large animals is expensive, time-consuming, highly regulated, and requires extremely specialized laboratory skills and a dedicated experimental site.

Therefore, the use of mouse models is recommended for the initial exploration of early drug screening, efficacy verification, mechanism clarification, and safety evaluation. Considering surgical manipulation, plaque imaging manifestation, and preliminary validation of large animal models, rats, and rabbits may be better choices. As research progresses and prepares for clinical trials, conducting verification in large animal models is crucial.

2.3. Material Design

To obtain benign anti-atherosclerosis effects, some general principles are supposed to be considered when constructing nanomaterials. Nanomaterials should possess superior bioavailability,

biocompatibility, stability, permeability, and desirable circulation time in vivo under physiological conditions, as well as accumulate at the target location as much as possible without damaging the surrounding healthy tissues via passive or active targeting.

2.3.1. Passive Targeting

Passive targeting refers that the nanomaterials being recruited to the plaque either through the high permeability of the leaky vasculature or the phagocytosis by the mononuclear phagocyte system (MPS). Similar to cancer, the EPR effect may be informative due to the abundant neovascularization and abnormal arrangement of endothelial cells within atherosclerosis. However, the EPR effect remains to be investigated because it is unpredictable in animal models and the endothelial junctions tend to be stabilized in advanced plaques. Another possibility is that nanomaterials are selectively ingested by certain immune cells, which carry a considerable proportion of the nanomedicines into the plaque.^[81] These two routes allow the nanomaterials to “passively target” the diseased organ or site, although the specific mechanism is not completely understood. Notably, it is highly dependent on the physicochemical characteristics of nanomaterials such as size, shape, and surface properties.^[82]

First, size has a profound impact on the biodistribution, pharmacokinetics, and half-life of nanomaterials upon intravenous injection. Nanomaterials whose size are smaller than 10 nm are easily cleared directly by the kidney, whereas nanomaterials are preferentially captured by the reticuloendothelial system in the liver and spleen when their size is larger than 50 nm, and oversized nanomaterials (micron-size) are difficult to enter plaque.^[83] It was demonstrated that as the size of nanomaterials increases in a limited range (from 40 nm to 200 nm), more capture by the reticuloendothelial system and shorter blood circulation times were observed. In a comparative study, polyion complex micelles of different sizes were constructed to evaluate the accumulation at the lesion site in a rat carotid balloon dilation model.^[84] Their work demonstrated that variation in the size of nanomaterials influenced their accumulation and therapeutic effects. After that, the same group further confirmed that resizing nanomaterials could adjust their interaction with macrophages in vascular diseases.^[85]

Second, several studies have suggested that the shape of nanomaterials (e.g., spherical, rod, disk, wire, oblate ellipsoids, etc.) affects the interaction between nanomaterials and cells, circulating half-life, and margination behavior. Although non-spherical nanomedicines are more challenging to prepare than spherical nanomaterials, they seem to be more favored in blood circulation and cell internalization.^[86] On the one hand, mononuclear macrophages in the liver and spleen internalize fewer nonspherical nanomaterials than spherical nanomaterials, thus prolonging the circulating half-life.^[87] On the other hand, the curvature of spherical nanomaterials limits their contact area with the endothelial surface, lowering the tendency of margination and adhesion.^[88] In a plate flow chamber model, rod particles with high aspect ratios manifested superior adhesive properties in comparison with conventional spherical particles.^[89] Another research aimed to explore the influence of different shape parameters on the targeting thrombi function in mice models.^[90] Like-

wise, rod nanomaterials are more powerful in terms of targeting effect, and the influence of shape is much stronger than that of various targeting peptides. Therefore, nonspherical nanomaterials seem to be more suitable as carriers for targeting atherosclerosis. Furthermore, nanomaterials with different shapes exhibit a preference for various inflammatory cell subpopulations. Researchers designed three types of nanostructures with the same surface chemical properties, including micelles, polymersomes, and filomicelles, to investigate the selective uptake of cell subpopulations by structural morphology differences. The study indicated that polymersomes were preferentially taken up by macrophages and DCs in the spleen and lymph nodes with a longer residence time. Micelles showed superior specificity for macrophages and DCs in the liver, while filomicelles were preferentially taken up by granulocytes in the blood. In addition, DCs in atherosclerotic plaques demonstrated a significant preference for polymersomes.^[91]

What is more, the surface property is another crucial aspect in the design of nanomaterials. For example, the surface charge affects cellular uptake and blood circulation time. The positively charged nanomaterials are more readily internalized by cells compared to their negative or neutral counterparts, probably due to the interactions with negatively charged sialic acid groups on the surface of macrophage membrane.^[92] The CD36 on macrophages or foam cells can slightly reinforce the internalization of the negatively charged nanomaterials. In addition, nanomaterials without surface modification are usually hydrophobic and easily cleared by macrophages in the liver and spleen, hindering the delivery of the nanomaterials. To address it, hydrophilic polymers like polyethylene glycol (PEG) or amphoteric polymers are applied to coat the nanomaterials, forming a hydrated shell.^[93] This surface coating can additionally work as an intermediate medium to modify more functional components into nanomaterials. Notably, nanomaterials are exposed to physiological fluids in vivo and apt to bind proteins or other biomolecules to form “protein corona”. The charged or hydrophobic nanomaterials tend to adsorb more proteins and induce protein denaturation than their neutral and hydrophilic counterparts.^[94] These protein crowns will alter the basic features of the nanomaterials including targeting performance, biodistribution, immunogenicity, and toxicity and even confer new functions on them.^[95]

2.3.2. Active Targeting

Active targeting typically entails attaching specific targeting agents to the nanoparticle or constructing a stimulus-responsive smart nanocarrier for effective diagnosis and/or therapy. Compared to passive targeting, active targeting allows higher intralésion localization and fewer side effects in a shorter time, due to the reduced single dosage and administration frequency.

For one thing, the specific pathological components and overexpressed molecules during atherosclerotic progression offer properly targeted goals for the active targeting of nanomaterials. Most of these active targeting strategies rely on the interaction between antigen and antibody as well as ligand and receptor. Currently, the active targeting aims of nanomaterials mainly include macrophages,^[96] endothelial cells,^[97]

neovascularization,^[98] thrombus,^[99] and extracellular matrix proteins.^[100]

Macrophage, a kind of phagocyte, acts as one of the most important cell types in atherosclerosis. The strategy for constructing actively targeted nanomaterials is mainly based on the typical surface marker (e.g., CD44, CD68, and CD47) and cellular phagocytic function of macrophage.^[101] This function involves high expression of CD36, SR-A1, LOX-1, mannose receptors, and phosphatidylserine (PS) receptors. After macrophages engulf lipids, foam cells are formed, and osteopontin (OPN) as well as ABCA1 are further abnormally expressed. Therefore, existing literatures have chosen corresponding antibodies, peptides, or ligands for modification of nanomaterials to achieve active targeting for these types of cells. Activated endothelial cells overexpress VCAM-1, ICAM-1, P/E-selectin,^[102] $\alpha v \beta 3$ integrin,^[103] and stabilin-2,^[100] thus antibodies or peptides with high affinity to these biomarkers have been widely applied for active targeting. In addition, $\alpha v \beta 3$ integrin is a promising candidate for the visualization or mitigation of neovascularization. In terms of thrombosis, platelets adhere and network fibrin and red blood cells together to form aggregates, and several ligands targeting fibrin and platelets have been developed to detect or competitively inhibit the formation of thrombus. In addition, the extracellular matrix proteins involve collagens, elastic fibers, laminins, and glycoproteins.^[104] These ingredients occupy more than half of the plaque area, so they can be actively targeted to reflect the degree of luminal stenosis and plaque stability.

For another, in the pathological transformation of the normal arterial wall structure, many variations in the lesion components occur, specifically the expression of molecules as described above, the change of the enzyme profile (such as matrix metalloproteinases within the atherosclerotic plaque site) and hemodynamics as well as the local microenvironment (e.g., pH, temperature and oxidative stress).^[105] Therefore, it is possible to construct therapeutic or diagnostic systems under specific stimulus-response based on the differences between the interior of the lesion and the normal tissues, thereby mitigating the interference with normal cells. Representative stimulus-response paradigms include a localized acidic environment-sensitive chemical bond breaking,^[106] a ROS-responsive drug release, and the transition between hydrophobic and hydrophilic states mediated by the lipid microenvironment within the atherosclerotic plaque.^[107]

3. Nanomaterials

3.1. Inorganic Nanomaterials

According to the reported literature, inorganic nanomaterials applied to atherosclerosis can be divided into metallic and non-metallic nanomaterials.

3.1.1. Nonmetallic Nanomaterials

Nonmetallic nanomaterials such as mesoporous silica and carbon-based nanomaterials are widely used in atherosclerosis. Mesoporous silica nanoparticles (MSNs) have a particle size of 10–600 nm and a pore size of 2–50 nm with a large surface

area, unique mesh-like pore structure, regular pore channels, and adjustable pore size. The adjustable central pore structure and high loading of cargo facilitate its function as a nanocarrier to improve the water solubility of drugs and decrease the side effects.^[108] In addition to filling inward as a shell structure, MSN can also be used as a platform for the growth of other materials (Figure 3a).^[109] Besides, carbon-based nanomaterials come in a variety of shapes and types, and in recent years, a myriad of novel carbon-based nanomaterials have attracted a lot of attention, such as graphene, carbon nanotubes, nanodiamonds, and nanodots, etc.^[110] Several carbon-based nanomaterials own unique structures and properties with high photothermal conversion efficiency and distinct FL effect, which are suitable for photothermal therapy (PTT), PA imaging, and FL tracing (e.g., carbon nanotubes,^[111] carbon nanocages,^[112] graphene oxide,^[113] and carbon quantum dots).^[114]

3.1.2. Metallic Nanomaterials

Gold nanoparticles (AuNPs) are currently the most widely used metal nanomaterials in the field of nanomedicine and are usually obtained by the reduction of inorganic acids containing gold in the presence of stabilizers (Figure 3b).^[115] AuNPs have controlled morphology and such as spheres, nanorods, and nanocages. AuNPs-based PTT and PA imaging for atherosclerosis are feasible due to the presence of surface plasmon resonance (SPR) effects, and CT tracing on the basis of AuNPs is possible because of the large atomic number.^[116] Among the metal oxides, iron oxide with marvelous magnetic properties can be applied to MR imaging. Cerium oxide (CeO₂), cobalt oxide (Co₃O₄) and manganese oxide (Mn₂O₃, Mn₃O₄) nanoenzymes with multienzyme-like activities are also gaining attention for their ability to scavenge ROS and alleviate inflammation.^[117] Semiconductor quantum dots (QDs) are excellent fluorescent tracers owing to their intrinsic optical characteristics.^[118] QDs have high photoluminescence quantum yields and photostability, which is promising in multimodal imaging and theranostic. Transition metal carbides, nitrides, and carbonitrides (MXene) have a 2D sheet-like structure with a huge surface area and abundant functional groups, which can be used as a carrier of many objects (Figure 3c).^[119] Additionally, the light absorption and photothermal conversion efficiency in the near-infrared region (NIR) of MXene is helpful for atherosclerotic PA imaging.^[120]

3.2. Organic Nanomaterials

3.2.1. Lipid-Associated Nanomaterials

Lipid-associated nanomaterials mainly include liposomes and reconstituted high-density lipoprotein nanoparticles (rHDL NPs). Liposomes have a phospholipid bilayer structure, which is composed of components such as cholesterol and phospholipids in a self-assembly behavior. As an excellent drug delivery vehicle with high biocompatibility, a wide range of deliverable drugs, easy surface modification, and controllable drug release, liposomes have been widely used in a variety of disease models.^[121] Similarly, rHDL is composed of endogenous apolipoprotein A-1

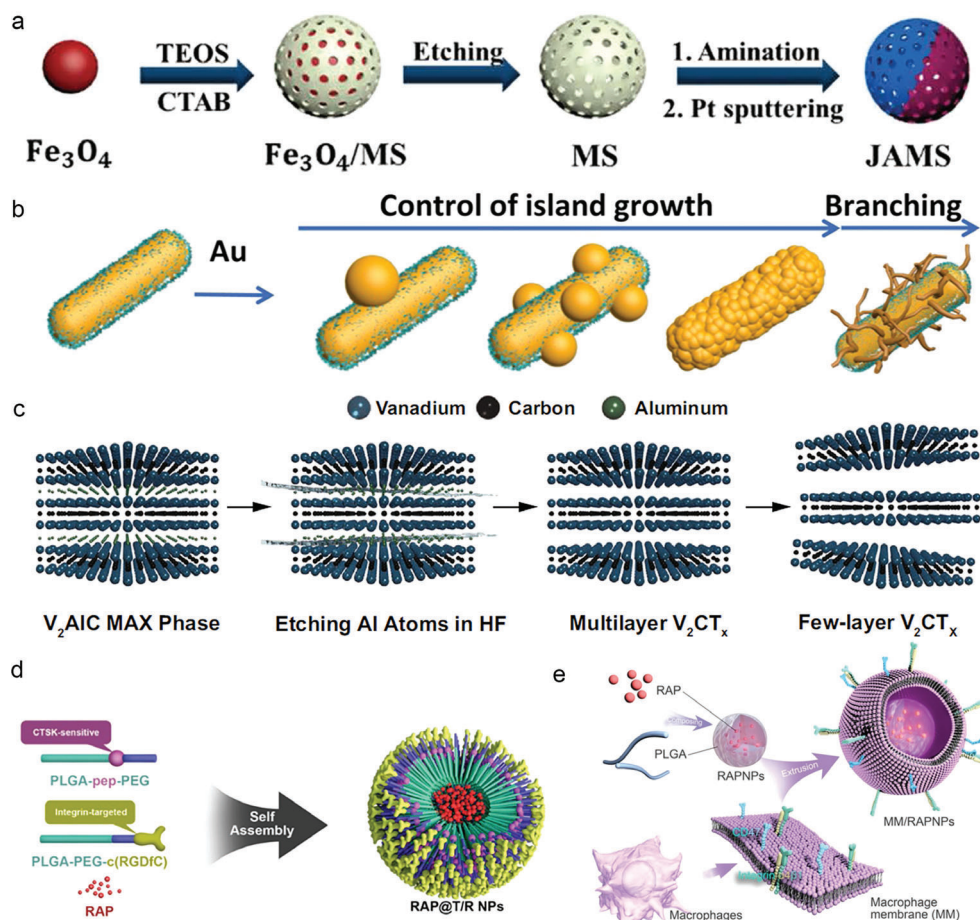


Figure 3. Representative schematic diagrams of typical nanomaterials such as a) MSNs, b) AuNPs and c) MXene. a) Reproduced with permission.^[109] Copyright 2020, Royal Society of Chemistry. b) Reproduced with permission.^[115] Copyright 2020, Wiley-VCH. c) Reproduced with permission.^[119a] Copyright 2021, Springer Nature. d) Representative illustration of polymeric nanomaterials (RAP@T/R NPs). Reproduced with permission.^[124] Copyright 2022, Ivyspring International Publisher. e) Schematic diagram of biomimetic cell membrane-coated nanomaterials (MM/RAPNPs). Reproduced with permission.^[131] Copyright 2021, Ivyspring International Publisher.

(ApoA-1), phospholipids, cholesterol, and cholesteryl esters inherent in the body. Cholesteryl esters act as the hydrophobic core that can encapsulate hydrophobic substances, and the other components act as the hydrophilic surfaces that can carry hydrophilic components. Particularly, rHDL NPs have anti-inflammatory and antioxidant effects, and mediate the reverse cholesterol transport in foam cells via ABCA1, ABCG1, and SR-1 to alleviate the lipid burden, making it especially suitable for atherosclerotic treatment.^[122]

3.2.2. Polymeric Nanomaterials

Polymeric nanomaterials, with diverse structures and compositions, could be fabricated by using natural polymers including dextran, cyclodextrin and chitosan, as well as synthetic polymers such as poly(ethylene glycol) (PEG), poly(ethylene imine) (PEI), Poly-L-lysine (PLL), polyamidoamine (PAMAM) and poly (lactic co-glycolic acid) (PLGA).^[123] They have strong plasticity and can introduce surfactants with different structures, thereby fulfilling various changes in biological functions (Figure 3d).^[124] On the

one hand, many drug carriers or nanoparticles use polymers as surface coatings and exist in the form of polymeric micelles. Polymeric micelles have high stability and biodegradability and are apt to reduce phagocytosis of the reticuloendothelial system to achieve longer blood circulation time. On the other hand, polymers participate in the construction of dendrimers. Dendrimers are artificial macromolecules with tree-like shapes, which have a well-defined 3D structure and are usually composed of a core, polymeric chains, and surface functional groups. The internal cavity structure assists drug loading, the polymerization algebra is easy to adjust, and a large number of functional groups on the surface facilitates molecular coupling, enabling precise control of size, shape, and function.^[125]

3.3. Biomimetic Nanomaterials

In recent years, biomimetic nanomaterials have gained widespread attention as a novel delivery strategy.^[126] These biomimetic nanomaterials mainly consist of nanoparticles and external biomimetic components, including biomimetic cell

membranes, living cells, viruses, and bacteria. They retain the intrinsic characteristics of nanoparticles while acquiring extra properties of biological structures (e.g., immune escape, long circulation, and targeted delivery). Among them, cell membrane-coated nanoparticles are popular in the treatment of atherosclerosis and are obtained by co-extrusion methods or ultrasound methods.

Currently, the BMT used to regulate inflammation and lipids in atherosclerosis is often limited by the first-pass effect and local low blood drug concentrations. Biomimetic nanomaterials endow nanoparticles with a longer circulation time, lasting drug release capabilities, and higher drug utilization. This may be related to the negative charge carried by cell membranes, which can reduce the rapid adsorption of most positively charged nanoparticles with cells in the bloodstream. Erythrocyte membranes were developed to encapsulate rapamycin, which took advantage of natural “don’t eat me” CD47 molecules on the surface to evade phagocytosis, prolonged the half-life in the bloodstream, and achieved targeted slow release of drugs across the leaks of endothelial cells and atherosclerotic microvessels.^[127] Additionally, gene editing technology could introduce functional probes like peptides, proteins, small molecules, etc. into red cells to achieve functional expansion, however, this section remains to be studied.^[128] Endothelial cell membranes, due to the large number of self-recognition proteins on the surface, had homologous targeting ability, making them efficient candidates for targeted atherosclerosis.^[129] According to literature reports, platelets^[130] and macrophages^[131] possess positive inflammatory tropism,^[132] which may be another alternative method (Figure 3e). Among them, nanoparticles coated with macrophage membranes are more favored. It has been found that the antigens such as the SR on the surface of macrophages can bind ox-LDL, reducing the uptake of lipids by macrophages and inhibiting the formation of foam cells. Moreover, the presence of membrane antigens sequestered key proinflammatory factors and chemokines, which was superior to live cell delivery in reducing inflammation within plaques.^[133]

In summary, biomimetic nanomaterials exhibit improved pharmacokinetics, excellent plaque-targeting ability, and controllable engineered design, some of which even have therapeutic effects, providing a promising platform for the treatment of atherosclerosis.

4. Diagnostic Imaging

For most, before the outbreak of the endpoint event, atherosclerosis is a relatively recessive disease without corresponding overt characteristics. Once the disease advances, the efficacy of drug treatment is limited, and the surgical treatment is accompanied by great damage. Therefore, scientists desperately wish that diagnostic tools could fulfill early diagnosis, provide an accurate assessment of atherosclerotic burden, and clarify future risk stratification, which is hard to achieve with conventional imaging tools and their contrast agents. In recent decades, a variety of nanoprobe flooded into our horizon as the nanoscale size allows easier access to the interior of plaque and more intuitive visualization of the pathological process by the EPR effect. Besides, coupled with antibodies, polypeptides, or other targeting ligands, the

nanoprobes can bind specifically to the surface molecules of certain cells or tissues to evaluate specific mechanisms or processes. An increasing number of research demonstrated that the application of nanoprobe can facilitate drug delivery, reduce dosage, enhance the ability to anticipate risks, and guide the subsequent treatment. Obviously, the employment of nanoprobe is opening a new door in atherosclerotic diagnosis.^[134] We summarize the basic features of nanoprobe for atherosclerotic diagnosis in recent years (Table 2).

4.1. Magnetic Resonance Imaging

MR imaging has been already used to diagnose coronary artery disease by utilizing nuclear magnetic resonance phenomena of certain atomic nuclei in tissues. Compared to other modalities, MR imaging has advantages like higher soft tissue resolution, deeper tissue penetration, and no ionizing radiation. MR imaging can offer partial information related to the thickness of the fiber cap, the size of the lipid necrosis core, and hemorrhage via different imaging sequences. However, low sensitivity, long operation time, and motion artifacts are the limitations of MR imaging in the diagnosis of atherosclerosis. The emergence of nanomaterials can assist in solving the above problems. Paramagnetic nanomaterials can fulfill precise positioning, improve sensitivity as well as safety, and obviously distinguish lesions from healthy tissue. Specifically, paramagnetic gadolinium (Gd)-based nanoparticles and superparamagnetic iron oxide nanoparticles (SPIONs) are the most common MR imaging nanotracers in atherosclerosis.^[135]

On the one hand, Gd-based MR contrast agents exhibit high signal on T1 weighting, which shortens the T1 relaxation time by affecting the relaxation rate of the surrounding water protons,^[136] but the toxicity of gadolinium ion limits its biological application.^[137] Therefore, Gd chelates have been prepared to improve their biocompatibility, for example, 1,4,7,10-tetraazacyclododecane-1,4,7,10-tetraacetic acid (Gd-DOTA) and diethylene triamine pentaacetic acid (Gd-DTPA).^[138] Due to the specific accumulation of tropoelastin within the plaque, Gd₄-TESMA made up of four Gd (III)-DOTA-monoamide chelate conjugated with a tropoelastin-binding peptide (the VVGS-peptide) was introduced to illustrate the location and size of plaque through MR imaging tropoelastin.^[139] In another research, Gd-DTPA was incorporated in the CNP, a complex nanoparticle self-assembled by protamine peptide TPP1880 and low molecular weight fucoidan LMWF8875, to target P-selectin overexpressed on the inflammatory endothelial cells surface.^[140]

On the other hand, iron oxide nanoparticles-based MR contrast agents exhibit low signal on T2 weighting, which shortens T2 value by altering the local magnetic field strength and accelerating dephasing mediated by spin-spin effects. It is reported that very small iron oxide nanoparticles could be engulfed and enriched by mononuclear macrophages accumulating in inflammatory atherosclerosis.^[141] To further enhance the targeting function of SPIONs to plaque, OPN-modified Fe₃O₄ nanoparticles (Cy5.5-OPN-DMSA-MNPs, named as COD-MNPs) were designed as MR imaging probe to indicate the lesions considering the overexpressed OPN on foamy macrophages.^[142] In another

Table 2. A summary of the application of nanomaterials in atherosclerosis.

Application method	Modality	Nanomaterials	Size	Targeting strategy	Animal models	Biomedical applications and mechanisms	Refs.
Diagnosis	MR imaging	Tropoelastin-binding peptide coupled tetrameric Gd ₄ -TESMA	/	Tropoelastin-binding peptide (the VVGS-peptide) target tropoelastin in plaque	ApoE -/- mice	Gd-mediated T1 weighted MR imaging	[139]
		DTPA/fucoidan/peptide complex nanoparticles	243.6 nm ± 10.0 nm (TEM)	Target P-selectin overexpressing endothelial cells.	/	Gd-mediated T1 weighted MR imaging	[140]
		Cy5.5-OPN-DMSA-MNPs (COD-MNPs)	DMSA-MNPs core: 7.3 nm ± 0.6 nm (DLS)	OPN antibody target OPN on foam macrophage	ApoE -/- mice	Iron oxide nanoparticles-mediated T2 weighted MR imaging	[142]
		Hyaluronan-conjugated iron oxide nanoworms (HA-NWs)	The length of HA-NW: 65 nm ± 15 nm	Hyaluronan target CD44 on endothelium cells	ApoE -/- mice	Iron oxide nanoparticles-mediated T2 weighted MR imaging	[144]
	CT imaging	N1177	259 nm	Phagocytosis by macrophages and quantification of macrophage burden	High-fat fed and balloon damaged New Zealand White rabbits	Iodinated nanotracer-mediated CT imaging	[151]
		Fib-GC-AuNP	127.4 nm ± 2.7 nm	Target fibrin in thrombi	C57Bl/6 mice with FeCl ₃ -induced carotid thrombosis and/or embolic ischemic stroke	AuNPs-mediated CT imaging	[153]
		11-MUDA AuNP	31.5 nm	Label and track monocytes	ApoE-/- mice	AuNPs-mediated CT imaging	[154]
		AuNP	12.5 nm	Phagocytosis by macrophages and quantification of macrophage burden	Balloon damaged New Zealand white rabbits	AuNPs-mediated CT imaging	[156]
Radionuclide imaging		¹⁸ F-Sodium Fluoride	/	Calcification imaging	Excised carotid specimens	¹⁸ F-mediated PET imaging	[157]
		⁸⁹ Zr-DFO-Gal ₃ -F(ab') ₂ mAb	/	Target the Galectin-3 and macrophage	ApoE -/- mice	⁸⁹ Zr-mediated PET imaging	[159a]
		⁸⁹ Zr-labeled maleylated human serum albumin (⁸⁹ Zr-HSA)	/	Target the macrophage scavenger receptor SR-A1	ApoE -/- mice	⁸⁹ Zr-mediated PET imaging	[159b]
		⁸⁹ Zr-labeled liposomes	106.0 nm ± 5.2 nm	Passive targeting	High-fat fed and balloon damaged New Zealand White rabbits	⁸⁹ Zr-mediated PET imaging	[161]
		⁶⁴ Cu-DAPTA-Combs	10%DAPTA-Comb 14.8 nm, 25%DAPTA-Comb 15.2 nm, 40%DAPTA-Comb 10.9 nm	Target the CCR5 in plaque	ApoE -/- mice and excised carotid specimens	⁶⁴ Cu-mediated PET imaging	[162]
		H-ferritin nanocages (⁹⁹ mTc-HFn)	16 nm	Phagocytosis into macrophages and quantification of macrophage burden	ApoE -/- mice	⁹⁹ mTc-mediated SPECT imaging	[163]

(Continued)

Table 2. (Continued)

Application method	Modality	Nanomaterials	Size	Targeting strategy	Animal models	Biomedical applications and mechanisms	Refs.
FL imaging		ApoA-I-Cy5.5	/	Protease-activatable fluorescent probe to analyze ApoA-I-degrading activities	Human ApoB transgenic LDL ^{-/-} atherosclerotic mice (ATX)	Cyanine-mediated FL imaging	[165]
		TBNC@Mp	100 nm to 120 nm	Platelet membrane target foam macrophage	SD rats with high-fat diets and vitamin D3	Naphthalimide-mediated FL imaging	[166]
		Pyrene-based naked-eye colorimetric and fluorescent turn-on probe (S-CIO)	/	Imaging endogenous HClO ⁻ , ClO ⁻ promoted oxidative cleavage reaction	RAW264.7 cells, an arterial vessel inflammation nude mouse model and human serum	Pyrene-mediated FL imaging	[168]
		IONP-ICG	IONP-ICG5 (35.9 nm ± 8.2 nm), IONP-ICG10 (34.1 nm ± 10.1 nm), IONP-ICG20 (34.9 nm ± 9.2 nm)	Passive target	Spontaneously hyperlipidemic (SHL) mice with a disrupted ApoE gene	Indocyanine green (ICG)-mediated FL imaging	[169]
		P-ICG2-PS-Lip	180 nm (TEM)	Phosphatidylserine(PS) target on macrophages	ApoE ^{-/-} mice and WHHL rabbits	Indocyanine green (ICG)-mediated FL imaging	[172]
		Anti-CD47-modified TPE-T-RCN NPs (anti-CD47 NPs)	105.1 nm ± 0.2 nm (DLS)	Anti-CD47 antibody target CD47 on SMC and macrophages	ApoE ^{-/-} mice and excised carotid specimens	D-π-A type AIE luminogen-mediated FL imaging	[173]
		PbS/CdS/ZnS quantum dots	5.6 nm (TEM) 20 nm (DLS)	Highly penetrating thermal transient thermometry discriminated between the ischemic and inflammatory phases	A murine model of hindlimb ischemia	QDs-mediated FL imaging	[176]
		Dextran-mimetic HgCdSe-based QDs	5.5 nm ± 0.9 nm (TEM)	Dextran target macrophages	C57BL/6 mice with HFD	QDs-mediated FL imaging	[177]
	PA imaging	OPN Ab/Ti ₃ C ₂ /ICG nanoprobe	Lateral size of less than 500, the thickness of about 1.5 nm (TEM)	OPN antibody target OPN on foam cell	ApoE ^{-/-} mice	Ti ₃ C ₂ and ICG-mediated PA imaging	[120]
		Ultrasensitive carbon nanotubes (SWNTs)	2 nm × 200 nm (width × length)	Target the Ly-6Chi monocytes subpopulation	FVB mice with high-fat diet; intraperitoneal injections of streptozotocin; ligate left common carotid artery	SWNTs-mediated PA imaging	[111]
		PBD-CD36 nanoparticles	50 nm (TEM)	CD36 antibody target CD36 on inflammatory cells	ApoE ^{-/-} mice	Semiconductor nanomaterial PBD-mediated PA imaging	[182]
		Ratiometric semiconducting polymer nanoparticles (RSPN)	20 nm (TEM)	Passive target	ApoE ^{-/-} mice and ApoE ^{-/-} mice complicated with pneumonia	Semiconductor polymer nanomaterial-mediated PA imaging	[183]

(Continued)

Table 2. (Continued)

Application method	Modality	Nanomaterials	Size	Targeting strategy	Animal models	Biomedical applications and mechanisms	Refs.
OCT	Multimodal imaging	AuNPs	/	Passive target	Non-animal	AuNPs-mediated OCT imaging	[186]
		Semiconductor QDs	5 nm ± 2 nm (TEM)	Passive target	Rabbits	QDs-mediated OCT imaging	[187]
		Zinc-doped ferrite nanoparticles (Zn _{0.4} Fe _{2.6} O ₄)	zinc doped ferrite (ZF) core: 24 nm ± 2 nm (TEM)	Heat shock protein (Hsp)-70 antibodies target atherosclerotic inflammatory site.	ApoE ^{-/-} mice	I. Zinc-mediated CT imaging, II. Ferrite nanocomplex-mediated MR imaging	[188]
		VUSPIO-TEG4	/	The scFv fragment of TEG4 antibody target the activated platelets (integrin αIIbβ3)	ApoE ^{-/-} mice and New Zealand rabbits (NZW)	I. Fluorochromes-mediated FL imaging, II. Iron oxide nanoparticles-mediated MR imaging	[189]
Therapy	Drug delivery	PP1-IO@MS-IR820, PIMI	90 nm (TEM)	PP1 target scavenger receptors A1 (SR-A1) on foam macrophages	ApoE ^{-/-} mice	I. NIRF dye (IR820)-mediated FL imaging, II. Iron oxide nanoparticles-mediated MR imaging	[190]
		⁸⁹ Zr/BODIPY-labeled ¹⁹ F-HDL	Small: 40 nm middle: 105 nm, large: 180 (DLS)	HDL target myeloid cells	ApoE ^{-/-} mice	I. ¹⁹ F-HDL-mediated ¹⁹ F MR imaging, II. ⁸⁹ Zr-mediated gamma imaging, III. Cholesteryl BODIPY-mediated optical techniques	[81]
		5-HT-Fe ₃ O ₄ -Cy7 nanoparticles (SHFeC NPs)	20.97 nm ± 2.23 nm (TEM) 50.27 nm ± 18.96 nm (DLS)	5-hydroxytryptamine (5-HT) target active MPO	ApoE ^{-/-} mice	I. Iron oxide nanoparticles-mediated magnetic particle imaging, II. Cy7-mediated FL imaging, III. CTA for anatomical information	[191]
		Simvastatin/EGCG-coated liposomes (SE LNPs)	20 nm (TEM), 208.90 nm ± 3.99 nm (DLS)	Passive target	ApoE ^{-/-} mice	Remove ROS, inhibit apoptosis, induce M2 macrophage polarization, decrease inflammation cytokines	[203]
Therapy	Drug delivery	Simvastatin-loaded nanoliposomes	106.8 nm ± 22.5 nm (DLS)	Passive target	/	Anti-inflammatory and promote cholesterol efflux	[204]
		GW3965-loaded Lyp-1 liposomes	77.5 nm ± 4.0 nm (DLS)	The cyclic peptide Lyp-1 target to gC1q receptor (p32) on foam cell	LDLr ^{-/-} mice	GW3965 activate LXR on foam cell, improve the induction of ABCA1/ABCG1, and promote the excess cholesterol efflux	[205]
		NLRP3 siRNA-loaded VCAM-1 binding peptide targeting cationic liposomes (siRNA PCLs).	138 nm ± 40 nm (DLS)	VCAM-1-binding peptide target VCAM-1 on endothelial cells.	ApoE ^{-/-} mice	Inhibit the formation of NLRP3 inflammasome, thereby inhibit subsequent inflammatory reactions	[206a]

(Continued)

Table 2. (Continued)

Application method	Modality	Nanomaterials	Size	Targeting strategy	Animal models	Biomedical applications and mechanisms	Refs.
		PPAR γ agonist of pioglitazone (PIO)-loaded, PtdSer and DSPE-PEG2000-cRCDFK modified liposome (AP-Lipo)	About 120 nm	cRCDFK peptide target to $\alpha v \beta 3$ integrin on endothelial cells.	ApoE $^{-/-}$ mice	Decrease M1 macrophages, increase M2 macrophages, secrete anti-inflammation cytokines	[207]
		Rapamycin (RAP)-loaded, platelets membrane-coated nanoparticles (RAP-PNP)	145.7 nm \pm 6.7 nm	Congenital adhesion of platelets to damaged vascular endothelium	ApoE $^{-/-}$ mice	Anti-inflammatory, reduce plaque burden	[208]
		Rapamycin (RAP)-loaded hybrid platelets membrane biomimetic liposomes	About 90 nm (TEM and DLS)	Congenital adhesion of platelets to damaged vascular endothelium	ApoE $^{-/-}$ mice	Anti-inflammatory, reduce plaque burden	[209]
		SHPTi-loaded, macrophage membrane-coated biomimetic nanoparticles	199.1 nm (DLS)	The inherent protein on macrophage membrane ensures the actively chemotactic towards the inflammatory lesion site	ApoE $^{-/-}$ mice	SHPTi block CD47-SIRP α signaling pathway, enhance efferocytosis, stabilize atherosclerosis	[211]
		Colchicine-loaded, modified macrophage-membrane (MMM)-coated PLGA nanoparticles	202.02 nm	Integrin $\alpha 4 \beta 1$ target to vascular cell adhesion protein 1 (VCAM-1) on vascular endothelial cells	ApoE $^{-/-}$ mice	Strongly anti-inflammatory and stable vulnerable plaque	[212]
		Simvastatin acid (SA)-loaded dendrimer nanoparticles adsorbed toRBCs (SA PAM@RBCs)	About 100 nm (TEM)	I) Shear stress separate nanoparticles from RBCs II) ROS promotes SA PAM to release simvastatin acid	ApoE $^{-/-}$ mice	Eliminate hydrogen peroxide, reduce lipid content, and reduce plaque area	[213]
		Quercetin (QT)-loaded macrophage-liposome conjugate (MP-QT-NP)	105 nm (DLS)	The inherent chemotactic ability of macrophage towards the inflammatory lesion site	ApoE $^{-/-}$ mice	I. β -CD dissolve plaque cholesterol, II. quercetin (QT) remove active oxygen, III. inhibit inflammation, promote polarization of M1 to M2 macrophages	[214]
		PEDE-loaded, cRCDFK-modified PEG-PCL (PEDE RNP)	148.2 nm \pm 68.7 nm (DLS)	cRCDFK peptide target to $\alpha v \beta 3$ integrin on endothelial cells.	ApoE $^{-/-}$ mice	Inhibit angiogenesis, stabilize plaque, and prevent plaque rupture	[215]
		ROS-responsive simvastatin nanoprodrug combined ticagrelor-loaded drug delivery system (TPTS/C/T)	189 nm (DLS)	ROS responsive and fibronectin-targeted	ApoE $^{-/-}$ mice	Anti-inflammatory and anti-oxidant stress, inhibit macrophage proliferation	[216a]

(Continued)

Table 2. (Continued)

Application method	Modality	Nanomaterials	Size	Targeting strategy	Animal models	Biomedical applications and mechanisms	Refs.
Phototherapy		Naringenin (Nrg)-loaded, folic acid-coated lipid-polymer nanoparticle (FA-LNPs/Nrg)	128.2 nm \pm 5.8nm(DLS)	Folic acid mediated stride over the intestinal mucosal-epithelial barrier and target to folate receptor β on M1 macrophages	ApoE $^{-/-}$ mice	Anti-inflammatory, reduce the plaque burden	[217]
		Vascular endothelial growth factor /paclitaxel-loaded porous micro/nanomotor	Micron level	Anti-VCAM-1 antibody target VCAM-1 on endothelial cells	ApoE $^{-/-}$ mice	Release VEGF and paclitaxel under near-infrared light excitation, Promote endothelial proliferation, anti-inflammatory	[218a]
		Anti-interleukin-1 β (anti-IL-1 β)-loaded mesoporous silica nanoparticles MSNs @ anti-IL-1 β	183.29 nm \pm 17.16 nm	Passive target	ApoE $^{-/-}$ mice	Protect vascular endothelial cells, inhibit VSMC proliferation and phenotype transformation, and improve local microenvironment.	[219]
		Curcumin-loaded, HA-coated mesoporous MnO ₂ nanoparticles	About 200 nm (TEM)	Hyaluronic acid (oHA) target CD44 on macrophage	ApoE $^{-/-}$ mice	Promote M2 polarization, restore lipid efflux and remove lipids	[220]
		Rapamycin-loaded UiO-66-NH-FAM-IL-1Ra (RUF)	About 100 nm	IL-1Ra target macrophage	ApoE $^{-/-}$ mice	Promote M2 polarization, induce autophagy, anti-inflammatory and antioxidant stress	[221]
		Mesoporous-silica-coated upconversion fluorescent nanoparticles encapsulating chlorin e6 (UCNPs-Ce6)	/	Passive target	/	Induce macrophage apoptosis by mitochondrial caspase pathway	[222]
		Ultrasmall CuCo ₂ S ₄ Nanocrystals	14 nm(TEM)	Passive target	ApoE $^{-/-}$ mice	Photothermal ablate inflammatory macrophages	[227]
		CS-CNCS@Ce6/DS	204.5 nm \pm 21.9nm(DLS)	Dextran sulfates target the type A scavenger receptor (SR-A)	ApoE $^{-/-}$ mice	Ablate Activated Macrophages	[112]
		PM-PAAO-UCNPs	Around 120 nm (DLS)	Platelet membrane target macrophage-derived foam cells	ApoE $^{-/-}$ mice	Reduce macrophage-derived foam cells	[226]
		MoO ₃ nanoclusters	Around 40 nm (TEM), around 70 nm(DLS)	Platelet membrane target macrophage-derived foam cells	ApoE $^{-/-}$ mice	Ablate inflammatory macrophages	[228]
		Black TiO ₂ -hyaluronan-porphine (bTiO ₂ -HA-p)	211 nm \pm 2 nm(DLS)	HA target CD44 on macrophages	/	Mildly induce foam cell apoptosis, promote cholesterol efflux, and reduce lipid intake	[232]
							(Continued)

Table 2. (Continued)

Application method	Modality	Nanomaterials	Size	Targeting strategy	Animal models	Biomedical applications and mechanisms	Refs.
SDT		5-aminolevulinic acid (ALA)	/	Passive target	Adult male New Zealand white rabbits	Macrophage apoptosis and apoptotic cell clearance	[234]
		5-aminolevulinic acid (ALA)	/	Passive target	New Zealand white rabbits and ApoE ^{-/-} mice	Foam cell apoptosis and efferocytosis, cholesterol efflux	[235a]
		Sinoporphyrin sodium (DVDMS)	/	Passive target	New Zealand white rabbits and ApoE ^{-/-} mice	Macrophage apoptosis-induced endothelial cell apoptosis	[236]
		Sinoporphyrin sodium (DVDMS)	/	Passive target	New Zealand white rabbits and ApoE ^{-/-} mice	Reduce iron retention in macrophages, inhibit the ferritin expression, treat intraplaque hemorrhage (IPH)	[237]
Nanoimmunotherapy		TRAF6i-HDL	20.7 nm ± 3.0 nm	HDL target scavenger receptor type B-1 (SR-B1) on macrophages	ApoE ^{-/-} mice	Block the interaction between CD40 and tumor necrosis factor receptor-associated factor 6 (TRAF6); reduce monocyte migration	[243]
		PEI-Au nanoparticles/shSiglec-1/PEI-ASA	92 nm(DLS)	Passive Targeting	ApoE ^{-/-} mice	I. shSiglec-1 blocks the recognition and interaction between macrophages and CD8 ⁺ T cells and NKT cells II. ASA promotes cholesterol efflux, inhibits Th17 cells differentiation, and remodels immune microenvironment	[244]
Gas therapy		Simvastatin-loaded high-density lipoprotein (S-HDL) nanoparticles	23.6 nm ± 3.7 nm	HDL target scavenger receptor type B-1 (SR-B1) on macrophages	ApoE ^{-/-} mice	Clear excessive inflammatory cells, reduce plaque burden	[245]
		NO-delivering HDL-like particles (SNO HDL NPs)	13.12 nm ± 0.65 nm (DLS)	HDL target scavenger receptor type B-1 (SR-B1) on macrophages and VSMCs	ApoE ^{-/-} mice	Improve macrophage efflux cholesterol, inhibit aortic SMC migration, reduce inflammation.	[247]
		Dendrimer nanopatform carrying 18 NO release units	/	/	/	Regulate NO release, maintain endothelial stability	[248]
		L-arginine (LA) and lovastatin (LV)-coated PLGA nanoparticle	114.0 nm ± 1.65 nm (DLS)	Passive target	ApoE ^{-/-} mice	Improve the expression of eNOS and p-eNOS, increase NO generation; deliver lovastatin	[249a]
		PLT membrane coated l-arginine and γ -Fe ₂ O ₃ magnetic nanoparticles (PAMNs)	215.50 nm ± 8.05 nm (DLS)	Platelets membrane target damaged blood vessel	Ischemic stroke mice	Increase NO generation, cause vasodilation, disrupt the local PLT aggregation	[249b]

(Continued)

Table 2. (Continued)

Application method	Modality	Nanomaterials	Size	Targeting strategy	Animal models	Biomedical applications and mechanisms	Refs.
Theranostic	MR imaging-based	Lipophilic nanomotor PMA-TPP/PTX-loaded with drug PTX and lipophilic triphenylphosphine (TPP)	About 200 nm (DLS)	Balloons located	High-fat-fed rabbits	I. NO nanomotor enhances drug penetration and retention, improve endothelial function, reduce ROS II. PTX inhibits intimal hyperplasia	[249c]
		Palladium hydride nanopocket cubes (PdH _{0.12} NPCs)	75.38 nm (DLS)	Passive target	ApoE ^{-/-} mice	I. Hydrogen promotes cholesterol transport II. Pd reduces ROS and ox-LDL generation	[251]
		Tetrapod needle-like PdH nanoparticle delivered by living macrophages	Tetrapod: 100 nm the edge length: 60 nm	Living macrophages target to the inflammatory site	ApoE ^{-/-} mice	I. Hydrogen reduces inflammation II. palladium removes ROS III. spike-like structure promotes macrophage autophagy	[252]
		Trehalose-L arginine-phosphatidylserine (TAP) carrier-free nanomotor	Around 200 (TEM)	Phosphatidylserine (PS) target macrophages in the AS	ApoE ^{-/-} mice	I. L arginine produces NO drive into plaque II. trehalose promotes macrophages autophagy	[250]
		Rosuvastatin/Gd-coated, HA-coated hybrid liposomal cerasomes (CCs) named as (HA-CC-RST)	178 nm (DLS)	Hyaluronic acid (HA) target CD44 on macrophages	ApoE ^{-/-} mice	I. Rosuvastatin-mediated drug delivery therapy II. Gd mediated MR imaging	[274a]
		Glucagon-like peptide-1 receptor (GLP-1R) agonists/gadolinium chelates-coated nanoparticles (GlpNP)	53.7 nm	Passive target	ApoE ^{-/-} mice	I. GLP-1R promotes cholesterol efflux and stable plaque II. gadolinium chelates-mediated MR imaging	[274b]
		Mito-magneto (MM)-loaded, stearyl-TPP/stearyl mannose-coated HDL-mimicking nanoparticles	140–180 nm (DLS)	I) Mannose target to mannose receptors (MMR) on macrophages II) stearyl-TPP target mitochondrion	BALB/c Albino mice	I. HDL-mimicking-mediated reverse cholesterol transport (RCT) II. mito-magneto (based on iron oxide)-mediated MR imaging	[275]
							(Continued)

Table 2. (Continued)

Application method	Modality	Nanomaterials	Size	Targeting strategy	Animal models	Biomedical applications and mechanisms	Refs.
FL imaging-based		Mannose-coated; lobe-glucitazone and Cy7-loaded (MMR-Lobe-Cy)	207.2 nm ± 34.79 nm (DLS)	Mannose target to mannose receptors (MMR) on lipid-overloaded macrophages	Rabbits	I. Lobe-glucitazone-mediated rapidly anti-inflammatory II. Cy7-mediated OCT-NIR imaging	[276b]
		Prednisolone (Pred)-fluorophore (TP)-loaded PMPC-PMEMA (PMM) nanoparticles (TPP@PMM)	57.5 nm ± 0.15 nm (DLS)	ROS responsive structures	ApoE ^{-/-} mice	I. ROS-responsive cleavage of the linker moiety releases prednisolone, which inhibits foam cell formation and reduces lipid uptake, leading to anti-inflammatory effects. II. AIE fluorophore-mediated two-photon AIE bioimaging	[276c]
		(Ru(bpy) ₃ @SiO ₂ -mSiO ₂ @SRT1720@AntiCD36	225.3 nm (DLS)	AntiCD36 target CD36 on macrophage	ApoE ^{-/-} mice	I. SRT1720 (SIRT1 activator) reduces the expression of proinflammatory factors, the number of foam cells, and promotes the reverse transport of cholesterol, Ru(bpy) ₃ Cl ₂ -mediated FL imaging	[277]
		Upconversion nanoparticle (UCNP) and gold nanoparticles (AuNPs)-coated chlorophyll-modified liposomal	150-250 nm	ROS responsive structures	/	I. Light excites chlorophyll, electrons are transferred to gold, and electrons on gold react with H ⁺ to generate hydrogen to remove ROS. II. Förster resonance energy transfer (FRET)-associated FL imaging reflects ROS levels.	[278]
		Hexyl 5-aminolevulinatide hydrochloride (HAL)-loaded M2 macrophage-derived exosomes (M2 Exo)	About 190 nm	M2 Exo have inherent inflammation tropism	ApoE ^{-/-} mice	I. M2 Exo carries anti-inflammatory factors that inhibits inflammation, the catabolic metabolites CO and bilirubin of HAL have anti-inflammatory effects. II. The metabolic intermediate protoporphyrin IX (PpIX) of HAL has red fluorescence.	[279]

(Continued)

Table 2. (Continued)

Application method	Modality	Nanomaterials	Size	Targeting strategy	Animal models	Biomedical applications and mechanisms	Refs.
US and MR imaging-based		Fe ₃ O ₄ (F)/ perfluorohexane (P)/DiR (D)-loaded and dextran sulfate (D)-coated PLGA-PEG-PLGA nanoparticles (FPD@CD)	255.9 nm ± 2.94 nm (DLS)	Dextran sulfate (DS) target SR-A on macrophage	APOE ^{-/-} mice	I. Perfluorohexane (PFH) under low-intensity focused ultrasound (LIFU) promotes macrophage apoptosis. II. Fe ₃ O ₄ -mediated MR imaging, perfluorohexane-mediated ultrasound, and DiR-mediated near-infrared fluorescence (NIRF) imaging	[280]
						I. HMME-mediated SDT induces neovessel endothelial cells apoptosis and improves hypoxia II. MnFe ₂ O ₄ -mediated MR imaging, PFP mediated US and PA imaging	
US, PA, and MR imaging-based		PFP-HMME @PLGA/MnFe ₂ O ₄ -ramucirumab nanoparticles (PHPMR NPs)	347.4 nm (DLS)	Anti-VEGFR-2 antibody target VEGF on endothelial cells	Plaque-bearing rabbits	I. HMME-mediated SDT induces neovessel endothelial cells apoptosis and improves hypoxia II. MnFe ₂ O ₄ -mediated MR imaging, PFP mediated US and PA imaging	[98]
						I. Hyaluronan-mediated anti-inflammation, ⁸⁹ Zr-mediated PET imaging II. Hydrogen peroxide reacts with boronic ester in BM to generate an anti-inflammatory drug 4-hydroxybenzyl alcohol (HBA).	
US, FL, and PA imaging-based		⁸⁹ Zr-labeled hyaluronan nanoparticles (⁸⁹ Zr-HA-NPs) Indocyanine green-loaded boronated maltodextrin (ICG-BM) nanoparticles	32 nm ± 0.5 nm (AFM) About 500 nm (DLS and TEM)	Hyaluronic acid (HA) target CD44 on macrophage Passive target	ApoE ^{-/-} mice and New Zealand White rabbits Ischemic mice	I. Hydrogen peroxide reacts with boronic ester in BM to generate an anti-inflammatory drug 4-hydroxybenzyl alcohol (HBA). II. Hydrogen peroxide degrades boronic ester and generates carbon dioxide bubbles to mediate US and PA imaging. III. Indocyanine green (ICG)-mediated FL and PA imaging	[297a] [297b]
						I. Au-mediated PTT ablation II. Au-mediated CT imaging	
CT imaging-based		Gold nanorods	About 68 nm × 15 nm	Passive target	ApoE ^{-/-} mice	I. Au-mediated PTT ablation II. Au-mediated CT imaging	[298]

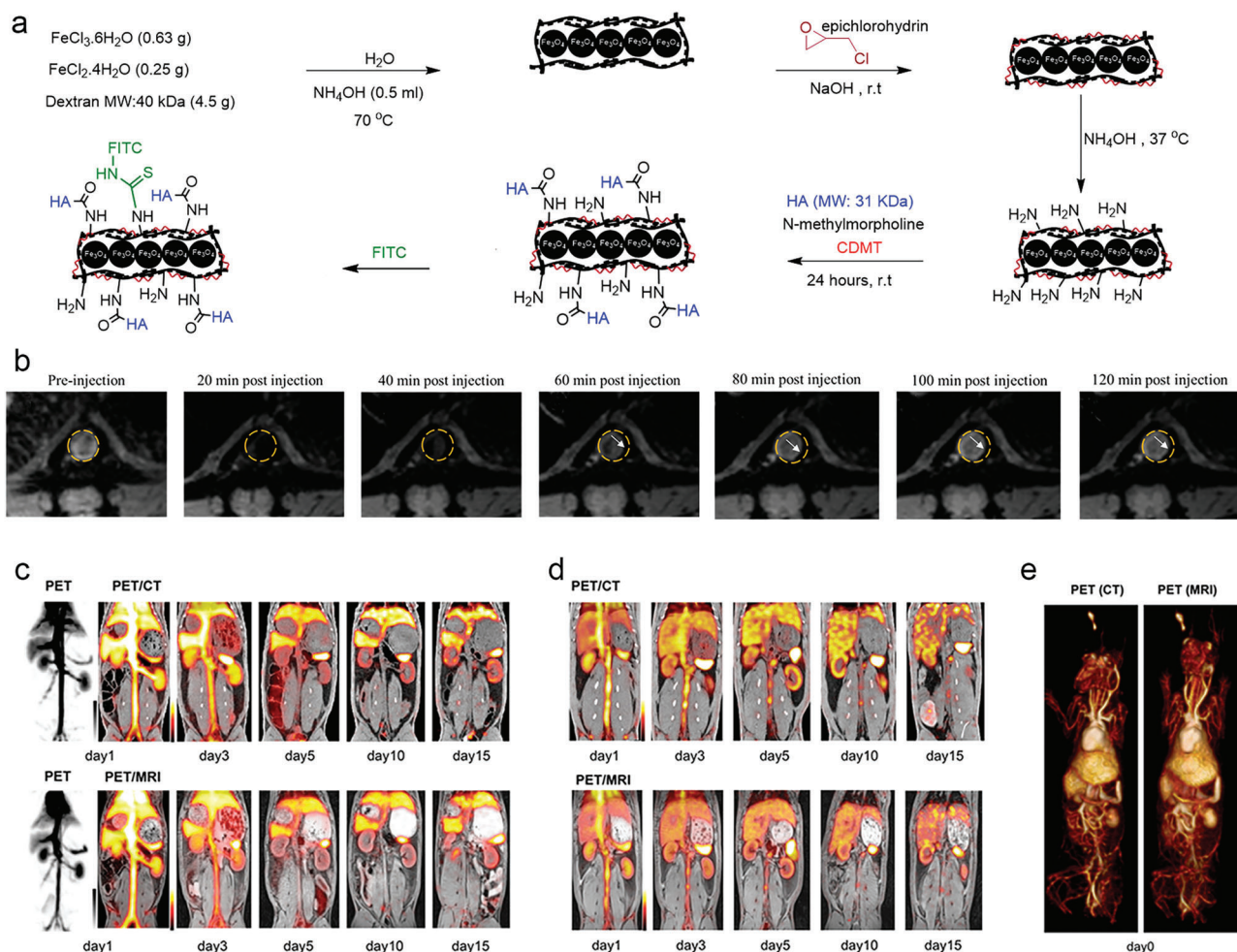


Figure 4. a) Schematic route illustration of the synthetic process of hyaluronan-conjugated HA-NWs. b) T2-weighted MR images of the aorta at different time points after injection of HA-NWs (8 mg Fe per kg body weight). a, b) Reproduced with permission.^[144] Copyright 2018, American Chemical Society. c) Biodistribution of ⁸⁹Zr-liposomes presented by PET and PET/CT (the upper chart) as well as PET and PET/MR imaging (the lower chart) in healthy rabbits at different time points after intravenous injection. d) Biodistribution of ⁸⁹Zr-liposomes presented by PET/CT (the upper) and PET/MR imaging (the lower) in atherosclerosis rabbits at different time points after intravenous injection. e) MIP from (c) PET/CT and (d) PET/MR imaging on day 0 after intravenous injection. c–e) Reproduced with permission.^[161] Copyright 2020, American Chemical Society.

report, biomimetic nanomaterials were introduced to further improve the dispersibility and biosafety of SPIONs owing their live cell origin and the mutual recognition of cell surface markers.^[143] In addition, it reported that engineering the morphology of nanomaterials is significant to its targeting function. Hossaini Nasr and co-workers constructed hyaluronan-conjugated iron oxide nanoworms (named as HA-NWs) with elongated shapes through the coprecipitation method to figure out the influence of the morphology of nanomaterials to MR imaging (Figure 4a). Both in vitro and in vivo experiments suggested the higher uptake and lower inflammatory response of HA-NWs than that of HA-SPIONs. Besides, a series of T2 weighted MR images were presented via serial MR imaging, indicating the signal intensity of plaque reduced to 20% after 20 min compared with pre-injection and kept its level until 120 min after injection (Figure 4b).^[144] Compared to the detection threshold of Gd-based NPs, SPIONs owed better imaging sensitivity and biosafety with favorable magnetic property.^[145]

4.2. Computed Tomography Imaging

CT imaging sketches a complete picture of the cardiovascular system at high speed and does not suffer from cardiac and respiratory artifacts. Additionally, the calcified component inherent in the plaque will appear as high-density in CT images. Nevertheless, it is limited by ionization radiation and is difficult to detect the early lesions at the cellular level. Based on the photoelectric effect and the Compton effect, CT contrast agents commonly are elements with a large atomic number such as iodine (I), gold (Au), bromine (Br), barium (Ba), bismuth (Bi), tantalum (Ta), while most research on CT nanotracker in atherosclerosis pays attention to iodine and gold.

After intravenous injection, iodine will be rapidly cleared by the kidneys, resulting in a limited imaging time window. Therefore, higher dose needs to be injected in order to realize the desired effect. However, iodine is toxic when in direct contact with blood or tissue components. To address it, nanoemulsions,^[146]

liposomal,^[147] dendrimers,^[148] polymeric NPs were prepared to weaken the direct contact between iodine and biological components.^[149] Extraordinarily, Hyafil et al. designed an iodinated nanotracer for CT imaging called N1177 to perform inflammatory macrophages imaging, which consists of ethyl-3,5-bis(acetylamino)-2,4,6-triiodobenzoate and surfactant.^[150] In another research, N1177 was used to identify ruptured plaques.^[151] The median CT value of ruptured plaques was 74 HU, which was approximately twice as high as that of unruptured plaques (32 HU).

AuNPs have the advantages of controlled shape and size, high biocompatibility, simple surface modification, and diversified functions.^[152] According to the thrombosis at the local site of atherosclerotic plaque and thromboembolism at distant sites due to plaque rupture, fibrin-targeting peptides-loaded AuNPs were developed to achieve the visualization of thrombus composition and the assessment of thrombolytic effect with tissue plasminogen activator via CT imaging.^[153] Besides, as monocytes play an important role in atherosclerotic pathology, Chhour et al. first used AuNPs-labeled monocytes for tracing their migration and recruitment from blood to atherosclerotic plaques by non-invasive CT imaging.^[154] It examined the effect of surface modification of AuNPs on monocytes with different ligands and demonstrated that AuNPs with small hydrodynamic diameters and negative zeta potentials were more accessible to monocytes. In another research, AuNPs were utilized in combination with photon-counting CT k-edge imaging,^[155] a technique capable of analyzing the photon energy, reclassifying it to fulfill high spatial resolution imaging, and preventing confusion from calcifications in conventional CT images.^[156] The researchers adopted an iodinated contrast agent to reflect the lumen structure and AuNPs to indicate the macrophage burden in the vessel wall to simultaneously achieve anatomic and molecular CT imaging.

4.3. Radionuclide Imaging

Radionuclides or radionuclide labeled substances are introduced into the body to participate in tissue metabolism, emitting nuclear rays that can penetrate tissues and be detected noninvasively by radionuclide imaging from the body surface to reflect specific pathophysiological processes. The radionuclide imaging modalities can be divided into two types: positron emission tomography (PET) and single-photon emission CT (SPECT) depending on the type of radionuclide. Radionuclide imaging allows extremely high detection sensitivity for metabolism, which belongs to functional imaging. However, the disadvantages include low anatomical resolution and the interference from surrounding tissues, hence it is generally applied in fusion with MR or CT imaging to improve anatomical background.

As for PET, NaF could bind to hydroxyapatite in calcification,^[157] and a previous study verified the significant accumulation of ¹⁸F-NaF in plaque calcification using Yucatan minipigs as a model.^[158] Their results confirmed that ¹⁸F-NaF-mediated PET imaging is a valid detection tool for identifying atherosclerotic calcification. Besides, radionuclides can directly label the corresponding antibodies, peptides, or ligands for selective tracing of a particular pathological process with high accuracy.^[159] What's more, metal positronium nuclides

such as ⁸⁹Zr, ⁶⁴Cu, ^{99m}Tc, ⁶⁸Ga, etc. with longer half-life time have gradually attracted more attention in recent years.^[160] In a report, Lobatto et al. structured ⁸⁹Zr radiolabeled liposomes chelated with deferoxamine B, which provided new perspectives related to synergistic drug delivery therapy.^[161] It was observed that the blood pool and vascular-rich organs were first filled, and over time, the liposomes in the blood pool were progressively cleared and the mononuclear phagocyte system was progressively brightened in healthy rabbits (Figure 4c). Then ⁸⁹Zr-labeled liposomes were injected into model rabbits, and when the contrast agent in the normal blood pool subsided, patchy atherosclerosis plaques could be clearly shown on PET/CT (Figure 4d). PET maximum intensity projections (MIP) offered a more stereoscopic view of the biodistribution of the ⁸⁹Zr-labeled liposomes (Figure 4e). As for ⁶⁴Cu, here is another experimentation, Detering and co-workers constructed CCR5-targeted amphiphilic comb copolymers, denoted as D-Ala-peptide T-amide (DAPTA-Comb), which were synthesized and matched with ⁶⁴Cu as radiolabel with favorable half-life.^[162] By changing the ratio of various copolymers, the physicochemical state and surface function were precisely controlled.

Regarding SPECT, Liang and co-workers conducted an intriguing study in which they isolated and purified natural human H-ferritin nanocages from *Escherichia coli*.^[163] Chelation of ^{99m}Tc with H-ferritin in the presence of N-hydroxysuccinimide ester MAG3 conferred H-ferritin the ability to be imaged via SPECT/CT for the quantitative analysis of vulnerable plaque. Signal intensity analysis was in good agreement with the plaque area revealed by oil red O staining of the isolated arteries. Gamma imaging of the isolated arteries was performed to further verify the presence of plaque much more clearly. In addition, the high contrast and low background signal of ^{99m}Tc-ferritin allowed them not only to indicate the progression of atherosclerotic plaques but also to be employed as a sensitive tool to monitor the anti-inflammatory effects.

4.4. Fluorescence Imaging

FL imaging, an emergent imaging technique for noninvasive visualization, is used for bioanalysis, disease monitoring and drug distribution thanks to its high sensitivity, low cost, and rapid acquisition and processing of images. It relies on optical materials with light absorption capabilities, especially NIR fluorescent materials with deeper imaging capabilities and higher signal-to-noise ratio. Organic small molecule fluorescent dyes (within a few kDa) such as rhodamine, coumarin,^[164] cyanine,^[165] naphthimide,^[166] BODIPY,^[167] pyrene,^[168] indocyanine green (ICG),^[169] etc. with superior optical properties are already used and make a contribution to multimodality imaging. Additionally, the development of nanomaterials offers new possibilities for FL detection of atherosclerosis. At present, there are three feasible approaches including (I) autofluorescence of tissues, (II) nanomodification of fluorescent dyes, or (III) the construction of fluorescent nanoprobe.

First, the autofluorescence properties of endogenous complexes such as some lipid components (e.g., insoluble lipid or ceroid), ox-LDL, collagen, heme, and its metabolites bilirubin can be employed to reflect compositional changes at different stages

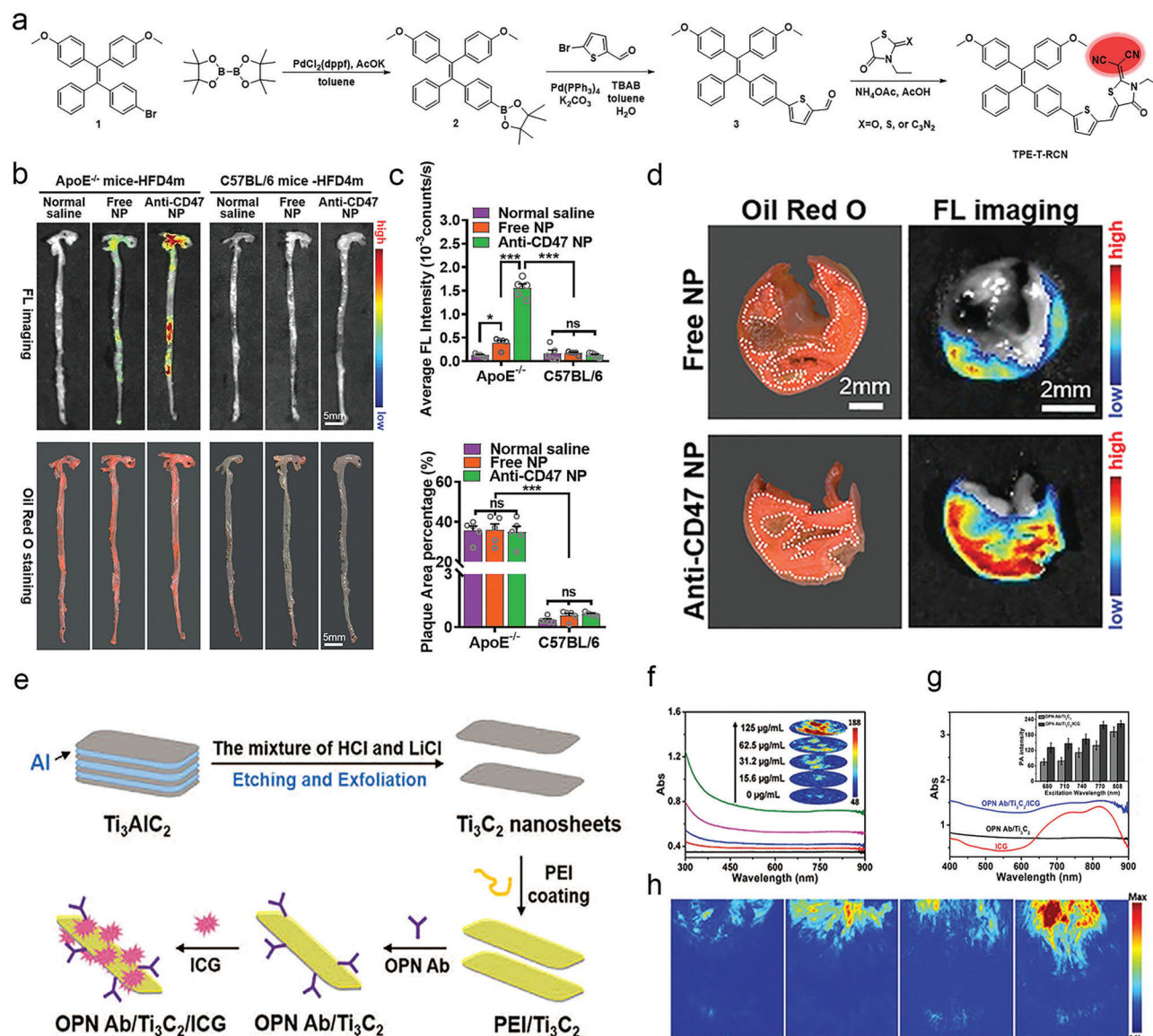


Figure 5. a) Preparation route of TPE-T-RCN. b) Typical fluorescence images and Oil Red O staining images of the isolated aorta from HFD-fed 4 months ApoE^{-/-} mice and HFD-fed 4 months C57BL/6 mice under different treatments (intravenous inject normal saline, free NP, anti-CD47 NP). c) Average fluorescence intensity value (upper) and the percentage of plaque area (lower) of the isolated aortas in every group. *P < 0.05, ***P < 0.001 and ns: not significant. d) Representative Oil Red O staining images and fluorescence images of human fresh carotid atherectomy specimens after different treatments (incubate with free NPs or anti-CD47 NPs for 2 h). a–d) Reproduced with permission.^[173] Copyright 2022, Wiley-VCH. e) Synthetic route to OPN Ab/Ti₃C₂/ICG. f) UV-vis absorption spectra and PA images under excitation wavelengths of 808 nm of Ti₃C₂ nanosheet (insert picture) with different concentrations. g) Absorption spectra before and after loading ICG as well as the distinguishable PA intensity of OPN Ab/Ti₃C₂ and OPN Ab/Ti₃C₂/ICG at different excitation wavelengths (inset picture). h) In vivo PA imaging of mice. Mice were divided into four groups: I) atherosclerotic mice without any treatment, II) atherosclerotic mice i.v. with Ti₃C₂/ICG, III) healthy mice i.v. with OPN Ab/Ti₃C₂/ICG, IV) atherosclerosis mice i.v. with OPN Ab/Ti₃C₂/ICG. e–h) Reproduced with permission.^[120] Copyright 2020, Wiley-VCH.

of atherosclerosis.^[170] Besides, functional group substitutions, surface modification, encapsulation, or optimization of ligands are able to retain intrinsic properties of FL agents while also improving their bio-imaging applications.^[171] Recently, Narita et al. synthesized a cleavable peptide-ICG2 and encapsulated it into PS-loaded liposomes, which actively drive them to macrophages in embolism-vulnerable plaques.^[172] These nanotracers undergone FL quenching at the existence of peptide linker in nor-

mal conditions. After taken up by macrophages, lysosomal enzyme and cathepsin B cleaved the peptide linker and terminated FL quenching, as a result, the fluorescence signaling was detectable in the deeper tissue. Another attractive research reported a dicyanomethylene-substituted rhodamine derivative (TPE-T-RCN), an aggregation-induced emission (AIE) nanoluminogen to perform atherosclerotic FL imaging (Figure 5).^[173] 3D geometric structures confirmed that it was a D- π -A type AIE lumino-

gen with tetraphenylethene (TPE) as the electron donor group, dicyanomethylene unit (CN) as the electron acceptor group, and thiophene (T) as the π -conjugate to achieve the optimal photoluminescence quantum yield. TPE-T-RCN was encapsulated with DSPE-PEG and coupled with CD47 (a “do not eat me” signal) antibody to form the final FL nanoprobe. After 12 h injection of FL nanoprobe, the aorta of the experimental and control mice was excised intactly and performed by FL imaging and oil red O staining. The plaque areas in the aorta of the atherosclerotic mice were almost identical, whereas the imaging capabilities were totally distinct. What is more, there was a significant correspondence between FL signal and plaque site in anti-CD47 NPs treated group (Figure 5b-d). Significant accumulation of FL nanoprobe at the plaque site was observed with immunofluorescence imaging, which was hardly visible in the control group.

Additionally, nanomaterials with applications in FL imaging include QDs, AuNPs, carbon-based nanomaterials, upconversion nanoparticles (UCNPs), etc.^[174] Wherein, QDs perhaps are the most critical nanomaterials, which possess long FL lifetime.^[175] PbS/CdS/ZnS QDs were introduced to identify the ischemic phase from the inflammatory phase due to their unique FL brightness and thermal sensitivity.^[176] Besides, Deng et al. first constructed dextran-mimetic and HgCdSe-based QD probes (Q-Dex) to point the atherosclerotic area.^[177]

4.5. Photoacoustic Imaging

PA imaging combines the high resolution of optical imaging with the deep penetration of acoustic imaging. Principally, thermal expansion caused by absorbers under laser light generates acoustic waves. PA imaging can detect acoustic waves in tissue at a depth of several centimeters and overcome the “soft limits” of optical depth.^[178] Research in PA imaging focus on pre-clinical study and aims to optimize imaging systems as well as algorithms and explores more suitable absorbers. Intravascular photoacoustic (IVPA), a tool for plaque components imaging, has been used to identify endogenous absorbers such as lipid, haemoglobin and collagen. In particular, the chronic deposition of lipid with its characteristic absorption peaks at 1210 nm in atherosclerotic plaques could be selected as a biomarker to indicate the accumulation of foam cells and the size of lipid core within plaque.^[179] Not only lipid core size, Cao et al. further analyze lipid composition to achieve tissue-type characterization via IVPA.^[180]

A safer option is screening the lesion from the body surface directly, but exogenous absorbers must be introduced to solve the weakened penetration problem caused by increased detection distance. For displaying inflammatory cells within the plaque, Ge et al. constructed a PA contrast agent based on NIR fluorescence probe ICG and osteopontin antibody (OPN Ab) co-loaded Ti₃C₂ nanosheet (OPN Ab/Ti₃C₂/ICG) to target inflammatory foam cells and distinguish the vulnerable atherosclerosis plaque (Figure 5e).^[120] The nanosheet had obvious absorption at 808 nm in a concentration-dependent manner, and the loading of ICG further enhanced its PA performance (Figure 5f,g). In vivo experiments demonstrated that OPN Ab/Ti₃C₂/ICG nanosheet could

develop as a promising candidate which particularly accumulated in atherosclerotic plaque and achieved noninvasive PA imaging at the molecule level (Figure 5h). In previous research, Smith et al. found that single-walled carbon nanotubes (SWNTs) could specifically target the Ly-6C^{hi} monocytes subpopulation in circulating blood cells.^[181] Inspired by it, PEG-coated SWNTs with long circulation times and favorable photothermal conversion efficiency were presented by the same group to detect the inflamed arterial plaque.^[111] Similar to this idea, Xie et al. investigated the PA performance of PBD, a semiconductor nanomaterial with absorbance in the NIR II, fulfilling a huge hint of resolution.^[182] In this report, PEG was selected to improve the water solubility of PBD while acting as a bridge to CD36 antibodies, facilitating specific PA imaging of foam cells. In addition, a novel ratiometric semiconducting polymer nanoparticle (RSPN) was proposed to reflect the oxidative stress level with an internal PA reference in ApoE^{-/-} mice complicated with pneumonia from normal mice, which revealed significant potential for detecting vulnerable plaque via PA imaging.^[183]

4.6. Optical Coherence Tomography (OCT)

OCT detects the reflection, scattering, and other signals of biological tissues by utilizing their light transmission properties, which are then converted into electrical signals and reconstructed into images through computer analysis. However, due to the inherent limitations of light penetration, it is difficult to detect atherosclerotic plaques from the body surface, making endovascular imaging necessary. Intravascular OCT is a multifunctional and high-resolution clinical tool that helps identify the morphology of blood vessels and plaques, their internal components, and plaque vulnerability, and can contribute to investigating the mechanisms of plaque erosion and healing.^[184] However, as the probe is placed in the bloodstream, the image is distorted by red blood cells, larger plaques, and thrombotic lesions.

Optical nanoprobe that target specific molecules expressed during different stages of plaque development can be beneficial in improving the detection sensitivity of intravascular OCT. By attaching to these specific molecules, these probes can provide contrast and enhance the visualization of plaque components during imaging. There have not been many studies on nanomaterials in this area to date. Au nanoparticles are crucial in providing OCT signals due to their strong backscattering cross-section.^[185] Gold nanoshells, excited by OCT at 1300 nm, produced clear images of individual cells, which had been validated in both suspended and adherent cells.^[186] Another study involved infrared emitting quantum dots (IR-QDs), which also produced sufficient backscattering when excited by a single-line laser OCT at 1300 nm. According to theoretical calculations, the scattering cross-section of a single IR-QD is nine orders of magnitude smaller than that of gold nanoshells, which may be due to their significant differences in volume. However, at equal mass concentrations, the OCT intensity of both was almost the same, and IR-QDs re-emitted light at 1600 nm, which could be used for additional FL imaging.^[187] From a clinical perspective, the next step is to give these nanomaterials targeting abilities so that specific component imaging of atherosclerosis can be unlocked.

4.7. Multimodal Imaging

The various single imaging methods have significantly contributed to the atherosclerotic diagnosis, nevertheless, their intrinsic limitations make it difficult to meet the requirements of resolution, sensitivity, and selectivity at the same time. Multimodal imaging permits us to compensate for shortcomings, achieve complementary strengths, and obtain much accurate information at the early diagnosis stage of the disease. Multimodal imaging, whether fusion imaging (one machine for multiple technologies) like PET/CT, SPECT/CT and PA imaging or the combined application of multiple imaging techniques, relies on imaging probes as vehicles. The small size, large specific surface area, high payload, and intelligent design of the multimodal imaging nanoprobe allow each probe to carry more substances and information for the detection by multimodal techniques.

Previously, zinc-doped ferrite nanocomplex was fabricated to improve the spatial resolution of MR imaging and achieve MR/CT bimodal imaging, which allowed stronger negative MR contrast and lower toxicity in comparison with commercial ferrite nanoparticles.^[188] For dual-mode imaging, although MR imaging has already provided high anatomical resolution, it still requires the assistance of a high-sensitivity device. Regarding PEG as a bridge, a near-infrared fluorochromes-carried and ligand-attached SPION was designed to target atherosclerotic activated platelets, which achieved the superimposition of two imaging elements.^[189] Similarly, Wu et al. prepared the mesoporous silica layer-coated, NIRF dye (IR820)-loaded and PP1 (a foamy macrophage-targeted peptide)-coupled SPION, noted as PP1-IO@MS-IR820 (PIMI), to perform MR/FL bimodal imaging.^[190]

As for multimodal imaging, to evaluate the inflow of immune cells, Senders et al. constructed a nanoprobe with bone marrow cell specificity to perform immunokinetic studies.^[81] They innovatively wrapped the perfluoro-crown ether core with the HDL derivative ApoA-1 and phospholipids, abbreviated as ¹⁹F-HDL, followed by loading ⁸⁹Zr and cholesteryl BODIPY to perform ¹⁹F MR imaging. The half-life time of ⁸⁹Zr is 78.4 h, only permitted high-sensitivity monitoring for 3 days in vivo, while the join of fluorine core allowed quantitative study for up to 28 d after a single injection via ¹⁹F MR imaging. Gamma imaging and optical techniques such as flow cytometry were performed additionally to study cell subpopulations ex vivo. Besides, ¹⁹F MR imaging and flow cytometry indicated that the intraplaque inflammatory cells were mainly Ly6C^{high} monocytes recruited from the bone marrow and spleen in the intermediate stage of atherosclerosis, whereas were mainly the local proliferation of macrophages in the advanced stage. Additionally, the novel multimodal imaging probe 5-HT-Fe₃O₄-Cy7 nanoparticles (5HFeC NPs) via FL/CT angiography/magnetic particle imaging (MPI) was constructed for the detection of excessive active MPO and inflammatory conditions within vulnerable plaque.^[191] Regarding SPIONs as the contrast agent, MPI (a novel tomographic method) greatly reduced the dose of SPIONs due to their high sensitivity. However, high sensitivity is often accompanied by the loss of spatial resolution, so CT angiography was selected as the contributor to provide anatomical information. What's more, the zero-signal attenuation of MPI compensated for the problem caused by the limited penetration depth of FL imaging.

4.8. Clinical Studies of Atherosclerosis Diagnosis in Nanomedicine

There are some reports on the clinical research of ultra-small superparamagnetic iron oxide (USPIO) in atherosclerosis. Initially, the first-generation FDA-approved USPIO contrast agent Ferumoxtran (Sinerem) was designed for lymph node and tumor imaging.^[192] Subsequently, researchers discovered signal loss in atherosclerotic plaques, suggesting its potential for atherosclerosis imaging and exploration.^[193] However, in 2010, its application was restricted due to liver function damage and was subsequently withdrawn from the market.

The second-generation USPIO contrast agent Ferumoxytol (Feraheme) was originally intended as an iron replacement therapy for treating iron deficiency anemia. Ferumoxytol consists of iron oxide nanoparticle core coated with carboxymethyl dextran.^[194] In atherosclerotic research, it gained attention due to its ability to accumulate in inflammatory tissue surrounding atherosclerotic plaques, possibly due to a specific mechanism related to plaque permeability.^[195] The optimal time for evaluating atherosclerosis was found to be 48 h after injection.^[196] Additionally, Ferumoxytol can be used as a non-invasive imaging method for diagnosing diseases related to coronary artery disease, vascular inflammation, and heart disease and peripheral artery disease (PAD).^[197]

Overall, for the diagnosis of atherosclerosis, MR imaging plays a crucial role, often utilizes iron oxide nanoparticles as a core and obtains certain results in clinical trials. CT imaging relies on elements with high atomic numbers, with gold nanoparticles as a typical representative, constructing different forms. FL imaging is diverse in design, but always centers around certain endogenous metabolites, various modified/unmodified small molecule fluorescent dyes, and materials platforms with fluorescent emission properties such as UCNP and quantum dots. Nuclear medicine imaging relies on labeled radioactive isotopes, while photoacoustic imaging depends on intrinsic absorption differences of biological components or material systems with absorption capacity in the NIR. It is noteworthy that US imaging is still a diagnostic system with a lot of exploration space in the nanomedicine field for atherosclerosis. The above-mentioned imaging methods have their own strengths and weaknesses, and sometimes it is difficult to fulfill synchronous improvement of sensitivity and resolution. Therefore, the multi-modal imaging mode for atherosclerosis has emerged to make up for the shortcomings of the single imaging methods and contributes to obtain more comprehensive and accurate information. The multimodal imaging modalities are constantly developing and innovating by preparing diverse multimodal nanoprobe. The targeting molecules and templates mentioned above also can be further designed for atherosclerotic treatment.

5. Therapy

The BMT for atherosclerosis includes lowering blood lipids, anti-hypertension, anti-thrombosis, and anti-platelet treatment, which needs to be taken for the whole life and may cause systemic side effects, such as liver and kidney damage. If the lesion is advanced and leads to severe vascular occlusion, surgical

intervention is required (e.g., stent implantation, intraluminal endarterectomy, or bypass surgery). Although the above methods have achieved certain outcomes in clinical practice, it is still urgent to develop new treatment strategies to optimize the existing treatment protocol. Nanotechnology-based therapeutic systems are used to finely regulate specific stages of atherosclerotic development. In this section, we mainly discuss the potential application of nanosystems in the improvement of atherosclerosis including drug delivery, phototherapy, SDT, immunotherapy, and gas therapy (Table 2).

5.1. Drug Delivery

To further reduce the systemic toxicity of drugs and increase their circulation time in the body, researchers innovatively introduce nanocarriers to specifically deliver drugs into the targeted lesions. Afterward, the research scope extended from traditional drugs to various small molecule regulators, proteins, cytokines, and gene components. Besides, nanocarriers have gradually expanded to liposomes,^[198] biomimetic nanomaterials,^[199] polymers,^[26a] micelles,^[200] mesoporous structures,^[201] and metal-organic framework (MOFs).^[202]

Liposomes have been widely used for the delivery of nanomedicines in various fields due to their nontoxic structures, excellent biocompatibility, easy biodegradation and the protective function of drug.^[203] Statins have the ability to regulate lipids, combat inflammation, and stabilize plaque, but they are lipid-soluble drugs that cannot be directly injected into veins and the long-term oral administration of statins will impair liver function. Therefore, the group developed a stable simvastatin (STAT)-loaded liposome and verified the excellent ability of the liposome to promote cholesterol efflux and its anti-inflammatory properties.^[204] Besides statins, Benne et al. prepared LXR agonists-loaded and cyclic peptide Lyp-1-modified liposomes in which Lyp-1 can target the gC1q receptor on foam cell surfaces, and the encapsulation efficiency is close to 100%. After internalization, the released LXR agonists upregulated the expression level of ABCA1 and ABCG1, resulting in a significant reduction in plaque burden and inflammatory macrophages.^[205] In addition, liposomes have also been utilized for targeted delivery of gene regulators such as NLRP3 siRNA which inhibits the formation of inflammasomes and miRNA-146a which restricts NF- κ B inflammation pathway activation.^[206] Interestingly, Wu et al. designed an apoptotic body biomimetic nanoliposome (AP-Lipo) to deliver drug to the atherosclerotic macrophages with maximum efficiency to reduce plaque burden.^[207] PS and cRGDFK peptide-coupled DSPE-PEG were inserted into PPAR γ agonist pioglitazone (PIO)-loaded liposomes, in which PS emitted "eat me" signal and promoted the phagocytosis of inflammatory macrophages. The experimental results confirmed that AP-Lipo significantly induced the phenotypic transition of macrophages from M1 to M2, increased the proportion of collagen, and stabilized the plaque.

Biomimetic nanoparticles retain partial basic structures and characteristics of cells, which can be used to wrap nanoparticles, increase biocompatibility, reduce immunogenicity, and improve targeting ability. Considering the inherent adhesion ability of platelets to damaged endothelium, a platelet membrane-coated

PLGA nano-delivery platform loaded with rapamycin (RAP-PNP) was designed to target plaques with high drug loading rate up to $3.55 \pm 0.06\%$. Compared with free rapamycin, RAP-PNP further reduced the area of plaques.^[208] In vitro, the binding capacity of RAP-PNP conferred by platelet membranes was verified in static conditions and flow-chamber model, respectively, and the uptake of RAP-PNP by foam cells was significantly enhanced. Considering that the extraction of platelet membrane requires a large supply of platelets, a new strategy of fusing platelets with artificial liposomes was proposed, which greatly improved the utilization of platelets (Figure 6a,b).^[209] In vivo, rapamycin-loaded and platelet membrane-fused liposomes (RAP-P-Lipo) were successfully accumulated in the plaques of the atherosclerotic model mice, which was not observed in free liposomes and was negligible in healthy C57 mice (Figure 6c). Histological sections of the aortic valve also showed that the fused structure had a highly co-localized distribution with collagen, activated endothelial cells, and macrophages. After eight weeks of treatment, the aortas of mice in each group were obtained for analysis. The plaque area was significantly reduced, and the burden of macrophages was relieved, which had statistical significance both in the gross staining by Oil Red O and in the histological sections (Figure 6d–f). Compared with platelets, the inherent inflammatory chemotactic ability of macrophages has also attracted widespread attention.^[210] Sha et al. encapsulated SHP₁ inhibitor (SHP1i) into liposome nanoparticles with macrophage membrane layer, and the membrane structure could competitively bind to ox-LDL and lipopolysaccharide, thereby reducing anti-inflammatory factors, ROS, and iNOS production. The loaded SHP₁i blocked the CD47-SIRP α "don't eat me" signaling pathway, promoting macrophages to engulf apoptotic cells (efferocytosis).^[211] In another report, CD47 plasmid was transfected into macrophages to express a large amount of anti-phagocytosis protein CD47 to effectively evade phagocytosis by the reticuloendothelial system. At the same time, endothelin-1 was used to stimulate macrophages to overexpress integrins $\alpha 4/\beta 1$ and selectively bind to VCAM-1 on the surface of endothelial cells, delivering potent anti-inflammatory drug colchicine and providing a new strategy for the application of biomimetic cell membranes.^[212]

Cell-mediated drug delivery aims at using the inherent homing or chemotactic abilities of live cells to carry nanodrugs to the site of lesions. A simvastatin acid-loaded dendritic polymer attached to red blood cells (SA PAM@RBCs) was constructed with $95.8 \pm 3.1\%$ encapsulation rate and $65.3 \pm 2.1\%$ drug loading rate, which responded to local shear stress and ROS. Briefly, the drug entered the bloodstream with red blood cells and reached the atherosclerotic site. Under the local high shear stress, the dendritic polymer detached from the surface of the red blood cells, and a large amount of ROS promoted SA PAM protonation to further release SA.^[213] In another report, a macrophage-liposome living cell hitchhiking strategy was proposed innovatively to achieve precise delivery of β -cyclodextrin and quercetin.^[214] The host-guest binding of β -cyclodextrin to adamantane mediated the attachment of quercetin-loaded liposomes to the surface of macrophage (Figure 6g). Then the macrophage-liposome conjugate entered the plaque depending on the intrinsic inflammatory chemotaxis of macrophages and released quercetin. The research indicated that β -cyclodextrin was stably anchored to macrophages

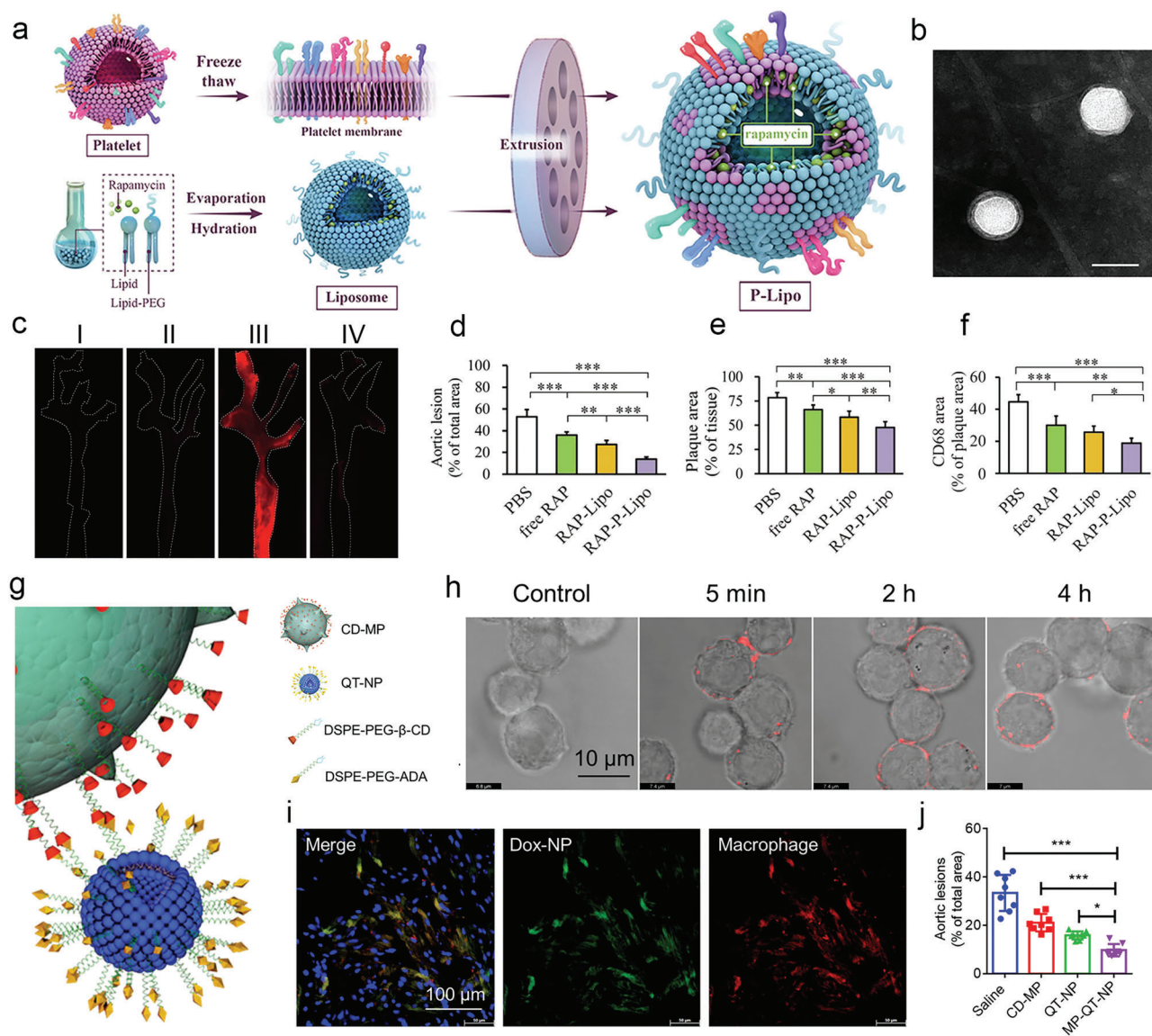


Figure 6. a) Illustration for the preparation of RAP-P-Lipo. b) TEM image of RAP-P-Lipo. c) Fluorescent images of the isolated aorta after different treatments (red: DiI-labeled liposomes, I: PBS group, II: Lipo group, III: P-Lipo group, IV: P-Lipo+C57 Mice group). d) Quantitative analysis of plaque area as a percentage of the total aortic area. Quantitative analysis of e) the plaque area and f) macrophage content in sections of the aortic valve ($n = 6$). $p < 0.05$, $**p < 0.01$, and $***p < 0.001$. a–f) Reproduced with permission.^[209] Copyright 2023, Elsevier. g) Schematic diagram of the macrophage-liposome conjugate. h) Confocal laser scanning microscope (CLSM) after co-incubation of macrophages with rhodamine-loaded liposomes at different times. i) FL imaging of aortic slices (blue: DAPI; green: Dox-loaded liposomes; red: DiI-labeled macrophages). j) Quantitative analysis of plaque area of total area. $*P \leq 0.05$, $**P \leq 0.01$, and $***P \leq 0.001$. g–j) Reproduced with permission.^[214] Copyright 2022, Elsevier.

within 8 h and mediated the binding of macrophages and liposomes within 4 h via the reacting with adamantane (Figure 6h). After injection into mice, the macrophage-liposome conjugate showed a significant colocalization with macrophages, indicating excellent targeting ability for drug delivery (Figure 6i). Quercetin, as an antioxidant stress drug, could activate the NRF2 pathway, reduce local ROS levels and inhibit plaque inflammation. In addition, the β -CD anchored on macrophages could dissolve cholesterol and increase lipid efflux. The synergistic effect of quercetin and β -cyclodextrin reduced the proportion of the area of aortic plaques from 34.6% to 8.6% (Figure 6j).

Polymeric nanoparticles have been widely used as promising candidates for drug delivery due to their variable size, easy surface modification, and controllable drug release. Li et al. established cRGD-modified polymeric nanoparticles that specifically deliver angiogenesis inhibitors pigment epithelium-derived factor (PEDF) with $91.7 \pm 2.6\%$ entrapment efficiency to endothelial cells to stabilize plaques.^[215] In addition, the multiple sites on the surface of the polymer make it easy to construct intelligent responsive delivery systems, which can stably and continuously release loaded drugs under stimulation, thereby effectively reducing off-target effects.^[216] Furthermore, folic acid-modified

lipid-polymeric nanoparticles encapsulating naringenin (Nrg) were found to effectively overcome the intestinal mucosal barrier and accumulate in atherosclerotic macrophages to exert an anti-inflammatory effect.^[217]

In addition to the commonly used drug delivery platforms mentioned above, other nanosystems, such as mesoporous systems, MOFs, tubular systems, and metal nanoparticles have also been elaborated for atherosclerotic drug delivery in recent years.^[218] For example, Pu et al. designed a mesoporous silica system with a pore size of 15.5 nm to deliver anti-IL-1 β , which effectively protected blood vessels, and inhibited VSMC proliferation and inflammatory phenotype transformation.^[219] Manganese dioxide (MnO₂) was also developed as a mesoporous structure and added with metal coordination to deliver curcumin, achieving a loading efficiency of up to 54%.^[220] Additionally, a MOFs structure based on UiO-66 (named RUF1) was constructed to co-load rapamycin and interleukin-1 receptor antagonists, achieving synergistic therapeutic effects. They regulated macrophage phenotype, promoted autophagy, and enhanced the immune regulatory function against atherosclerosis.^[221]

5.2. Phototherapy

Phototherapy refers to the process of generating ROS or heating up under the excitation of the light at a specific wavelength, converting light energy into chemical or thermal energy to kill specific cells (e.g., macrophages, and endothelium). For the treatment of atherosclerosis, phototherapy mainly includes photodynamic therapy (PDT) and photothermal therapy (PTT).

PDT usually refers to the process of promoting the generation of ROS and inducing chemical damage by photosensitizers under light irradiation.^[222] The previous reports included Ce6-mediated foam cell autophagy and cholesterol efflux,^[223] IR780-mediated inflammatory cell ablation,^[224] and curcumin-induced VSMC autophagy.^[225] To solve the problem of weak penetration ability of light, Ma et al. incorporated Ce6 into micelles together with UCNPs to handle atherosclerosis, which activated Ce6 to produce ROS at 980 nm excitation wavelength. Considering the affinity of platelets to early atherosclerotic plaques, the nanoparticles were further coated with platelet membranes, named as PM-PAAO-UCNPs. The in vitro experiments demonstrated that UC-NPs conferred superior tissue penetration to PM-PAAO-UCNPs while generating considerable ROS. The in vivo experiments revealed that PM-PAAO-UCNPs-mediated PDT (980 nm, 10 mW, 30 min) significantly reduced plaque volume and lipid area, decreased the secretion of pro-inflammatory factors (IL-6 and TNF- α) and promoted the secretion of anti-inflammatory factors (TGF- β and IL-10).^[226]

Nanomaterials^[227] with high photothermal conversion efficiency can be used to perform PTT, which is the process of converting light energy into heat energy and inducing physical damage to eliminate specific pathological components.^[228] Peng et al. designed a ternary semiconductor with up to 43% photothermal conversion efficiency based on theoretical calculations, achieving good macrophage ablation effects.^[229] In addition, the light-responsive thermal effect generated a thermophoresis phenomenon, promoting the movement of nanomaterials and drug release.^[218a,230]

Further combining PDT with PTT, Chlorin e6 (Ce6) was loaded with carbon nanocages and then electrostatic adsorbed dextran sulfate (DS) to target SR-A on the surface of activated macrophages, which killed inflammatory macrophages and reduced inflammatory factor secretion via PTT/PDT (808 nm (1 W cm⁻²)/633 nm (80 mW cm⁻²), 5 min).^[112] However, high temperatures could cause damage to the tissue, hence mild phototherapy has been proposed and gained more recognition in various inflammatory disease models including atherosclerosis. This study used polydopamine nanoparticles as the core to generate photothermal effects with OPN antibody as the targeting component. After 10 min of irradiation with the 808 nm laser, mild PPT was produced to promote fibrosis within the lesion, stabilizing the plaque without causing damage to the blood vessels.^[231] Intriguingly, a black TiO₂ modified with HA and porphyrin was constructed (denoted as bTiO₂-HA-P) to perform mild PTT in combination with PDT (Figure 7a). Porphyrin, a traditional photosensitizer, generated singlet oxygen (¹O₂) to promote foam cells apoptosis under NIR irradiation, and the black TiO₂ nanoparticles with high photothermal conversion efficiency exerted PTT under 808 nm and 1 W cm⁻² for 10 min. This mild PTT upregulated the expression of ABCA1 to promote cholesterol efflux, downregulated the LDLr expression to reduce lipid endocytosis, and eventually reduced foam cell formation, while raising the temperature to 44.5 °C as well as promoting the expression of HSP27 to maintain PDT-mediated macrophage apoptosis within a stable range and reduce the adverse effects of excessive necrosis and apoptosis (Figure 7b,c).^[232]

5.3. Sonodynamic Therapy (SDT)

SDT refers to the production of transient ROS from acoustic sensitizers with the exist of energy by cavitation effect under ultrasound excitation.^[233] SDT is similar to PDT, but its significant advantage is the large increase in penetration depth, reaching up to several centimeters in soft tissues.^[13b]

Tian et al. proposed that 5-aminolevulinic acid (ALA)-mediated SDT (1.5 W cm⁻²) could alleviate plaque progression in the early year.^[234] Then they explored different intensities of ultrasound and the influence on atherosclerosis, the results showed that high-intensity ultrasound-mediated cell necrosis, while low-intensity ultrasound-induced cell apoptosis and cell burial of inflammatory cells, which was beneficial to alleviate the lesion. Furthermore, the investigators focused on the action mode of ALA-mediated low-intensity ultrasound in advanced APOE^{-/-} atherosclerotic mice. They found that SDT (0.5 W cm⁻², 15 min) promoted cholesterol efflux via the PPAR γ pathway and induced the apoptosis of inflammatory macrophages through the mitochondrial pathway. While upregulating the expression of Merck to promote efferocytosis, which greatly diminished the inflammatory macrophages as well as the inflammatory burden within the plaque and rapidly stabilized the atherosclerosis.^[235] Meanwhile, sonosensitizers sinoporphyrin sodium (DVDMS)-mediated SDT (mice: 0.8 W cm⁻², rabbits: 1.5 W cm⁻², both 30% duty factor, 15 min) was used to promote macrophage and endothelial cell apoptosis and inhibit neovascularization.^[236] Another report indicated that DVDMS-mediated SDT (mice: 0.4 W cm⁻², rabbits: 1.5 W cm⁻², 15 min) upregulated PFN1 expression

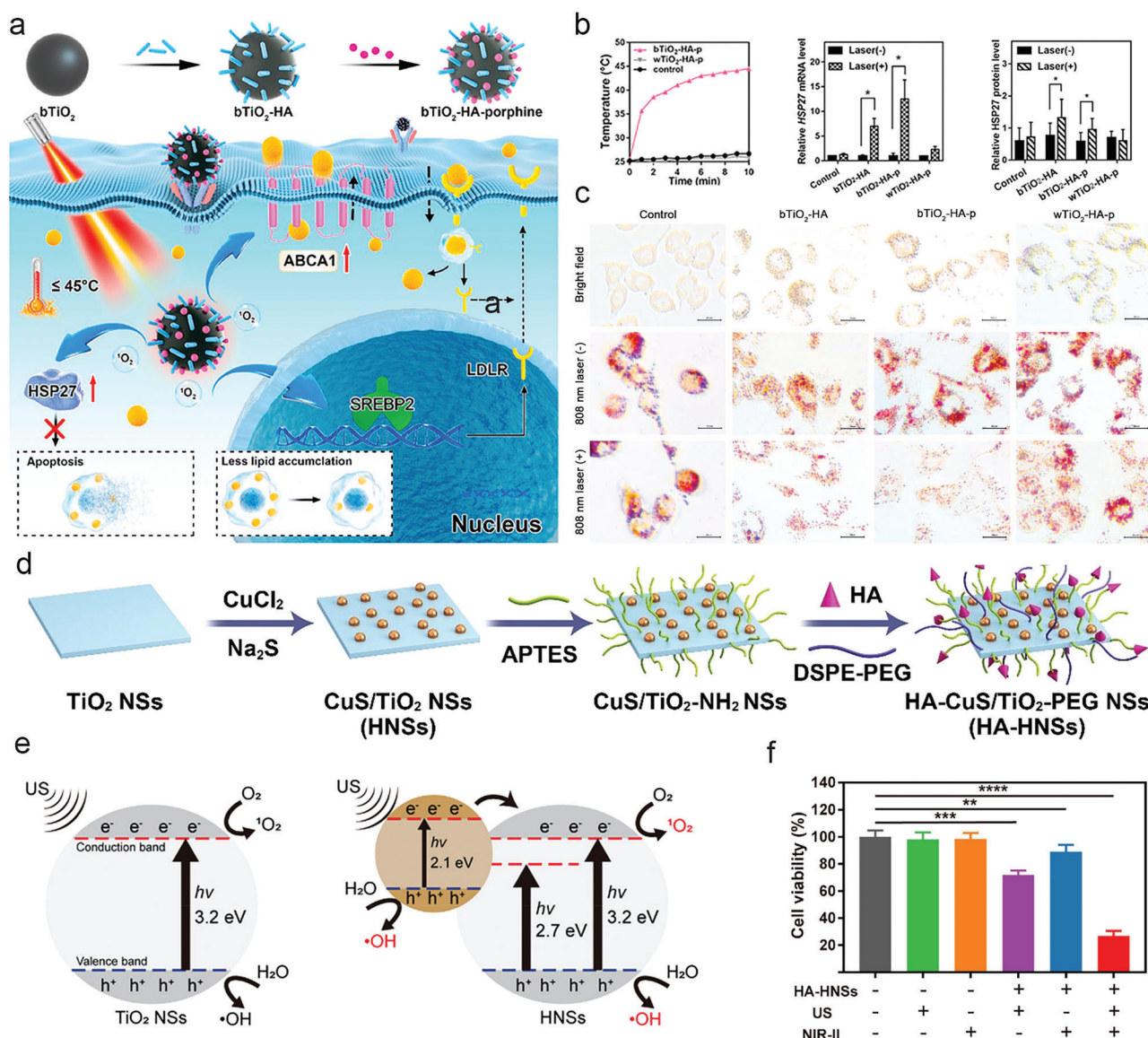


Figure 7. a) Schematic diagram of the synthesis process of bTiO₂-HA-P and its therapy strategy. b) Temperature curves of bTiO₂-HA-p and wTiO₂-HA-p at 808 nm laser (left) and relative HSP27 mRNA level (middle) and protein level (right) after different treatments. c) Representative Oil Red O staining images after different treatments to assess the lipid burden of foam cells. **p* < 0.05. a–c) Reproduced with permission.^[232] Copyright 2022, Elsevier. d) Schematic diagram of HA-HNSs. e) The principle of HA-HNSs-mediated SDT. (f) Viability of macrophages under different treatments (*n* = 3). *, *P* < 0.05; **, *P* < 0.01; ***, *P* < 0.001; ****, *P* < 0.0001. d–f) Reproduced with permission.^[241] Copyright 2023, American Chemical Society.

by activating the ROS-Nrf2-PFN1 signaling pathway and promoted transferrin efflux, which reduced iron retention in plaques and especially in the macrophages.^[237]

Another representative sonosensitizer is a natural extract represented by hydroxysafflower yellow and curcumin. The former induced THP-1 macrophage autophagy and cleared local inflammation in plaque by inhibiting PI3K/Akt/mTOR induction under US irradiation.^[238] The sonodynamic effect of curcumin mediated THP-1 macrophage clearance by inducing mitochondrial damage.^[239] To further improve the solubility and efficacy of natural products, a curcumin nanosuspension-mediated SDT (0.4 W cm⁻², 1.0 MHz, 15 min) stabilized with PVPK30 and

SDS was developed to enhance macrophage apoptosis under the mitochondrial injury pathway and interfere with macrophage polarization.^[240]

In addition, inorganic TiO₂ was selected to prevent early plaque progression due to its narrow bandgap (Figure 7d). This study combined SDT (0.5 W cm⁻², 10 min) with PTT (0.8 W cm⁻², 10 min) by preparing CuS/TiO₂ heterostructured nanosheets (abbreviated as HA-HNSs), which possessed a better electron-hole separation effect (Figure 7e). The in vitro results showed that synergistic therapy synergistically induced macrophage apoptosis and inflammation clearance (Figure 7f).^[241]

5.4. Immunotherapy

With the progressive understanding of atherosclerotic pathology, the current view holds that atherosclerosis has a complex immune inflammatory reaction, making immunotherapy possible.^[242] Early acute inflammatory cells are enriched in plaque, attracted major contributors (mononuclear macrophages), and eventually macrophages interacted with neutrophils and T cells to maintain inflammation. Immunotherapy can regulate the intraplaque inflammatory microenvironment by cutting off or alleviating the cascade response of the inflammatory network.^[243]

Recently, a nano-immunoplateform named ASPA was reported, which combined shSiglec-1 with PEI-Au NPs by electrostatic adsorption, and it was wrapped with pH-responsive polyethylenimine-acetylsalicylic acid (PEI-ASA) to regulate the atherosclerotic inflammatory microenvironment (**Figure 8a**). In order to verify the acid-responsive hydrolysis of ASPA and the release of shSiglec and ASA, physiologically relevant buffers at different pH were used to simulate the *in vivo* environment, and the high-performance liquid chromatography (HPLC) and ¹H NMR spectrum were performed after co-incubation. The results indicated that ASA can be released up to 90.2% at pH 5 buffer, but only 12.8% at pH 7.4 buffer. On the one hand, shSiglec-1 silenced CD169 on macrophages, blocked the mutual recognition and interaction between macrophages and CD8⁺ T cells and NKT cells, and inhibited the lipids antigen presentation, which eventually reduced the infiltration of inflammatory cells (**Figure 8b,c**). On the other hand, the ASA up-regulated peroxisome proliferator-activated receptor α (PPAR- α) and γ (PPAR- γ) (**Figure 8d**). The former reduced the inflammatory Th17 cell differentiation and cooperatively inhibited the expression of inflammatory factors (**Figure 8e**). The latter participated in the cholesterol efflux pathway, decreased the formation of foam cells, and further impaired the lipid antigen presentation of macrophages (**Figure 8f**). Finally, ASPA successfully changed the atherosclerotic immune microenvironment and turned it from a complex thermal environment to a stable cold environment by remodeling various immune cells.^[244]

Besides, rHDL is also a promising nano-immunotherapeutic agent, which can specifically aim at myeloid cells. The researchers used phospholipid DMPC/MHPC and ApoA1 as ingredients to prepare r-HDL on a large scale and loaded it with simvastatin via microfluidic homogenization. Radionuclide imaging demonstrated high enrichment of r-HDL in the liver, kidney, spleen, and artery, while flow cytometry results manifested excellent myeloid targeting ability of r-HDL. After the tail vein injection in ApoE^{-/-} mice on Western diet, the aorta was removed for analysis, and the results showed that immunotherapy rapidly attenuated excessive inflammatory cells within the lesion and reduced plaque burden.^[245]

Collectively, although the reviewed immunotherapies have achieved significant efficacy, as for the immune system, the slightest nudge causes the widest chain reaction. Therefore, it requires a deep understanding of cell subsets, surface markers, and their role in different disease stages. Furthermore, immunotherapy is expected to achieve high precision in targeting therapies by modulating the size, surface charge, and ligand of nanoparticles. And now, the paradigm of nanomedicine has shifted from

simply avoiding the immune system to actively engaging with it in a meaningful way.

5.5. Gas Therapy

Gas therapy is a new treatment modality based on special gas signal molecules that participate in various physiological regulation of cells and tissues.^[246] It has received wide attention in many fields due to its high efficiency and safety. Currently, the gases used in the treatment of atherosclerosis are nitric oxide (NO) and hydrogen (H₂). NO, as a special endogenous substance, can regulate vasodilation, repair endothelial damage, reconstruct the endothelial barrier, and reduce oxidative stress, but its synthesis is impaired during atherosclerosis. To solve this problem, one of the methods is directly introducing exogenous NO into the lesion, and the liposomes, dendrimers, and macromolecular backbones are candidates as NO carriers. For example, Rink et al. assembled the NO transporter protein RSON and HDL together to construct bio-nanoparticles that integrated NO delivery and lipid regulation, reducing the atherosclerotic burden and ischemia-reperfusion injury.^[247] Similarly, to maintain favorable NO concentration, a dendrimer nanoplateform carrying 18 NO release units was constructed to finely modulate the slow release of NO.^[248] Another alternative is delivering NO donor L-arginine into the atherosclerotic plaques to produce endogenous NO.^[249]

Interestingly, the concept of “nanomotor” has been proposed recently that regarded NO production as a driving force to enhance the abilities of nanoparticles for the targeting, retention, and penetration into atherosclerotic plaques. In this research, carrier-free nanomotor based on trehalose-L arginine-phosphatidylserine (Tr-Arg-PS) was structured to enable cascade targeting of intraplaque macrophages (**Figure 8g**). First, L-arginine reacted with the high levels iNOS as well as ROS in the microenvironment of plaque and produced NO as driving force to achieve primary targeting, then relied on the affinity of PS to macrophages to realize secondary targeting. Motion is the key behavior of nanomotor. Brownian motion was only observed in normal RAW264.7 macrophages and HUVEC cells, while significant displacement of nanomotor for up to 24 h was observed in LPS-induced inflammation cell models (**Figure 8h**). The CLSM results also exhibited significant enrichment of Tr-Arg-PS with motor structure in inflammatory cells (**Figure 8i**). After sequential treatments, the nanomotor repaired the integrity and consistency of the vascular endothelial barrier and presented the well-aligned endothelium (**Figure 8j**).^[250]

H₂, an exogenous gas, has been reported to alleviate oxidative stress, reduce the expression of pro-inflammatory cytokines, and promote cholesterol efflux from macrophages. However, it is difficult to directly deliver H₂ in the blood circulation, so metallic palladium has been used as a hydrogen carrier as its interstitial void can accommodate hydrogen atoms. Palladium had been reported to come in a variety of shapes, and Xu et al. constructed a palladium nanopocket cube that can load up to 0.12% hydrogen atoms. The superior hydrogen storage and release activated the PPAR- γ pathway, promoted lipid efflux and alleviated atherosclerosis.^[251] Attractively, a tetrapod needle-like PdH nanoparticle was designed to perform living cell delivery depending on the chemotaxis towards macrophages within the plaque

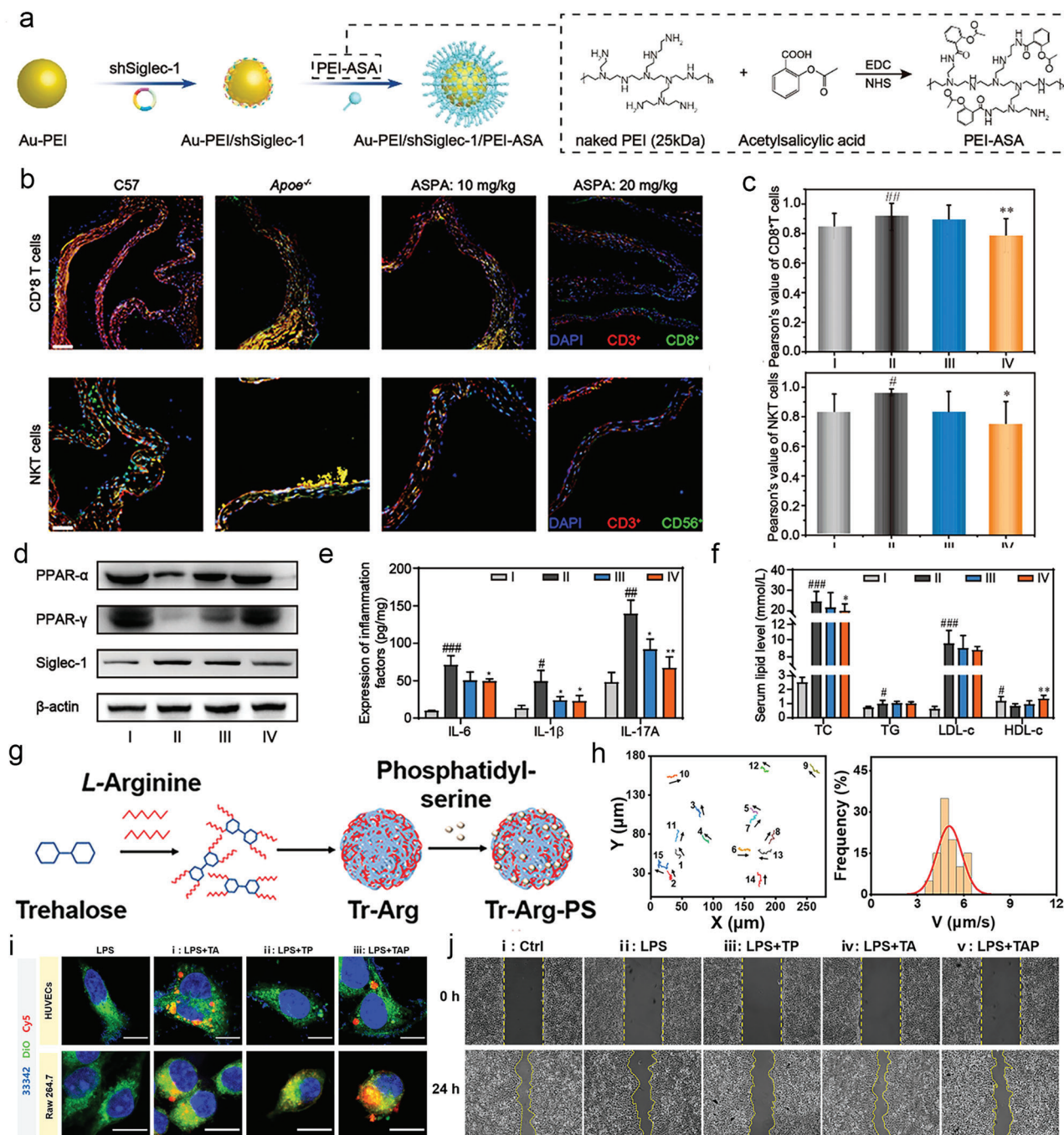


Figure 8. a) The diagrammatic sketch of ASPA and the covalent binding of PEI-ASA. b) Typical immunofluorescence images and c) their quantitative analysis indicating CD8⁺T cells and NKT cells from the cardiac valve of healthy and atherosclerotic mice under different treatments. d) The results of PPAR-α, PPAR-γ, and Siglec-1 protein expression. e) The expression of IL-6, IL-1β, and IL-17A in extracted aortas after corresponding treatments. f) The levels of serum lipids. I: C57 group, II: *Apoe*^{-/-} group, III: ASPA: 10 mg per kg group, IV: ASPA: 20 mg per kg group. #*p* < 0.05, ##*p* < 0.01; **p* < 0.05, ***p* < 0.01, ****p* < 0.001. a–f) Reproduced with permission.^[244] Copyright 2022, American Chemical Society. g) Composition strategy of Tr-Arg-PS. h) Motion trajectories (left) and velocities (right) of TAP nanomotors. i) Confocal laser scanning microscope (CLSM) of cells uptake (red: sample, blue: nucleus, green: cell membrane). j) Representative microscope images of scratch wound healing assay under different treatments of HUVECs. g–j) Reproduced with permission.^[250] Copyright 2022, American Chemical Society.

microenvironment. After entering the plaque, H₂ was released from nanoparticle-loaded live cells in several minutes under the 808 nm NIR laser irradiation. In addition, the hydrogen carrier palladium had nanoenzyme activity to remove ROS in the lesion and the spike-like structure was able to induce macrophage autophagy, demonstrating significant therapeutic effects.^[252]

5.6. Clinical Studies of Atherosclerosis Therapy in Nanomedicine

Although nanomaterials have demonstrated efficacy in animals with atherosclerosis, there are currently no formally approved nanomedicines, and only a few have entered clinical trials. Liposomes have received broad attention as excellent candidates. Previous reports on atherosclerosis clinical trials have included liposomal nanoparticle encapsulating prednisolone (LN-PLP) and paclitaxel-associated cholesterol-rich non-protein nanoemulsion (PTX-LDE). Based on the safety and efficacy validation of LN-PLP in rabbits, it has been approved for clinical trials.^[253] LN-PLP exhibited a long half-life of 45–63 h, which was 7–15 times that of free prednisolone. In addition, preoperative injection of LN-PLP through the brachial vein of patients undergoing arterial stripping surgery showed targeting of macrophages but lacked anti-inflammatory efficacy.^[254] Another study administered PTX-LDE to severely atherosclerotic patients every three weeks for six consecutive weeks. This preliminary study suggested that using high-dose PTX-LDE (175 mg m⁻² body surface area) was safe. Four out of eight subjects in the experimental group had an average plaque volume reduction, but this was not statistically significant.^[255] Hence, longer-term observations may be necessary.

In vivo, HDL participates in reverse cholesterol transport, so the use of rHDL mimetics may be feasible. The first rHDL (ETC-216) composed of ApoAI Milano and palmitoyl-oleoyl phosphatidyl choline (POPC) was associated with a significant reduction in plaque volume in acute coronary syndrome patients.^[256] However, clinical trials were suspended due to adverse reactions such as increased neutrophils and decreased lymphocytes. Subsequently, improvements were made to the formula, resulting in MDCO-216. Results from a single-ascending-dose phase I study showed that the drug promoted ABCA1-mediated cholesterol efflux in healthy individuals and stable coronary heart disease patients.^[257] However, in another randomized clinical trial focused on acute coronary syndrome patients, MDCO-216 (*n* = 59) was compared with a placebo (*n* = 67) while all patients received statin therapy, and the addition of MDCO-216 did not further reduce plaque volume.^[258] However, MDCO-216 demonstrated good overall safety and tolerability, leaving room for further exploration.

CER-001 is composed of ApoAI, dipalmitoylphosphatidylglycerol (DPPG), and sphingomyelin (SPM). Similarly, two clinical trials investigated the effect of CER-001 on plaque regression in patients with acute coronary syndrome. The results showed that neither a low-dose regimen (3 mg kg⁻¹) for up to 10 weeks nor a dose-escalation approach reduced coronary atherosclerosis.^[259] CSL111 is formed by the combination of native ApoAI and phospholipids. In a randomized controlled trial, short-term administration of CSL111 resulted in a statistically significant improvement in plaque characteristic index and coronary artery score,

but there was still no statistically significant regression of plaque volume.^[260] CSL112 is another discoidal rHDL NPs similar to CSL111.^[261] The in vitro experiments have clearly demonstrated its ability to promote cholesterol efflux and reshape plaque characteristics. Single-dose (NCT01129661) and multi-dose escalating trials (NCT01281774) have completed phase I clinical trials, aiming to study the safety, tolerability, and pharmacokinetics of CSL112.^[257] The results of both two trials confirmed that CSL112 administration can increase ApoAI and pre-β1-HDL, but cannot seem to increase lipids promoting atherothrombotic risk, and no serious adverse events occurred.^[262] In another multicenter escalating dose trial (NCT02427035), there were no significant changes in liver and kidney function for all investigators, even in patients with moderate renal impairment.^[263] In addition, three phase II clinical trials have been completed. First, a single escalating dose trial of CSL112 (1.7 g, 3.4 g, and 6.8 g) was determined to be well tolerated in stable atherosclerotic patients.^[264] Subsequently, it was further determined that a dose of 6g of CSL112 was acceptable in patients with moderate renal impairment.^[265] And regardless of weight, gender, and race, a 6g dose of CSL112 is beneficial for acute myocardial infarction patients.^[262a,266] Encouraged by these findings, a phase III clinical trial (NCT03473223) is currently actively being conducted to study the efficacy and safety of CSL112 in patients with acute coronary syndrome.

Apart from the lipid-based nanomaterials mentioned above, other types of nanomaterials have also been applied in clinical trials. A randomized, double-blinded, placebo-controlled clinical trial revealed that the natural compound curcumin micelle (80 mg once daily for 3 months) can prevent atherosclerosis by reducing high-sensitivity C-reactive protein in type II diabetic patients with mild to moderate coronary artery disease (CAD).^[267]

Another team developed a silica-gold core-shell nanoparticle (NANO) for the treatment of atherosclerosis using plasmonic photothermal therapy (PPTT).^[268] The results showed that the treatment of NANO and PPTT indeed regressed total atheroma volume (TAV) and reduced mortality, complications, and thrombosis. However, the side effects cannot be ignored, such as an increase in the incidence of defects in erythrocyte membranes in patients treated with NANO.^[269] To improve long-term safety and efficacy, the lesion preparation such as treated with stent first or treated with predilation by drug-coated balloon prior to NANO treatment was found to be beneficial.^[270]

Compared to bare metal stents, drug-eluting stents (DES) are more effective in reducing restenosis and improving blood flow in patients receiving coronary stent implantation. COBRA PzF is a thin strut cobalt-chromium alloy stent coated with Polyzenef. A single-center clinical trial of 155 stents in 100 patients conducted a one-year follow-up and no acute adverse events were observed, providing an opportunity for further research on COBRA PzF.^[271] However, this was a small-scale clinical trial with no control group. Subsequently, Maillard et al. conducted a multicenter prospective study (e-Cobra) including 980 patients aiming to evaluate the safety and effectiveness of COBRA PzF in short-term dual antiplatelet therapy (DAPT) patients. The patients were followed up for one year, and only 9% of them had major adverse cardiovascular events (MACE), and 0.7% of them experienced stent thrombosis.^[272] Furthermore, the team compared the COBRA PzF stents followed by DAPT for 14 days with FDA-approved DES followed by guideline-recommended (3–6 months) DAPT ther-

apy, and found that the former therapy reduced bleeding without promoting thrombosis.^[273] It should be noted that these results are from small-scale and limited control group clinical trials, so more research and verification are needed before making any decisions.

6. Theranostic

Combining contrast agents and therapeutic agents in a single atherosclerosis theranostic nanoplatform can integrate diagnostic, therapeutic, and monitoring functions. It facilitates the diagnosis and treatment of diseases, as well as streamlines monitoring of disease progression, evaluation of therapeutic efficacy, and timely adjustment of drug administration strategies, thus enabling personalized treatments. The development of a multifunctional theranostic nanoplatform for atherosclerosis is currently a hot research topic and remains challenging. In this section, we mainly discuss how nanomaterials have promoted the development of theranostic approaches and their current applications in atherosclerosis recently, with the aim of providing deep insight into the promotion of theranostic development (Table 2).

MR imaging-based theranostic still relied on gadolinium and iron oxide, and based on existing reports, they were mostly constructed by loading diagnostic probes and therapeutic components into the same nanosystem to form theranostic probes.^[274] Interestingly, in one report, an iron oxide-based mito-magneto (MM) played the significant role of MR imaging, exhibiting favorable high contrast. The team directly selected biomimetic HDL nanoparticles with therapeutic effects to achieve dual-targeted delivery of contrast agents to macrophages and mitochondria. This dual-targeting mode achieved molecular-level imaging of macrophages, reversed cholesterol transport (RCT), and oxidative stress relief targeted at mitochondria.^[275]

FL imaging-based theranostic have been found to be rapidly expanding in the field of cardiovascular disease, and substances that can produce fluorescence are diverse and easy to modify, making FL imaging an indispensable part of theranostic.^[276] In addition to the previously mentioned fluorescence imaging substances, Ru(bpy)₃Cl₂, a FL molecular probe, was loaded into mesoporous silica systems along with the SIRT1 activator SRT1720 and targeted macrophages via coating CD36 antibody. Real-time monitoring of inflammation cells in plaques was realized while reducing cholesterol content in macrophages by SRT1720.^[277]

Besides, inspired by photosynthesis, a report proposed a chlorophyll a (Chla)-modified liposome that can produce H₂ under NIR light and continuously detect local ROS levels. The core of the liposome was coupled between lanthanide elements doped UCNP and AuNPs via the thioketal-based linker (Figure 9a). On the one hand, the distance between UCNP and AuNPs was short enough for Förster resonance energy transfer (FRET) in a normal environment. Therefore, the AuNPs (acceptor) were able to absorb the green upconversion luminescence (UCL) emitted by the UCNP (donor) upon 980 nm excitation. When the liposome entered the plaque and monitored the excessive ROS in the lesion, the linker broken, and the distance between UCNP and AuNPs increased. The green UCL (at 550 nm) emitted by the UCNP cannot be absorbed by AuNPs, so it achieved in situ detection of ROS levels. On the other hand, when UCNP were excited by

980 nm light, it produced red UCL (at 660 nm), which stimulated the photosensitizer Chla into the excited state and provided excitation electrons to AuNPs, while the citrates on the surface of UCNP provided protons, and the protons are reduced to H₂ by AuNPs, removing excess ROS (Figure 9b). The experimental results indicated that the higher the concentration of hydrogen peroxide (H₂O₂), the stronger the green fluorescence emitted, and there was a good linear relationship between them, without affecting the emission of red fluorescence (Figure 9c). At the same time, gas chromatography was used to measure the release of H₂ under exposure to the infrared laser, and the H₂ release amount gradually increased with the prolongation of irradiation time (Figure 9d). In vitro, after the irradiation with 980 nm near-infrared laser, the ROS, pro-inflammatory cytokine IL-1 β , and IL6 were significantly reduced. Consistent with the results of detection kits, FRET technology sensitively evaluated the level of H₂O₂ in cells. In summary, this report fulfilled the systematic combination of diagnosis and therapy by ingeniously applying the transfer of electrons and energy between donors and acceptors and the reduction catalysis of protons.^[278]

Another study used exosomes from M2 macrophages to carry hexyl 5-aminolevulinate hydrochloride (HAL@M2 Exo) by electroporation, fully utilizing the biosynthesis and metabolism of HAL for atherosclerotic diagnosis and treatment (Figure 9e). The metabolic intermediate of HAL was protoporphyrin IX (PPIX), a photosensitizer that emitted red fluorescence to track the lesion. Next, further biological metabolism occurred, which produced anti-inflammatory and antioxidant substances carbon monoxide (CO) and bilirubin. In addition, M2 exosomes had excellent inflammatory chemotaxis activity for plaque targeting, and they carried anti-inflammatory factors secreted by M2 macrophages to further clear local inflammation in the lesion. At the cellular level, FL imaging and quantitative analysis illustrated the red fluorescence emitted by PPIX and the green fluorescence of CO, which validated the feasibility of theranostic (Figure 9f,g).^[279]

US is an ideal device for detecting vascular diseases and is typically used for the real-time assessment of vascular wall lesions. Contrast-enhanced ultrasound relies on the intravenous injection of microbubbles to artificially enhance the contrast of blood, thereby imaging normal or pathological structures of blood vessels. Inspired by this, microbubble-mediated atherosclerotic theranostic has made significant progress recently.^[280] Since inflammatory macrophages within the plaque are an important part of atherosclerotic plaques, PLAG nanoparticles loaded with perfluorohexane (PFH) were designed to target macrophages for ultrasound imaging. At the same time, low-intensity focused US (LIFU) was applied to the lesion to induce PFH to undergo a gas-liquid phase transition. This process was accompanied by a series of physicochemical reactions known as the acoustic droplet vaporization (ADV) effect. In the ADV effect, bubbles regularly oscillated, expanded, contracted, or collapsed, potentially generated energy, destroyed cells, and promoted macrophage apoptosis, which achieved a similar effect to ablation, reversed plaque progression, and facilitated early diagnosis and intervention of vulnerable plaques.^[281] Similarly, perfluoropentane (PFP) can also be transformed into gas microbubbles through the ADV effect. A multifunctional nanoplatform with PFP as a core carrying sonosensitizer hematoporphyrin monomethyl ether (HMME) and MR/PA imaging probe MnFe₂O₄ was constructed to tar-

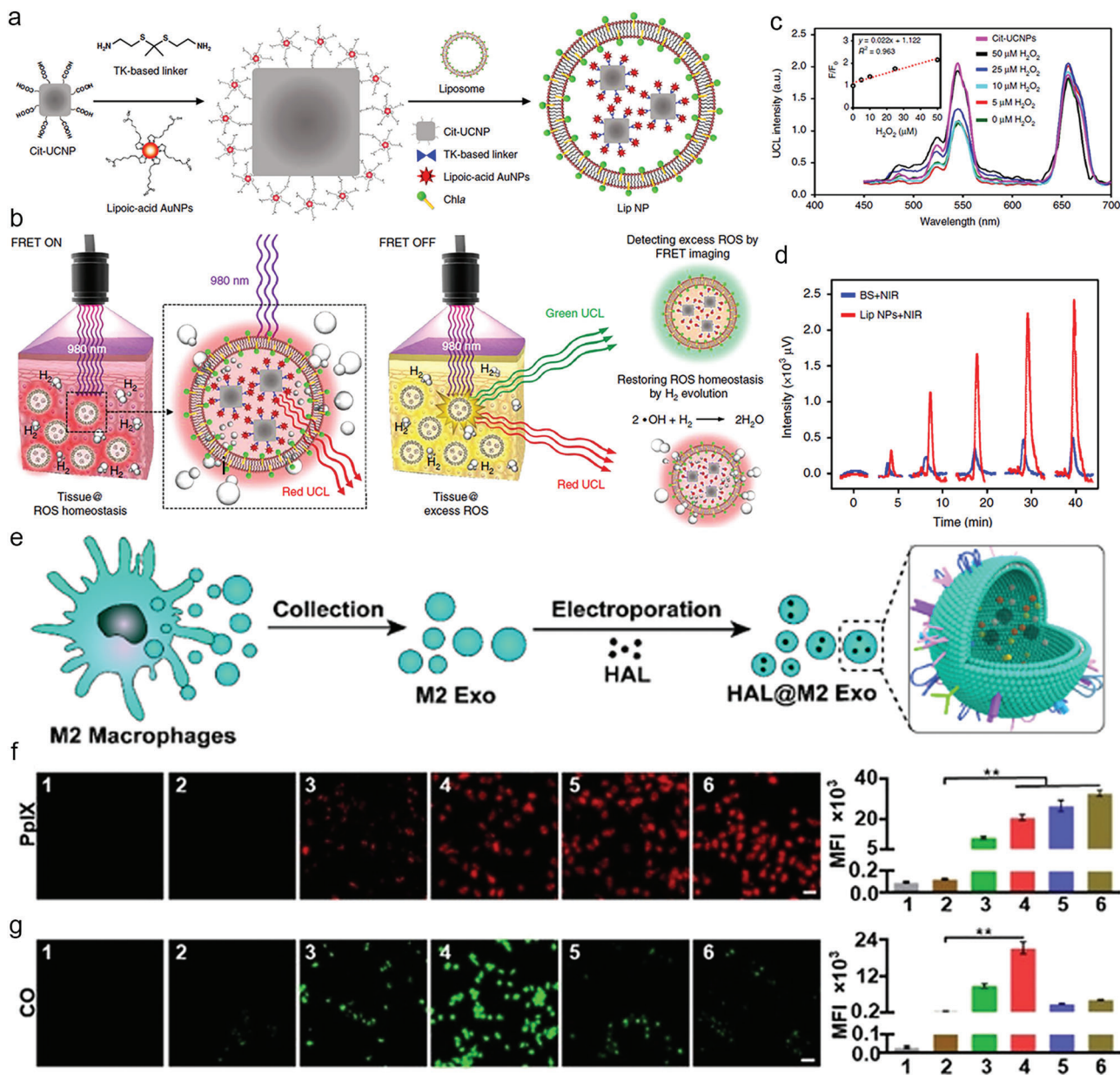


Figure 9. Schematic illustration of a) the composition of Lip NP b) and the principles of theranostic under light excitation of Lip NP. c) FL excitation spectra and linear correlation curve of Lip NP under different concentrations of H_2O_2 with a NIR laser (980 nm) for 30 min. d) H_2 release after irradiation at different times. a–d) Reproduced with permission.^[278] Copyright 2020, Springer Nature. e) Composition strategy of HAL@M2 Exo. FL imaging (left) and quantitative analysis (right) of f) PpIX and g) CO under different treatments (1. Control 2. M2 Exo 3. HAL 4. HAL@M2 Exo 5. HAL+HO-1 inhibitors 6. HAL@M2 Exo+HO-1 inhibitors, $n = 3$). e–g) Reproduced with permission.^[279] Copyright 2020, Wiley-VCH.

get neovascularization in atherosclerotic plaques. LIFU-mediated endothelial cell apoptosis achieved complete inhibition of neovascularization, and ultimately, the plaque became stable.^[98]

PA imaging-mediated theranostic made tremendous progress on latest research. A multifunctional and smart nanotheranostic agent controlled by pH and ROS dual switches with accurate cascade targeting ability for damaged endothelial cells, macrophages, and mitochondria has been proposed as a multi-channel diagnostic and therapeutic system for atherosclerosis (Figure 10a). This group innovatively synthesized a novel π -

conjugated polymer (PMeTPP-MBT) for in vivo PA imaging. Based on it, they connected the therapeutic components SS-31 peptide and astaxanthin to enable non-invasive early theranostic of atherosclerosis (named as PA/ASePSD). The maximum photoacoustic absorption peak of PA/ASePSD exists at 830 nm, and there is a good linear relationship between the signal intensity and concentration (Figure 10b–d). Briefly, SS-31 peptide was a versatile mitochondrial-targeting peptide that restored mitochondrial function while reduced intracellular ROS and suppressed the expression of CD36 and LOX-1 receptor on macrophage

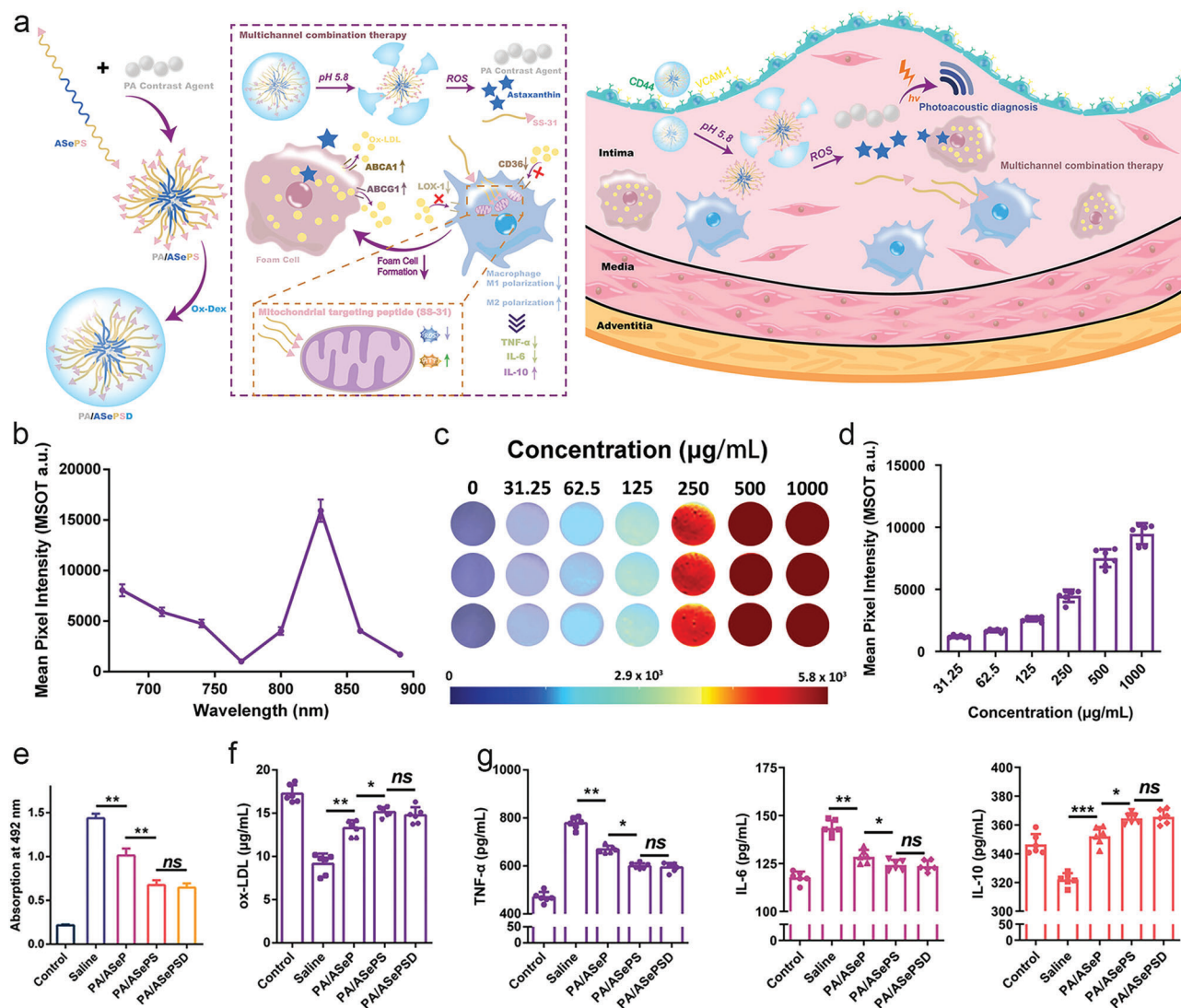


Figure 10. a) Schematic illustration of the composition structure and theranostic strategy of PMeTPP-MBT. b) Photoacoustic absorption spectrum of PA/ASePSD. c) Photoacoustic images and d) quantitative analysis of PA/ASePSD at different concentrations ($n = 3$). e) Quantitative analysis of intracellular Oil red staining and f) the ox-LDL in supernatant under different treatments. 3D reconstruction PA images of the aorta and carotid arteries. g) The expression of various inflammatory factors (TNF- α , IL-6, and IL-10) in macrophages ($n = 6$). * $p < 0.05$, ** $p < 0.01$, *** $p < 0.001$; ns, no significance. Reproduced with permission.^[282] Copyright 2023, Wiley-VCH.

surfaces. Oil red staining and quantitative analysis of foam cells after treatment with PA/ASePSD revealed a significant decrease in intracellular lipid content. Consistent with the results of Oil red, the increase in ox-LDL in the supernatant medium of the PA/ASePSD group confirmed the synergistic effect of inhibiting lipid endocytosis and enhancing lipid exocytosis (Figure 10e,f). Astaxanthin targeted foam cells and enhanced cholesterol efflux mediated by ABCA1/G-1, thereby reducing foaminess. The synergistic effects of both substances fulfilled lipid management and anti-inflammatory to atherosclerosis (Figure 10g), and the introduction of PA imaging provided a new perspective for atherosclerotic theranostic.^[282]

Vascular interventional surgery performs atherosclerotic diagnosis and treatment simultaneously in clinical practice, such as bare metal stents (BMS), drug-eluting stents (DES), and drug-

coated balloons (DCB). However, BMS causes re-narrowing,^[283] DES increases the risk of late thrombosis,^[284] and local retention and permeability of drugs in DCB are unsatisfactory.^[285] Nanomaterials for stent and balloon functionalization can enrich the types of interventional devices in vascular interventional surgery and improve the aforementioned issues. Inorganic nanomaterials such as TiO₂ and magnesium fluoride (MgF₂) nanofilm layers have been reported to promote endothelial cell growth and proliferation with confirmed biocompatibility in animals.^[286] Polymer nanomaterials are promising candidates for organic stent coatings due to their biodegradability and surface modifiability. Dopamine self-polymerizes in alkaline environments to form a polydopamine (PDA) film on the stent surface, enhancing stent corrosion resistance, and promoting endothelial cell proliferation while reducing VSMC proliferation.^[287] The breakdown

of PLGA ester linkages with oligomers and monomers is the main method for delivering drugs after hydrolysis.^[288] Interestingly, Huang et al. designed a NIR-controlled tip-separable microneedle-loaded balloon with anti-proliferation drugs paclitaxel encapsulated in the microneedle tip. A ring laser was placed in the catheter axis, emitting a NIR laser to heat and melt the phase-change material lauric acid (LA) when the catheter was slowly removed from the blood vessel. Then gently withdrawing the balloon kept the drug delivery tip in the atherosclerotic lesion, slowly releasing the drug under the regulation of PLGA and polycaprolactone (PCL).^[289] Additionally, several new polymers such as chitosan (CS),^[290] polycyclodextrin,^[291] polyurethane,^[292] and phosphorylcholine^[293] are also involved in the application of nano-coatings. Carbon-based nanomaterials such as carbon nanotubes and graphene oxide also have some reports due to their ability to promote cholesterol efflux and photoresponse performance.^[294] Inspired by mussels, biomimetic nanomaterial coating has carried out some research, in which mussel adhesive protein is extracted to replace polymer coating and enhance the adhesion of the coating to the stent.^[295] Further modification of groups on mussel adhesive proteins can connect biological effect molecules and exert anti-atherosclerosis applications.^[296] Encouraged by the above results, it is believed that nanomaterial coating stents and balloons provide an alternative theranostic strategy for patients.

In addition to the above, theranostic for atherosclerosis based on CT or nuclear medicine had also been reported.^[297] For example, AuNPs have a high atomic number and are suitable for CT imaging. Besides, they have a broad and distinct absorption peak in the NIR and a high photothermal conversion efficiency, which are capable of photothermal ablation.^[298] This multi-functional theranostic agent can utilize the inherent diagnostic and therapeutic properties of a single nanomaterial, greatly enhancing the utilization and providing innovative ideas for further therapy of inflammatory diseases.

7. Biosafety

The unique properties and application potential of nanomaterials have made nanomedicine a research hotspot in fields like disease diagnosis, drug delivery, molecular technology, etc. Although many engineered nanomaterials have shown enormous potential, most of the research for atherosclerosis is in its early stages, and there are some issues need to be resolved. Unlike conventional medical drugs, the special physicochemical properties of nanomaterials may have unpredictable behaviors and impacts on living organisms. Therefore, the issue of biosafety should be an important part of nanomedicine research for final clinical translation.^[299]

The biosafety assessment of nanomaterials in atherosclerosis involves multiple fields, such as nanotechnology, fluid dynamics, pathology, and toxicology, and it is a complex evaluation process. A comprehensive evaluation method is necessarily required, which typically includes the followings:

I. In vivo distribution and metabolism assessment of nanomaterials:^[300] The main factors that affect distribution and metabolism are the characteristics of nanomaterials, such as targeting substances, size, potential, shape,

stiffness, and route of administration.^[301] The evaluation typically requires the use of biological imaging techniques and other biological detection methods. It is worth noting that when nanomaterials enter the body, they may adsorb proteins and form a "protein corona," which slows down the clearance from the body or mediates special drug delivery methods.^[302] A literature validated the critical role of protein corona in atherosclerotic mice. Designed anionic liposomes interacted with proteins in the serum and formed a protein corona, in which the complement component C1q significantly mediated the cellular uptake of liposomes.^[121b] Subsequently, nanomaterials mostly enter tissues or organs through the bloodstream and are mainly metabolized and excreted by the liver, kidneys, and lungs.^[303] Wang and co-workers designed spherical MSNs with a diameter of 61.4 nm and found drug accumulation in the liver and gallbladder at 0.5 and 1 h after intravenous injection respectively, and gradually disappeared after 24 h, suggesting that the metabolic pathway may be the hepatobiliary system.^[277] In addition, disk-shaped rHDL NPs with a diameter of 23.6 nm were excreted through the hepatobiliary and urinary systems of atherosclerotic mice.^[245] It is consistent with previous views that small-sized nanomaterials (below 10 nm) are mainly metabolized by the kidneys after glomerular filtration, large nanomaterials (above 50 nm) are mainly metabolized by the liver, and medium-sized nanomaterials (10–50 nm) often exhibit the joint metabolic pattern.

II. Biological evaluation: It is supposed to evaluate the effect of nanomaterials on body weight, behavior, and mental state as well as biological molecules such as DNA, RNA, and proteins. The biological evaluation of nanomaterials needs to comprehensively consider the different stages of cellular interactions and tissue transportation, and the content involved is relatively extensive.^[304] For the diagnosis and/or therapy of atherosclerosis, intravenous injection is the most commonly used method. Nanomaterials often directly interact with blood components therefore it is particularly crucial to analyze the types, morphology, proportion, and number of complete blood cells. In addition, Wang et al. designed a biomimetic red blood cell membrane-coated PLGA nanomaterial for a one-month treatment, and regularly monitored the body weight of ApoE^{-/-} mice during the treatment period. After the treatment, further evaluation of the function index of vital organs such as the heart, liver, spleen, lungs, and kidneys was performed to obtain a more comprehensive biological assessment. This study demonstrated the biosafety advantages of biomimetic nanomaterials as a next-generation drug delivery system for atherosclerotic management.^[127]

III. Immunological evaluation: Nanomaterials that enter the body may have close contact with the immune system and cause direct or indirect effects.^[305] Immunological evaluation of nanomaterials needs to be started from both in vitro and in vivo aspects. In vitro evaluation includes co-culturing the nanomaterials with immune cells to observe their morphology, proliferation, differentiation, and changes in cytokines. The in vivo evaluation mainly involves immune activation evaluation and immune toxicity evaluation. For example, Lameijer and co-workers selected RAW264.7 cells and

bone marrow-derived macrophages to assess the immunological safety of rHDL NPs. Nanomaterials were cocultured with these macrophages and tested immune cell function. The results indicated that these rHDL NPs did not affect the expression of chemokine ligand 2 in macrophages, nor did it affect the immune response of macrophages to lipopolysaccharide. Further, the expression of cytokine chemokines such as IL-6, chemokine ligand 2, and TNF- α were detected within the normal range after the rHDL NPs were injected into atherosclerotic mice, and no systemic inflammatory response and potential adverse immune effects were observed. These results demonstrated the great potential of rHDL NPs as a new-generation nanoplatform for the treatment of atherosclerosis.^[243]

- IV. Toxicology evaluation: The toxicology evaluation of nanomaterials needs to evaluate toxic effects on cells, various organs, and biological systems, which mainly embraces acute and chronic toxicity evaluation.^[306] Cell culture, biological slice technology, and blood biochemical detection methods can assist toxicological evaluation to ensure the safe application of nanomaterials. It has been demonstrated that several types of nanomaterials for atherosclerosis exhibited low toxicity both in vitro and in vivo. On the one hand, cell proliferation, and death assessment is the most common method in vitro, and in one report, a kind of manganese ferrite (MnFe₂O₄)-based nanomaterial at the concentration of 31.25 $\mu\text{g mL}^{-1}$ was safe for the growth of RAEC cells.^[98] Another metal element Zr-contained MOFs did not lead to cytotoxic death at the concentration of 32 $\mu\text{g mL}^{-1}$ after co-incubation with cells for 24 h.^[221] Comparatively, organic nanomaterials without metal elements demonstrated superior results. For instance, a rapamycin-loaded polymer exhibited a safe concentration of up to 300 $\mu\text{g mL}^{-1}$ at the cellular level.^[124] On the other hand, the in vivo toxicity assessments require the observation of blood samples and major organs (e.g., heart, liver, spleen, lungs, and kidneys). The above MnFe₂O₄, MOFs, and polymer all exhibited outstanding biosafety and the blood indices and tissue sections had no significant differences between the treatment and control group. In addition, another study on palladium-hydrogen nanopocket cubes also analyzed serum triglycerides and HDL in atherosclerotic mice with no significant abnormalities, suggesting that nanomaterials are suitable for biological application.^[251]

It is worth noting that there are remarkable individual differences between nanomaterials, and they need to be treated differently during biological safety evaluation. Although breakthroughs have been made in the application of nanomaterials, we should not be complacent and need to consider the challenges they face in terms of biosafety and biocompatibility.^[307]

8. Summary and Prospect

In this review, we elaborate on the pathological basis of atherosclerosis, the characteristics of nanomaterials, the applications of nanomedicine in atherosclerosis, and the assessment of biosafety, in order to provide useful references for further research in this field. The application of nanomedicine

in atherosclerosis involves many pathological processes, such as inflammatory burden, immune cell infiltration, lipid accumulation, endothelial injury, glycolysis, neovascularization, and thrombosis. The commonly used nanoplatforms include liposome, micelle, polymer, metallic oxide, AuNP, carbon-based nanomaterial, QD, membrane-coated biomimetic nanoparticle, living cell, cell-derived extracellular vesicles, etc. These nanomaterials passively target plaques through the EPR effect, or specifically target certain components within plaques through modified proteins, peptides, and other ligands. On the one hand, the use of nanomaterials has expanded the imaging range from basic anatomical imaging to molecular functional imaging, including MR, CT, FL, radioisotopes, PA, OCT, and multimodal imaging, enabling early detection of plaques, distinguishing the stable and vulnerable plaques, and providing more optimized diagnostic data for the clinic. On the other hand, the methods of atherosclerotic therapy can be roughly categorized into five types, including drug delivery, phototherapy, SDT, immunotherapy, and gas therapy. It has demonstrated the remarkable abilities of these nanomaterials to inhibit plaque formation. Furthermore, the biosafety evaluation including in vivo distribution and metabolism assessment, biological evaluation, immunological evaluation, and toxicology evaluation of various nanomedicine for biomedical applications were thoroughly discussed (Figure 11).

In the past decade, the scientific community has witnessed significant breakthroughs in the biomedical applications of nanomaterials. In the field of nanomedicine, cardiovascular diseases have become the second-largest application branch after cancer. The term “atherosclerosis” is also appearing more frequently in the field of nanomedicine. Even though the application of nanomedicine is still in the research stage, it has demonstrated fascinating prospects based on the improvement of diagnostic capabilities, therapeutic effects, and even theranostic assessment. However, in order to achieve clinical translation and long-run development, there is still an urgent need to consider and address several crucial challenges and issues:

- I. The unknown interaction between nanomaterials and biological systems is a major obstacle to the application of nanomaterials in biomedical fields. Especially for atherosclerosis, a chronic cardiovascular disease, lesions spread over various parts of the body including the heart, brain, kidneys, and limbs. Before targeting the atherosclerotic lesions, nanomaterials generally encounter many biological components in the body and manifest a wide distribution range whether injected intravenously or orally. Therefore, scientists ought to conduct more detailed biocompatibility and biosafety assessments, including risk-benefit assessments for blood circulation, distribution, uptake, toxicity, immune activation, biodegradation, metabolism, and elimination. It is a critical prerequisite for achieving further clinical translation.
- II. Material design for atherosclerosis is cumbersome. An increasing number of reports tend to prepare multifunctional nanomaterials involving various chemical components, which may inadvertently increase the complexity of the nanoparticles. In the field of atherosclerotic theranostic, the complex components also bring unprecedented challenges to the biocompatibility assessment. For example, researchers cannot accurately evaluate the biological effects of

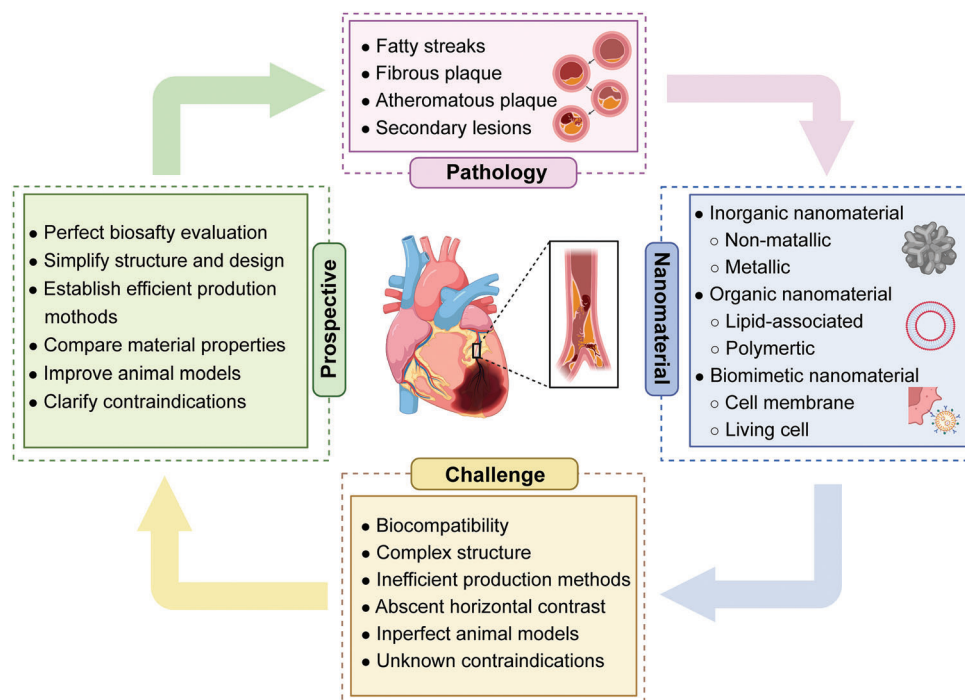


Figure 11. Schematic illustration of nanomedicine application (including pathological progress, the classification of nanomaterials, facing challenges and prospects) in atherosclerosis. Figure was created with BioRender.com.

each component under the premise of control variables, let alone speculate on the subtle results of interactions between various components. Thus, material design for atherosclerotic diagnosis and/or therapy should not be a combination and stacking of complex components but should fully explore the deeper and multifaceted effects of a certain material, subtract components from the material and make each component have a supportive and constructive relationship with each other.

- III. Nanomaterials need to be improved in production methods. Atherosclerosis is a highly prevalent chronic disease that requires long-term administration. However, most existing nanomaterials are prepared through manual synthesis in the laboratory and have low yields. These hand-prepared nanomaterials are often differences between batches including material size, yield, drug loading, and other parameters. Therefore, high-precision and large-scale commercial production methods need to be established to enhance the reproducibility of material parameters and performance, as well as meet clinical translation and application needs.
- IV. The nanomaterial system lacks horizontal comparison. The number of articles on treating atherosclerosis is increasing exponentially, and the nanomaterial system is diverse with most reports claiming significant efficacy. However, there has been no scientific and systematic evaluation of which nanomaterial has the optimal effect. According to existing reports, the pathological composition within atherosclerosis is uneven and unequal, which may be dominated by lipids, inflammatory cells, neovascularization, or matrix proteins. Therefore, the same nanomaterial may exhibit significantly different effects in different individuals. It is necessary to

compare the functions of nanomaterials based on the pathological types of atherosclerosis, which may be helpful for individualized diagnosis and treatment of patients.

- V. The animal models suitable for studying atherosclerosis need to be expanded. Most animal models used in atherosclerotic research related to nanomedicine are mice and rabbits. Although models used to simulate human atherosclerosis (such as ApoE^{-/-} mice, LDLr^{-/-} mice, balloon-injured rabbits) contribute to understanding the pathophysiology of atherosclerosis and validating the emerging therapies to some extent, their pathological condition differs from that of the human body. Moreover, large animals such as pigs and monkeys are costly. Therefore, establishing a mature atherosclerotic model that is similar to humans is an urgent problem that needs to be solved.
- VI. The contraindications of nanomedicine for the use of atherosclerosis are still unknown. Generally, patients with atherosclerosis are often accompanied by other complications including coronary heart disease, stroke, diabetes, obesity, liver and kidney dysfunction, etc. It is difficult to study the feasibility and/or contraindications of applying nanoparticles in complex disease populations. Therefore, it may be possible to identify contraindications of nanomedicine by constructing an animal model with multiple diseases.

These challenges exactly pose resistance to the development of nanomedicine to some degree. However, they also drive us to think further about the direction of our future efforts and guide us from multiple dimensions to promote the development and clinical translation of the next wave of nanomedicine in atherosclerosis theranostics. In addition to solving the above

obstacles, we must deepen our understanding of atherosclerosis to make great strides forward through more extensive research. In the future, as the key scientific issues and technical challenges related to nanomedicine are resolved, and the preparation methods and evaluation measures based on multidisciplinary fields are standardized, it is highly expected that the rapid development of nanomedicine can bring sustained innovation to the diagnosis and treatment of atherosclerosis, breaking further development constraints. It is believed that in the near future, we can definitely achieve significant progress and more exciting breakthroughs in the field of atherosclerosis and even the entire medical field through nanomedicine.

Acknowledgements

This work was supported by the National Key Research and Development Projects (Grants No. 2022YFC3602400), National Natural Science Foundation of China (Grants No. 82071931, 82130057, 82271997), National Science Foundation for Young Scientists of China (Grant No. 81903178, 82102085), Shanghai Science and Technology Program (Grant No. 21010500100, 22140901700, 22DZ2204700, 22142202200), Basic Research Program of Shanghai Municipal Government (Grant No. 21JC1406002), program from Science and Technology Commission of Shanghai Municipality (Grants No. 20Y11912400), the 2019 clinical research innovation, Shanghai Hospital Development Center (Grants No. SHDC12016233), Science and Technology Commission of Shanghai Municipality (Grants No. 124119a3201) and Innovative research team of high-level local universities in Shanghai.

Conflict of Interest

The authors declare no conflict of interest.

Keywords

atherosclerosis, biomaterials, diagnosis, nanomedicine, theranostic, therapy

Received: June 27, 2023
Revised: September 11, 2023
Published online: October 28, 2023

- [1] a) M. Zhou, H. Wang, X. Zeng, P. Yin, J. Zhu, W. Chen, X. Li, L. Wang, L. Wang, Y. Liu, J. Liu, M. Zhang, J. Qi, S. Yu, A. Afshin, E. Gakidou, S. Glenn, V. S. Krish, M. K. Miller-Petrie, W. C. Mountjoy-Venning, E. C. Mullany, S. B. Redford, H. Liu, M. Naghavi, S. I. Hay, L. Wang, C. J. L. Murray, X. Liang, *Lancet* **2019**, 394, 1145; b) P. Libby, *Nature* **2021**, 592, 524.
- [2] P. Libby, J. E. Buring, L. Badimon, G. K. Hansson, J. Deanfield, M. S. Bittencourt, L. Tokgözoğlu, E. F. Lewis, *Nat. Rev. Dis. Primers* **2019**, 5, 56.
- [3] a) M. R. Maurya, S. Gupta, J. Y.-S. Li, N. E. Ajami, Z. B. Chen, J. Y. J. Shyy, S. Chien, S. Subramaniam, *Proc. Natl. Acad. Sci. USA* **2021**, 118, e2023236118; b) Y. Pan, J. Jing, X. Cai, Z. Jin, S. Wang, Y. Wang, C. Zeng, X. Meng, J. Ji, L. Li, L. Lyu, Z. Zhang, L. Mei, H. Li, S. Li, T. Wei, Y. Wang, *JAMA Network Open* **2022**, 5, e2218307.
- [4] W. Herrington, B. Lacey, P. Sherliker, J. Armitage, S. Lewington, *Circ. Res.* **2016**, 118, 535.
- [5] a) N. S. Parikh, R. F. Gottesman, *J. Am. Coll. Cardiol.* **2021**, 77, 899; b) X. Zeng, S. Jiang, S. Ruan, L. Zhu, H. Lian, M. Liu, Z. Guo, J. Guo, C. Ye, Y. Cheng, J. Dong, *BMC Cancer* **2022**, 22, 534.
- [6] a) K. M. Sturgeon, L. Deng, S. M. Bluethmann, S. Zhou, D. M. Trifiletti, C. Jiang, S. P. Kelly, N. G. Zaorsky, *Eur. Heart J.* **2019**, 40, 3889; b) G. Riccardi, A. Giosuè, I. Calabrese, O. Vaccaro, *Cardiovasc. Res.* **2022**, 118, 1188; c) Y. Liu, X. Wang, Q. Zhang, G. Meng, L. Liu, H. Wu, Y. Gu, S. Zhang, Y. Wang, T. Zhang, M. J. Górski, S. Sun, X. Wang, M. Zhou, Q. Jia, K. Song, L. Tan, K. Niu, *Front. Nutr.* **2021**, 8, 723726.
- [7] N. V. Mushenkova, V. I. Summerhill, D. Zhang, E. B. Romanenko, A. V. Grechko, A. N. Orekhov, *Int. J. Mol. Sci.* **2020**, 21, 2992.
- [8] V. Aboyans, J.-B. Ricco, M.-L. E. L. Bartelink, M. Björck, M. Brodmann, T. Cohnert, J.-P. Collet, M. Czerny, M. De Carlo, S. Debusa, C. Espinola-Klein, T. Kahan, S. Kownator, L. Mazzolai, A. R. Naylor, M. Roffi, J. Rotherb, M. Sprynger, M. Tendera, G. Tepe, M. Venermo, C. Vlachopoulos, I. Desormais, *Rev. Esp. Cardiol.* **2018**, 71, 111.e1.
- [9] M. Lee, C.-Y. Cheng, Y.-L. Wu, J.-D. Lee, C.-Y. Hsu, B. Ovbiagele, *JAMA Neurol.* **2022**, 79, 349.
- [10] C. B. Newman, D. Preiss, J. A. Tobert, T. A. Jacobson, R. L. Page, L. B. Goldstein, C. Chin, L. R. Tannock, M. Miller, G. Raghuvier, P. B. Duell, E. A. Brinton, A. Pollak, L. T. Braun, F. K. Welty, *Arterioscler., Thromb., Vasc. Biol.* **2019**, 39, e38.
- [11] J. S. Lawton, J. E. Tamis-Holland, S. Bangalore, E. R. Bates, T. M. Beckie, J. M. Bischoff, J. A. Bittl, M. G. Cohen, J. M. DiMaio, C. W. Don, S. E. Fremes, M. F. Gaudino, Z. D. Goldberger, M. C. Grant, J. B. Jaswal, P. A. Kurlansky, R. Mehran, T. S. Metkus, L. C. Nnacheta, S. V. Rao, F. W. Sellke, G. Sharma, C. M. Yong, B. A. Zwischenberger, *Circulation* **2022**, 145, e4.
- [12] M. Venermo, M. Sprynger, I. Desormais, M. Björck, M. Brodmann, T. Cohnert, M. De Carlo, C. Espinola-Klein, S. Kownator, L. Mazzolai, R. Naylor, C. Vlachopoulos, J.-B. Ricco, V. Aboyans, *Eur. J. Vasc. Endovasc. Surg.* **2019**, 58, 641.
- [13] a) Y. Zhang, M. Li, X. Gao, Y. Chen, T. Liu, *J. Hematol. Oncol.* **2019**, 12, 137; b) J. Ouyang, A. Xie, J. Zhou, R. Liu, L. Wang, H. Liu, N. Kong, W. Tao, *Chem. Soc. Rev.* **2022**, 51, 4996; c) X. Huang, N. Kong, X. Zhang, Y. Cao, R. Langer, W. Tao, *Nat. Med.* **2022**, 28, 2273.
- [14] a) R. M. Williams, S. Chen, R. E. Langenbacher, T. V. Galassi, J. D. Harvey, P. V. Jena, J. Budhathoki-Uprety, M. Luo, D. A. Heller, *Nat. Chem. Biol.* **2021**, 17, 129; b) L. Salvioni, L. Morelli, E. Ochoa, M. Labra, L. Fiandra, L. Palugan, D. Prosperi, M. Colombo, *Adv. Colloid Interface Sci.* **2021**, 293, 102437; c) Q. Zhang, Y. Ying, J. Ping, *Adv. Sci.* **2022**, 9, e2103414.
- [15] a) S. N. Bhatia, X. Chen, M. A. Dobrovolskaia, T. Lammers, *Nat. Rev. Cancer* **2022**, 22, 550; b) W. Tao, N. Kong, X. Ji, Y. Zhang, A. Sharma, J. Ouyang, B. Qi, J. Wang, N. Xie, C. Kang, H. Zhang, O. C. Farokhzad, J. S. Kim, *Chem. Soc. Rev.* **2019**, 48, 2891.
- [16] Y. Liu, Y. Cheng, C. Zhao, H. Wang, Y. Zhao, *Adv. Sci.* **2022**, 9, e2104272.
- [17] L. Yang, Z. Zhou, J. Song, X. Chen, *Chem. Soc. Rev.* **2019**, 48, 5140.
- [18] D. Furtado, M. Björnmalm, S. Ayton, A. I. Bush, K. Kempe, F. Caruso, *Adv. Mater.* **2018**, 30, 1801362.
- [19] Y. Shi, R. van der Meel, X. Chen, T. Lammers, *Theranostics* **2020**, 10, 7921.
- [20] M. P. Vincent, J. O. Navidzadeh, S. Bobbala, E. A. Scott, *Cancer Cell* **2022**, 40, 255.
- [21] a) X. Liang, H. Li, X. Li, X. Tian, A. Zhang, Q. Luo, J. Duan, Y. Chen, L. Pang, C. Li, X.-J. Liang, Y. Zeng, J. Yang, *Acta Pharm. Sin. B* **2022**, 36, 841; b) F. M. E. Segers, A. V. Ruder, M. M. Westra, T. Lammers, S. M. Dadfar, K. Roemhild, T. S. Lam, M. E. Kooi, K. B. J. M. Cleutjens, F. K. Verheyen, G. W. H. Schurink, G. R. Haenen, T. J. C. van Berkel, I. Bot, B. Halvorsen, J. C. Sluimer, E. A. L. Biessen, *Cardiovasc. Res.* **2023**, 118, 3346; c) X. Zhang, F. Centurion, A. Misra, S. Patel, Z. Gu, *Adv. Drug Delivery Rev.* **2023**, 194, 114709.
- [22] a) T. H. Nøst, K. Alcalá, I. Urbarova, K. S. Byrne, F. Guida, T. M. Sandanger, M. Johansson, *Eur. J. Epidemiol.* **2021**, 36, 841; b) B. R. Sharma, T.-D. Kanneganti, *Nat. Immunol.* **2021**, 22, 550; c) S. Xu,

- D. Kamato, P. J. Little, S. Nakagawa, J. Pelisek, Z. G. Jin, *Pharmacol. Ther.* **2019**, 196, 15; d) M. Di, Y. Zhang, R. Zeng, X. Liu, W. Chen, M. Zhang, C. Zhang, M. Li, M. Zhang, *Int. J. Biol. Sci.* **2021**, 17, 4122.
- [23] a) J. He, W. Zhang, X. Zhou, F. Xu, J. Zou, Q. Zhang, Y. Zhao, H. He, H. Yang, J. Liu, *Bioact. Mater.* **2023**, 19, 115; b) W. Tong, Y. Zhang, H. Hui, X. Feng, B. Ning, T. Yu, W. Wang, Y. Shang, G. Zhang, S. Zhang, F. Tian, W. He, Y. Chen, J. Tian, *EBioMedicine* **2023**, 90, 104509.
- [24] a) M. Punjabi, L. Xu, A. Ochoa-Espinosa, A. Kosareva, T. Wolff, A. Murtaja, A. Broisat, N. Devoogdt, B. A. Kaufmann, *Arterioscler., Thromb. Vasc. Biol.* **2019**, 39, 2520; b) M. L. Senders, S. Hernot, G. Carlucci, J. C. van de Voort, F. Fay, C. Calcagno, J. Tang, A. Alaarg, Y. Zhao, S. Ishino, A. Palmisano, G. Boeykens, A. E. Meerwaldt, B. L. Sanchez-Gaytan, S. Baxter, L. Zendman, M. E. Lobatto, N. A. Karakatsanis, P. M. Robson, A. Broisat, G. Raes, J. S. Lewis, S. Tsimikas, T. Reiner, Z. A. Fayad, N. Devoogdt, W. J. M. Mulder, C. Pérez-Medina, *JACC: Cardiovasc. Imaging* **2019**, 12, 2015.
- [25] a) N. Distasio, F. Dierick, T. Ebrahimian, M. Tabrizian, S. Lehoux, *Acta Biomater.* **2022**, 143, 356; b) X. Fu, X. Yu, J. Jiang, J. Yang, L. Chen, Z. Yang, C. Yu, *Nat. Commun.* **2022**, 13, 6528; c) E.-B. Zhan, H.-W. Du, *Prev. Med.* **2023**, 172, 107524.
- [26] a) Y. Dai, X. Sha, X. Song, X. Zhang, M. Xing, S. Liu, K. Xu, J. Li, *Int. J. Nanomed.* **2022**, 17, 5413; b) W. Zhang, Z. Lv, Y. Zhang, S. C. B. Gopinath, Y. Yuan, D. Huang, L. Miao, *Oxid. Med. Cell. Longevity* **2022**, 2022, 6006601.
- [27] M. A. Gimbrone, *Ann. N. Y. Acad. Sci.* **1987**, 516, 5.
- [28] S. González-Ramos, M. Paz-García, C. Rius, A. Del Monte-Monge, C. Rodríguez, V. Fernández-García, V. Andrés, J. Martínez-González, M. A. Lasunción, P. Martín-Sanz, O. Soehnlein, L. Boscá, *FASEB J.* **2019**, 33, 3912.
- [29] M. A. Gimbrone, G. García-Cardena, *Circ. Res.* **2016**, 118, 620.
- [30] B. A. Ference, J. J. P. Kastelein, A. L. Catapano, *JAMA, J. Am. Med. Assoc.* **2020**, 324, 595.
- [31] I. Tabas, K. J. Williams, J. Borén, *Circulation* **2007**, 116, 1832.
- [32] B. A. Ference, H. N. Ginsberg, I. Graham, K. K. Ray, C. J. Packard, E. Bruckert, R. A. Hegele, R. M. Krauss, F. J. Raal, H. Schunkert, G. F. Watts, J. Borén, S. Fazio, J. D. Horton, L. Masana, S. J. Nicholls, B. G. Nordestgaard, B. van de Sluis, M.-R. Taskinen, L. Tokgözoğlu, U. Landmesser, U. Laufs, O. Wiklund, J. K. Stock, M. J. Chapman, A. L. Catapano, *Eur. Heart J.* **2017**, 38, 2459.
- [33] S. Gao, D. Zhao, M. Wang, F. Zhao, X. Han, Y. Qi, J. Liu, *Can. J. Cardiol.* **2017**, 33, 1624.
- [34] S. Yui, T. Sasaki, A. Miyazaki, S. Horiuchi, M. Yamazaki, *Arterioscler. Thromb.* **1993**, 13, 331.
- [35] K. Kugiyama, S. A. Kerns, J. D. Morrisett, R. Roberts, P. D. Henry, *Nature* **1990**, 344, 160.
- [36] a) Y. M. Park, *Exp. Mol. Med.* **2014**, 46, e99; b) M. Febbraio, D. P. Hajjar, R. L. Silverstein, *J. Clin. Invest.* **2001**, 108, 785.
- [37] A. Akhmedov, I. Rozenberg, F. Paneni, G. G. Camici, Y. Shi, C. Doerries, A. Sledzinska, P. Mocharla, A. Breitenstein, C. Lohmann, S. Stein, T. von Lukowicz, M. O. Kurrer, J. Borén, B. Becher, F. C. Tanner, U. Landmesser, C. M. Matter, T. F. Lüscher, *Eur. Heart J.* **2014**, 35, 2839.
- [38] a) M. S. Brown, J. L. Goldstein, *Nature* **1990**, 343, 508; b) K. Li, W. Yao, X. Zheng, K. Liao, *Cell Res.* **2009**, 19, 1006.
- [39] B. W. Parks, A. J. Lusis, *N. Engl. J. Med.* **2013**, 369, 2352.
- [40] C. S. Robbins, I. Hilgendorf, G. F. Weber, I. Theurl, Y. Iwamoto, J. L. Figueiredo, R. Gorbato, G. K. Sukhova, L. M. Gerhardt, D. Smyth, C. C. Zavitz, E. A. Shikatani, M. Parsons, N. van Rooijen, H. Y. Lin, M. Husain, P. Libby, M. Nahrendorf, R. Weissleder, F. K. Swirski, *Nat. Med.* **2013**, 19, 1166.
- [41] S. Frambach, R. de Haas, J. A. M. Smeitink, G. A. Rongen, F. G. M. Russel, T. J. J. Schirris, *Pharmacol. Rev.* **2020**, 72, 152.
- [42] I. F. Charo, M. B. Taubman, *Circ. Res.* **2004**, 95, 858.
- [43] a) Y. Kojima, I. L. Weissman, N. J. Leeper, *Circulation* **2017**, 135, 476; b) B. D. Gerlach, P. B. Ampomah, A. Yurdagul, C. Liu, M. C. Lauring, X. Wang, C. Kasikara, N. Kong, J. Shi, W. Tao, I. Tabas, *Cell Metab.* **2021**, 33, 2445.
- [44] A. Tajbakhsh, M. Rezaee, P. T. Kovanen, A. Sahebkar, *Pharmacol. Ther.* **2018**, 188, 12.
- [45] D. A. Chistiakov, A. V. Grechko, V. A. Myasoedova, A. A. Melnichenko, A. N. Orekhov, *J. Cell. Mol. Med.* **2018**, 22, 1366.
- [46] Y. Döring, M. Drechsler, S. Wantha, K. Kemmerich, D. Lievens, S. Vijayan, R. L. Gallo, C. Weber, O. Soehnlein, *Circ. Res.* **2012**, 110, 1052.
- [47] X. Zhou, A. Nicoletti, R. Elhage, G. K. Hansson, *Circulation* **2000**, 102, 2919.
- [48] J. Li, K. Ley, *Arterioscler., Thromb., Vasc. Biol.* **2015**, 35, 40.
- [49] M. A. Houtkamp, O. J. de Boer, C. M. van der Loos, A. C. van der Wal, A. E. Becker, *J. Pathol.* **2001**, 193, 263.
- [50] J. Wang, A. K. Uryga, J. Reinhold, N. Figg, L. Baker, A. Finigan, K. Gray, S. Kumar, M. Clarke, M. Bennett, *Circulation* **2015**, 132, 1909.
- [51] P. Lacolley, V. Regnault, A. Nicoletti, Z. Li, J. B. Michel, *Cardiovasc. Res.* **2012**, 95, 194.
- [52] J. J. Boyle, P. L. Weissberg, M. R. Bennett, *Arterioscler., Thromb., Vasc. Biol.* **2002**, 22, 1624.
- [53] M. C. H. Clarke, T. D. Littlewood, N. Figg, J. J. Maguire, A. P. Davenport, M. Goddard, M. R. Bennett, *Circ. Res.* **2008**, 102, 1529.
- [54] G. L. Basatemur, H. F. Jørgensen, M. C. H. Clarke, M. R. Bennett, Z. Mallat, *Nat. Rev. Cardiol.* **2019**, 16, 727.
- [55] a) H. Pan, C. Xue, B. J. Auerbach, J. Fan, A. C. Bashore, J. Cui, D. Y. Yang, S. B. Trignano, W. Liu, J. Shi, C. O. Ihuegbu, E. C. Bush, J. Worley, L. Vlahos, P. Laise, R. A. Solomon, E. S. Connolly, A. Califano, P. A. Sims, H. Zhang, M. Li, M. P. Reilly, *Circulation* **2020**, 142, 2060; b) G. F. Alencar, K. M. Owsiany, S. Karnewar, K. Sukhvasi, G. Mocci, A. T. Nguyen, C. M. Williams, S. Shamsuzzaman, M. Mokry, C. A. Henderson, R. Haskins, R. A. Baylis, A. V. Finn, C. A. McNamara, E. R. Zunder, V. Venkata, G. Pasterkamp, J. Björkegren, S. Bekiranov, G. K. Owens, *Circulation* **2020**, 142, 2045.
- [56] a) S. H. Zhang, R. L. Reddick, J. A. Piedrahita, N. Maeda, *Science* **1992**, 258, 468; b) S. Ishibashi, M. S. Brown, J. L. Goldstein, R. D. Gerard, R. E. Hammer, J. Herz, *J. Clin. Invest.* **1993**, 92, 883.
- [57] a) F. A. Shelburne, S. H. Quarfordt, *J. Biol. Chem.* **1974**, 249, 1428; b) M. Miyata, J. D. Smith, *Nat. Genet.* **1996**, 14, 55; c) M. Ishigami, D. K. Swertfeger, M. S. Hui, N. A. Granholm, D. Y. Hui, *Arterioscler., Thromb., Vasc. Biol.* **2000**, 20, 1020.
- [58] a) F. Kuipers, J. M. van Ree, M. H. Hofker, H. Wolters, G. In't Veld, R. Havinga, R. J. Vonk, H. M. Princen, L. M. Havekes, *Hepatology* **1996**, 24, 241; b) A. D. Marais, *Pathology* **2019**, 51, 165.
- [59] P. A. VanderLaan, C. A. Reardon, R. A. Thisted, G. S. Getz, *J. Lipid Res.* **2009**, 50, 376.
- [60] D. Teupser, A. D. Persky, J. L. Breslow, *Arterioscler., Thromb., Vasc. Biol.* **2003**, 23, 1907.
- [61] S. Bonthu, D. D. Heistad, D. A. Chappell, K. G. Lamping, F. M. Faraci, *Arterioscler., Thromb., Vasc. Biol.* **1997**, 17, 2333.
- [62] B. J. van Vlijmen, A. M. van den Maagdenberg, M. J. Gijbels, H. van der Boom, H. HogenEsch, R. R. Frants, M. H. Hofker, L. M. Havekes, *J. Clin. Invest.* **1994**, 93, 1403.
- [63] M. J. Gijbels, M. van der Cammen, L. J. van der Laan, J. J. Emeis, L. M. Havekes, M. H. Hofker, G. Kraal, *Atherosclerosis* **1999**, 143, 15.
- [64] a) T. Sasaki, M. Kuzuya, K. Nakamura, X. W. Cheng, T. Shibata, K. Sato, A. Iguchi, *Arterioscler., Thromb., Vasc. Biol.* **2006**, 26, 1304; b) S.-x. Jin, L.-h. Shen, P. Nie, W. Yuan, L.-h. Hu, D.-d. Li, X.-j. Chen, X.-k. Zhang, B. He, *Arterioscler., Thromb., Vasc. Biol.* **2012**, 32, 2372; c) T. Matoba, K. Sato, K. Egashira, *Curr. Opin. Lipidol.* **2013**, 24, 419.
- [65] J. L. Van Herck, G. R. Y. De Meyer, W. Martinet, C. E. Van Hove, K. Foubert, M. H. Theunis, S. Apers, H. Bult, C. J. Vrints, A. G. Herman, *Circulation* **2009**, 120, 2478.

- [66] W. A. Thomas, W. S. Hartroft, *Circulation* **1959**, 19, 65.
- [67] L. Yu, R. Gao, X. Song, X. Li, J. Zhu, *J. Oleo Sci.* **2021**, 70, 1447.
- [68] M. Gao, G. Xin, X. Qiu, Y. Wang, G. Liu, *J. Biomed. Res.* **2016**, 31, 47.
- [69] S. D. Sithu, M. V. Malovichko, K. A. Riggs, N. S. Wickramasinghe, M. G. Winner, A. Agarwal, R. E. Hamed-Berair, A. Kalani, D. W. Riggs, A. Bhatnagar, S. Srivastava, *JCI Insight* **2017**, 2, e86442.
- [70] Y. Zhao, Y. Yang, R. Xing, X. Cui, Y. Xiao, L. Xie, P. You, T. Wang, L. Zeng, W. Peng, D. Li, H. Chen, M. Liu, *Atherosclerosis* **2018**, 271, 26.
- [71] J. Liang, E. Liu, Y. Yu, S. Kitajima, T. Koike, Y. Jin, M. Morimoto, K. Hatakeyama, Y. Asada, T. Watanabe, Y. Sasaguri, S. Watanabe, J. Fan, *Circulation* **2006**, 113, 1993.
- [72] Y. Watanabe, *Atherosclerosis* **1980**, 36, 261.
- [73] J. Fan, S. Kitajima, T. Watanabe, J. Xu, J. Zhang, E. Liu, Y. E. Chen, *Pharmacol. Ther.* **2015**, 146, 104.
- [74] E. J. Keliher, Y.-X. Ye, G. R. Wojtkiewicz, A. D. Aguirre, B. Tricot, M. L. Senders, H. Groenen, F. Fay, C. Perez-Medina, C. Calcagno, G. Carlucci, T. Reiner, Y. Sun, G. Courties, Y. Iwamoto, H.-Y. Kim, C. Wang, J. W. Chen, F. K. Swirski, H.-Y. Wey, J. Hooker, Z. A. Fayad, W. J. M. Mulder, R. Weissleder, M. Nahrendorf, *Nat. Commun.* **2017**, 8, 14064.
- [75] A. L. Al-Mashhadi, C. B. Poulsen, K. von Wachenfeldt, A.-K. Robertson, J. F. Bentzon, L. B. Nielsen, J. Thygesen, L. P. Tolbod, J. R. Larsen, S. K. Moestrup, B. Frendéus, B. Mortensen, L. Drouet, R. H. Al-Mashhadi, E. Falk, *J. Diabetes Res.* **2018**, 2018, 6823193.
- [76] D. Hamamdžić, R. L. Wilensky, *J. Diabetes Res.* **2013**, 2013, 761415.
- [77] M. Kim, H. B. Kim, D. S. Park, K. H. Cho, D. Y. Hyun, H. J. Kee, Y. J. Hong, M. H. Jeong, *Sci. Rep.* **2021**, 11, 13695.
- [78] a) A. F. Hedayat, K. H. Park, T. G. Kwon, J. R. Woollard, K. Jiang, D. F. Carlson, A. Lerman, L. O. Lerman, *Transl. Res.* **2018**, 192, 30; b) M. Otake, H. Kawaguchi, S. Enya, A. Kangawa, T. Koga, K. Matsuo, S. Yamada, M. M. Rahman, N. Miura, M. Shibata, A. Tanimoto, *In Vivo* **2021**, 35, 2025.
- [79] J. R. Kaplan, S. B. Manuck, *Ann. N. Y. Acad. Sci.* **1999**, 896, 145.
- [80] Y. Niu, B. Shen, Y. Cui, Y. Chen, J. Wang, L. Wang, Y. Kang, X. Zhao, W. Si, W. Li, A. P. Xiang, J. Zhou, X. Guo, Y. Bi, C. Si, B. Hu, G. Dong, H. Wang, Z. Zhou, T. Li, T. Tan, X. Pu, F. Wang, S. Ji, Q. Zhou, X. Huang, W. Ji, J. Sha, *Cell* **2014**, 156, 836.
- [81] M. L. Senders, A. E. Meerwaldt, M. M. T. van Leent, B. L. Sanchez-Gaytan, J. C. van de Voort, Y. C. Toner, A. Maier, E. D. Klein, N. A. T. Sullivan, A. M. Sofias, H. Groenen, C. Faries, R. S. Oosterwijk, E. M. van Leeuwen, F. Fay, E. Chepurko, T. Reiner, R. Duivenvoorden, L. Zangi, R. M. Dijkhuizen, S. Hak, F. K. Swirski, M. Nahrendorf, C. Pérez-Medina, A. J. P. Teunissen, Z. A. Fayad, C. Calcagno, G. J. Strijkers, W. J. M. Mulder, *Nat. Nanotechnol.* **2020**, 15, 398.
- [82] J. Tang, S. Baxter, A. Menon, A. Alaarg, B. L. Sanchez-Gaytan, F. Fay, Y. Zhao, M. Ouimet, M. S. Braza, V. A. Longo, D. Abdel-Atti, R. Duivenvoorden, C. Calcagno, G. Storm, S. Tsimikas, K. J. Moore, F. K. Swirski, M. Nahrendorf, E. A. Fisher, C. Pérez-Medina, Z. A. Fayad, T. Reiner, W. J. M. Mulder, *Proc. Natl. Acad. Sci. USA* **2016**, 113, E6731.
- [83] a) H. S. Choi, W. Liu, P. Misra, E. Tanaka, J. P. Zimmer, B. Itty Ipe, M. G. Bawendi, J. V. Frangioni, *Nat. Biotechnol.* **2007**, 25, 1165; b) Y.-N. Zhang, W. Poon, A. J. Tavares, I. D. McGilvray, W. C. W. Chan, *J. Controlled Release* **2016**, 240, 332.
- [84] R. Taniguchi, Y. Miura, H. Koyama, T. Chida, Y. Anraku, A. Kishimura, K. Shigematsu, K. Kataoka, T. Watanabe, *Mol. Pharmaceutics* **2016**, 13, 2108.
- [85] M. Suhara, Y. Miura, H. Cabral, D. Akagi, Y. Anraku, A. Kishimura, M. Sano, T. Miyazaki, N. Nakamura, A. Nishiyama, K. Kataoka, H. Koyama, K. Hoshina, *J. Controlled Release* **2018**, 286, 394.
- [86] a) X. Hu, J. Hu, J. Tian, Z. Ge, G. Zhang, K. Luo, S. Liu, *J. Am. Chem. Soc.* **2013**, 135, 17617; b) H. Li, W. Zhang, W. Tong, C. Gao, *ACS Appl. Mater. Interfaces* **2016**, 8, 11210.
- [87] a) S.-Y. Lin, W.-H. Hsu, J.-M. Lo, H.-C. Tsai, G.-H. Hsiue, *J. Controlled Release* **2011**, 154, 84; b) G. Sharma, D. T. Valenta, Y. Altman, S. Harvey, H. Xie, S. Mitragotri, J. W. Smith, *J. Controlled Release* **2010**, 147, 408.
- [88] a) N. Doshi, B. Prabhakarparandian, A. Rea-Ramsey, K. Pant, S. Sundaram, S. Mitragotri, *J. Controlled Release* **2010**, 146, 196; b) M. Cooley, A. Sarode, M. Hoore, D. A. Fedosov, S. Mitragotri, A. Sen Gupta, *Nanoscale* **2018**, 10, 15350.
- [89] A. J. Thompson, E. M. Mastria, O. Eniola-Adefeso, *Biomaterials* **2013**, 34, 5863.
- [90] A. M. Wen, Y. Wang, K. Jiang, G. C. Hsu, H. Gao, K. L. Lee, A. C. Yang, X. Yu, D. I. Simon, N. F. Steinmetz, *J. Mater. Chem. B* **2015**, 3, 6037.
- [91] S. Yi, S. D. Allen, Y.-G. Liu, B. Z. Ouyang, X. Li, P. Augsornworawat, E. B. Thorp, E. A. Scott, *ACS Nano* **2016**, 10, 11290.
- [92] J. Tang, M. Rakshit, H. M. Chua, A. Darwitan, L. T. H. Nguyen, A. Muktabar, S. Venkatraman, K. W. Ng, *Nanotechnology* **2021**, 32, 505105.
- [93] A. A. D'Souza, R. Shegokar, *Expert Opin. Drug Delivery* **2016**, 13, 1257.
- [94] a) M. Sarparanta, L. M. Bimbo, J. Rytkönen, E. Mäkilä, T. J. Laaksonen, P. Laaksonen, M. Nyman, J. Salonen, M. B. Linder, J. Hirvonen, H. A. Santos, A. J. Airaksinen, *Mol. Pharmaceutics* **2012**, 9, 654; b) S. M. Pustulka, K. Ling, S. L. Pish, J. A. Champion, *ACS Appl. Mater. Interfaces* **2020**, 12, 48284.
- [95] a) C. Cao, L. Zhang, B. Kent, S. Wong, C. J. Garvey, M. H. Stenzel, *Angew. Chem., Int. Ed.* **2021**, 60, 10342; b) A. Nandakumar, W. Wei, G. Siddiqui, H. Tang, Y. Li, A. Kakin, X. Wan, K. Koppel, S. Lin, T. P. Davis, D. T. Leong, D. J. Creek, F. Ding, Y. Song, P. C. Ke, *ACS Appl. Mater. Interfaces* **2021**, 13, 58238; c) W. Xiao, Y. Wang, H. Zhang, Y. Liu, R. Xie, X. He, Y. Zhou, L. Liang, H. Gao, *Biomaterials* **2021**, 274, 120888.
- [96] a) X. Huang, C. Liu, N. Kong, Y. Xiao, A. Yurdagul, I. Tabas, W. Tao, *Nat. Protoc.* **2022**, 17, 748; b) W. Tao, A. Yurdagul, N. Kong, W. Li, X. Wang, A. C. Doran, C. Feng, J. Wang, M. A. Islam, O. C. Farokhzad, I. Tabas, J. Shi, *Sci. Transl. Med.* **2020**, 12, e1063.
- [97] S. Wang, Y. Wang, X. Lai, J. Sun, M. Hu, M. Chen, C. Li, F. Xu, C. Fan, X. Liu, Y. Song, G. Chen, Y. Deng, *ACS Nano* **2023**, 17, 2761.
- [98] J. Yao, Z. Yang, L. Huang, C. Yang, J. Wang, Y. Cao, L. Hao, L. Zhang, J. Zhang, P. Li, Z. Wang, Y. Sun, H. Ran, *Adv. Sci.* **2021**, 8, e2100850.
- [99] C. N. Morrell, D. N. Pariser, Z. T. Hilt, D. Vega Ocasio, *Annu. Rev. Immunol.* **2019**, 37, 125.
- [100] C. P. Manta, T. Leibing, M. Friedrich, H. Nolte, M. Adrian, K. Schledzewski, J. Krzietzko, C. Kirkamm, C. David Schmid, Y. Xi, A. Stojanovic, S. Tonack, C. de la Torre, S. Hammad, S. Offermanns, M. Krüger, A. Cerwenka, M. Platten, S. Goerd, C. Géraud, *Circulation* **2022**, 146, 1783.
- [101] a) W. Chen, M. Schilperoort, Y. Cao, J. Shi, I. Tabas, W. Tao, *Nat. Rev. Cardiol.* **2022**, 19, 228; b) R. Ji, X. Li, C. Zhou, Q. Tian, C. Li, S. Xia, R. Wang, Y. Feng, W. Zhan, *Nanoscale* **2018**, 10, 20246.
- [102] H. B. Sager, P. Dutta, J. E. Dahlman, M. Hulsman, G. Courties, Y. Sun, T. Heidt, C. Vinegoni, A. Borodovsky, K. Fitzgerald, G. R. Wojtkiewicz, Y. Iwamoto, B. Tricot, O. F. Khan, K. J. Kauffman, Y. Xing, T. E. Shaw, P. Libby, R. Langer, R. Weissleder, F. K. Swirski, D. G. Anderson, M. Nahrendorf, *Sci. Transl. Med.* **2016**, 8, 342ra80.
- [103] A. J. Beer, J. Pelisek, P. Heider, A. Saraste, C. Reeps, S. Metz, S. Seidl, H. Kessler, H. J. Wester, H. H. Eckstein, M. Schwaiger, *JACC: Cardiovasc. Imaging* **2014**, 7, 178.
- [104] R. Mohindra, D. K. Agrawal, F. G. Thankam, *J. Cardiovasc. Transl. Res.* **2021**, 14, 647.
- [105] T. Weiss-Sadan, Y. Ben-Nun, D. Maimoun, E. Merquioli, I. Abd-Elrahman, I. Gotsman, G. Blum, *Theranostics* **2019**, 9, 5731.
- [106] N. Cheraga, Z. Ye, M. J. Xu, L. Zou, N. C. Sun, Y. Hang, C. J. Shan, Z. Z. Yang, L. J. Chen, N. P. Huang, *Nanoscale* **2022**, 14, 8709.

- [107] H. Xu, P. Y. She, B. X. Ma, Z. Y. Zhao, G. C. Li, Y. B. Wang, *Biomaterials* **2022**, 288, 121734.
- [108] K. Song, Z. Tang, Z. Song, S. Meng, X. Yang, H. Guo, Y. Zhu, X. Wang, *Pharmaceutics* **2022**, 14, 1265.
- [109] Y. Huang, T. Li, W. Gao, Q. Wang, X. Li, C. Mao, M. Zhou, M. Wan, J. Shen, *J. Mater. Chem. B* **2020**, 8, 5765.
- [110] a) A. Dunphy, K. Patel, S. Belperain, A. Pennington, N. H. L. Chiu, Z. Y. Yin, X. W. Zhu, B. Priebe, S. M. Tian, J. J. Wei, X. W. Yi, Z. Q. Jia, *Nanomaterials* **2021**, 11, 1116; b) A. M. Flores, N. Hosseini-Nassab, K.-U. Jarr, J. Ye, X. Zhu, R. Wirka, A. L. Koh, P. Tsantilas, Y. Wang, V. Nanda, Y. Kojima, Y. Zeng, M. Lotfi, R. Sinclair, I. L. Weissman, E. Ingelsson, B. R. Smith, N. J. Leeper, *Nat. Nanotechnol.* **2020**, 15, 154; c) F. Liu, N. Ding, D. Huo, G. Yang, K. Wei, G. Guan, Y. Li, J. Yang, T. Wang, Y. Wang, J. Tan, W. Zeng, C. Zhu, *Adv. Healthcare Mater.* **2019**, 8, e1900386.
- [111] M. Gifani, D. J. Eddins, H. Kosuge, Y. Zhang, S. L. A. Paluri, T. Larson, N. Leeper, L. A. Herzenberg, S. S. Gambhir, M. V. McConnell, E. E. B. Ghosn, B. R. Smith, *Adv. Funct. Mater.* **2021**, 31, 2101005.
- [112] J. Liu, B. Zhou, Y. Guo, A. Zhang, K. Yang, Y. He, J. Wang, Y. Cheng, D. Cui, *ACS Appl. Mater. Interfaces* **2021**, 13, 29349.
- [113] B. Oh, C. H. Lee, *Mol. Pharmaceutics* **2015**, 12, 3226.
- [114] a) W. Tao, O. C. Farokhzad, *Chem. Rev.* **2022**, 122, 5405; b) M. Rezaee, B. Behnam, M. Banach, A. Sahebkar, *Biotechnol. Adv.* **2018**, 36, 2232.
- [115] J. Jia, G. Y. Liu, W. J. Xu, X. L. Tian, S. B. Li, F. Han, Y. H. Feng, X. C. Dong, H. Y. Chen, *Angew. Chem., Int. Ed.* **2020**, 59, 14443.
- [116] C. Wang, X.-G. Nie, Y. Shi, Y. Zhou, J.-J. Xu, X.-H. Xia, H.-Y. Chen, *ACS Nano* **2017**, 11, 5897.
- [117] a) S. Bhagat, N. V. Srikanth Vallabani, V. Shutthanandan, M. Bowden, A. S. Karakoti, S. Singh, *J. Colloid Interface Sci.* **2018**, 513, 831; b) W. Zou, Y. Tang, H. Zeng, C. Wang, Y. Wu, *J. Hazard. Mater.* **2021**, 417, 125994; c) N. Singh, M. A. Savanur, S. Srivastava, P. D'Silva, G. Magesh, *Angew. Chem., Int. Ed.* **2017**, 56, 14267.
- [118] B. B. Karakoçak, A. Laradji, T. Primeau, M. Y. Berezin, S. Li, N. Ravi, *ACS Appl. Mater. Interfaces* **2021**, 13, 277.
- [119] a) W. Feng, X. Han, H. Hu, M. Chang, L. Ding, H. Xiang, Y. Chen, Y. Li, *Nat. Commun.* **2021**, 12, 2203; b) G. Yuan, X. Xia, J. Zhang, J. Huang, F. Xie, X. Li, D. Chen, C. Peng, *Biosens. Bioelectron.* **2023**, 221, 114424.
- [120] X. Ge, H. Cui, J. Kong, S.-Y. Lu, R. Zhan, J. Gao, Y. Xu, S. Lin, K. Meng, L. Zu, S. Guo, L. Zheng, *Adv. Mater.* **2020**, 32, 2000037.
- [121] a) D. E. Large, R. G. Abdelmessih, E. A. Fink, D. T. Auguste, *Adv. Drug Delivery Rev.* **2021**, 176, 113851; b) N. Benne, J. van Duijn, F. Lozano Vigario, R. J. T. Lebox, P. van Veelen, J. Kuiper, W. Jiskoot, B. Slütter, *J. Controlled Release* **2018**, 291, 135.
- [122] S. Jebari-Benslaiman, K. B. Uribe, A. Benito-Vicente, U. Galicia-Garcia, A. Larrea-Sebal, I. Santin, I. Alloza, K. Vandenbroeck, H. Ostolaza, C. Martín, *Small* **2022**, 18, e2105915.
- [123] D. Gimes, T. Trimaille, *Adv. Colloid Interface Sci.* **2021**, 294, 102483.
- [124] F. Fang, Y. H. Ni, H. C. Yu, H. M. Yin, F. Yang, C. L. Li, D. L. Sun, T. Pei, J. Ma, L. Deng, H. Y. Zhang, G. X. Wang, S. Li, Y. Shen, X. H. Liu, *Theranostics* **2022**, 12, 4200.
- [125] M. Yousefi, A. Narmani, S. M. Jafari, *Adv. Colloid Interface Sci.* **2020**, 278, 102125.
- [126] S. Li, L. Wang, Y. Gu, L. Lin, M. Zhang, M. Jin, C. Mao, J. Zhou, W. Zhang, X. Huang, C. Corbo, W. Tao, E. Lu, J. Liu, *Matter* **2021**, 4, 3621.
- [127] Y. Wang, K. Zhang, X. Qin, T. Li, J. Qiu, T. Yin, J. Huang, S. McGinty, G. Pontrelli, J. Ren, Q. Wang, W. Wu, G. Wang, *Adv. Sci.* **2019**, 6, 1900172.
- [128] J. Shi, L. Kundrat, N. Pishesha, A. Bilate, C. Theile, T. Maruyama, S. K. Dougan, H. L. Ploegh, H. F. Lodish, *Proc. Natl. Acad. Sci. USA* **2014**, 111, 10131.
- [129] W. Gao, H. Yang, X. Liu, Z. Liu, L. Tong, Y. Sun, W. Cao, Y. Cao, B. Tang, *Chem. Commun.* **2019**, 55, 11535.
- [130] L. Chen, Z. Zhou, C. Hu, M. F. Maitz, L. Yang, R. Luo, Y. Wang, *Research* **2022**, 2022, 9845459.
- [131] Y. Wang, K. Zhang, T. H. Li, A. Maruf, X. Qin, L. Luo, Y. Zhong, J. H. Qiu, S. McGinty, G. Pontrelli, X. L. Liao, W. Wu, G. X. Wang, *Theranostics* **2021**, 11, 164.
- [132] Z. Zhang, J. Zhou, C. Liu, J. Zhang, Y. Shibata, N. Kong, C. Corbo, M. B. Harris, W. Tao, *Trends Chem.* **2022**, 4, 420.
- [133] C. Gao, Q. X. Huang, C. H. Liu, C. H. T. Kwong, L. D. Yue, J. B. Wan, S. M. Y. Lee, R. B. Wang, *Nat. Commun.* **2020**, 11, 2622.
- [134] J. M. Tarkin, M. R. Dweck, N. R. Evans, R. A. P. Takx, A. J. Brown, A. Tawakol, Z. A. Fayad, J. H. F. Rudd, *Circ. Res.* **2016**, 118, 750.
- [135] R. Di Corato, F. Gazeau, C. Le Visage, D. Fayol, P. Levitz, F. Lux, D. Letourneur, N. Luciani, O. Tillement, C. Wilhelm, *ACS Nano* **2013**, 7, 7500.
- [136] E. Gallo, C. Diaferia, E. D. Gregorio, G. Morelli, E. Gianolio, A. Accardo, *Pharmaceutics* **2020**, 13, 19.
- [137] R. Chen, D. Ling, L. Zhao, S. Wang, Y. Liu, R. Bai, S. Baik, Y. Zhao, C. Chen, T. Hyeon, *ACS Nano* **2015**, 9, 12425.
- [138] a) P. Caravan, J. J. Ellison, T. J. McMurphy, R. B. Lauffer, *Chem. Rev.* **1999**, 99, 2293; b) C. Wang, D. Cheng, N. Jalali Motlagh, E. G. Kuellenberg, G. R. Wojtkiewicz, S. P. Schmidt, R. Stocker, J. W. Chen, *J. Med. Chem.* **2021**, 64, 5874.
- [139] F. Capuana, A. Phinikaridou, R. Stefania, S. Padovan, B. Lavin, S. Lacerda, E. Almouazen, Y. Chevalier, L. Heinrich-Balard, R. M. Botnar, S. Aime, G. Digilio, *J. Med. Chem.* **2021**, 64, 15250.
- [140] T. M. Cheng, R. Li, Y. C. J. Kao, C. H. Hsu, H. L. Chu, K. Y. Lu, C. A. Changou, C. C. Chang, L. H. Chang, M. L. Tsai, F. L. Mi, *Mater. Sci. Eng.: C* **2020**, 114, 111064.
- [141] M. R. Makowski, G. Varma, A. J. Wiethoff, A. Smith, K. Mattock, C. H. P. Hansen, A. Warley, M. Taupitz, T. Schaeffter, R. M. Botnar, *Circ.: Cardiovasc. Imaging* **2011**, 4, 295.
- [142] H. Qiao, Y. Wang, R. Zhang, Q. Gao, X. Liang, L. Gao, Z. Jiang, R. Qiao, D. Han, Y. Zhang, Y. Qiu, J. Tian, M. Gao, F. Cao, *Biomaterials* **2017**, 112, 336.
- [143] X. Huang, C. Lin, C. Luo, Y. Guo, J. Li, Y. Wang, J. Xu, Y. Zhang, H. Wang, Z. Liu, B. Chen, *Nanomedicine* **2021**, 33, 102348.
- [144] S. Hossaini Nasr, A. Tonson, M. H. El-Dakdouki, D. C. Zhu, D. Agnew, R. Wiseman, C. Qian, X. Huang, *ACS Appl. Mater. Interfaces* **2018**, 10, 11495.
- [145] A. Yilmaz, M. A. Dengler, H. van der Kuip, H. Yildiz, S. Rösch, S. Klumpp, K. Klingel, R. Kandolf, X. Helluy, K.-H. Hiller, P. M. Jakob, U. Sechtem, *Eur. Heart J.* **2013**, 34, 462.
- [146] a) W. H. Kong, W. J. Lee, Z. Y. Cui, K. H. Bae, T. G. Park, J. H. Kim, K. Park, S. W. Seo, *Biomaterials* **2007**, 28, 5555; b) A. de Vries, E. Custers, J. Lub, S. van den Bosch, K. Nicolay, H. Grull, *Biomaterials* **2010**, 31, 6537.
- [147] D. B. Elrod, R. Partha, D. Danila, S. W. Casscells, J. L. Conyers, *Nanomedicine* **2009**, 5, 42.
- [148] S. You, H.-Y. Jung, C. Lee, Y. H. Choe, J. Y. Heo, G.-T. Gang, S.-K. Byun, W. K. Kim, C.-H. Lee, D.-E. Kim, Y. I. Kim, Y. Kim, *J. Controlled Release* **2016**, 226, 258.
- [149] Q. Yin, F. Y. Yap, L. Yin, L. Ma, Q. Zhou, L. W. Dobrucki, T. M. Fan, R. C. Gaba, J. Cheng, *J. Am. Chem. Soc.* **2013**, 135, 13620.
- [150] a) F. Hyafil, J.-C. Cornily, J. E. Feig, R. Gordon, E. Vucic, V. Amirbekian, E. A. Fisher, V. Fuster, L. J. Feldman, Z. A. Fayad, *Nat. Med.* **2007**, 13, 636; b) F. Hyafil, J.-C. Cornily, J. H. F. Rudd, J. Machac, L. J. Feldman, Z. A. Fayad, *J. Nucl. Med.* **2009**, 50, 959.
- [151] J. L. Van Herck, G. R. Y. De Meyer, W. Martinet, R. A. Salgado, B. Shivalkar, R. De Mondt, H. Van De Ven, A. Ludwig, P. Van Der Veken, L. Van Vaeck, H. Bult, A. G. Herman, C. J. Vrints, *Basic Res. Cardiol.* **2010**, 105, 51.

- [152] D. P. Cormode, E. Roessl, A. Thran, T. Skajaa, R. E. Gordon, J.-P. Schlomka, V. Fuster, E. A. Fisher, W. J. M. Mulder, R. Proksa, Z. A. Fayad, *Radiology* **2010**, 256, 774.
- [153] J.-Y. Kim, J. H. Ryu, D. Schellingerhout, I.-C. Sun, S.-K. Lee, S. Jeon, J. Kim, I. C. Kwon, M. Nahrendorf, C.-H. Ahn, K. Kim, D.-E. Kim, *Theranostics* **2015**, 5, 1098.
- [154] P. Chhour, P. C. Naha, S. M. O'Neill, H. I. Litt, M. P. Reilly, V. A. Ferrari, D. P. Cormode, *Biomaterials* **2016**, 87, 93.
- [155] O. Lee, S. Kappler, C. Polster, K. Taguchi, *IEEE Trans. Med. Imaging* **2017**, 36, 2389.
- [156] S. A. Si-Mohamed, M. Sigovan, J. C. Hsu, V. Tatard-Leitman, L. Chalabreysse, P. C. Naha, T. Garrivier, R. Dessouky, M. Carnaru, L. Bousset, D. P. Cormode, P. C. Douek, *Radiology* **2021**, 300, 98.
- [157] A. Irkle, A. T. Vesey, D. Y. Lewis, J. N. Skepper, J. L. E. Bird, M. R. Dweck, F. R. Joshi, F. A. Gallagher, E. A. Warburton, M. R. Bennett, K. M. Brindle, D. E. Newby, J. H. Rudd, A. P. Davenport, *Nat. Commun.* **2015**, 6, 7495.
- [158] P. Nogales, C. Velasco, A. Mota-Cobián, L. González-Cintado, R. A. Mota, S. España, J. Mateo, J. F. Bentzon, *Arterioscler., Thromb., Vasc. Biol.* **2021**, 41, e480.
- [159] a) Z. Varasteh, F. De Rose, S. Mohanta, Y. Li, X. Zhang, B. Miritsch, G. Scafetta, C. Yin, H. B. Sager, S. Glasl, D. Gorpas, A. J. R. Habenicht, V. Ntziachristos, W. A. Weber, A. Bartolazzi, M. Schwaiger, C. D'Alessandria, *Theranostics* **2021**, 11, 1864; b) M. Ahmed, T. Tegnebratt, T. A. Tran, L. Lu, P. Damberg, A. Gisterå, L. Tarnawski, D. Bone, U. Hedin, P. Eriksson, S. Holmin, B. Gustafsson, K. Caidahl, *Int. J. Nanomed.* **2020**, 15, 6137; c) F. Hyafil, J. Pelisek, I. Laitinen, M. Schottelius, M. Mohring, Y. Döring, E. P. C. van der Vorst, M. Kallmayer, K. Steiger, A. Poschenrieder, J. Notni, J. Fischer, C. Baumgartner, C. Rischpler, S. G. Nekolla, C. Weber, H.-H. Eckstein, H.-J. Wester, M. Schwaiger, *J. Nucl. Med.* **2017**, 58, 499; d) E. J. Kim, S. Kim, H. S. Seo, Y. J. Lee, J. S. Eo, J. M. Jeong, B. Lee, J. Y. Kim, Y. M. Park, M. Jeong, *J. Nucl. Med.* **2016**, 57, 1792.
- [160] J. Pellico, I. Fernández-Barahona, J. Ruiz-Cabello, L. Gutiérrez, M. Muñoz-Hernando, M. J. Sánchez-Guisado, I. Aiestaran-Zelaia, L. Martínez-Parra, I. Rodríguez, J. Bentzon, F. Herranz, *ACS Appl. Mater. Interfaces* **2021**, 13, 45279.
- [161] M. E. Lobatto, T. Binderup, P. M. Robson, L. F. P. Giesen, C. Calcagno, J. Witjes, F. Fay, S. Baxter, C. H. Wessel, M. Eldib, J. Bini, S. D. Carlin, E. S. G. Stroes, G. Storm, A. Kjaer, J. S. Lewis, T. Reiner, Z. A. Fayad, W. J. M. Mulder, C. Pérez-Medina, *Bioconjugate Chem.* **2020**, 31, 360.
- [162] L. Detering, A. Abdilla, H. P. Luehmann, J. W. Williams, L.-H. Huang, D. Sultan, A. Elvington, G. S. Heo, P. K. Woodard, R. J. Gropler, G. J. Randolph, C. J. Hawker, Y. Liu, *Mol. Pharmaceutics* **2021**, 18, 1386.
- [163] M. Liang, H. Tan, J. Zhou, T. Wang, D. Duan, K. Fan, J. He, D. Cheng, H. Shi, H. S. Choi, X. Yan, *ACS Nano* **2018**, 12, 9300.
- [164] W.-L. Wu, H.-L. Ma, L.-L. Xi, M.-F. Huang, K.-M. Wang, J.-Y. Miao, B.-X. Zhao, *Talanta* **2019**, 194, 308.
- [165] F. Maafi, B. Li, C. Gebhard, M. R. Brodeur, W. Nachar, L. Villeneuve, F. Lesage, D. Rhainds, E. Rhéaume, J.-C. Tardif, *Atherosclerosis* **2017**, 258, 8.
- [166] Q. Wang, R. Lou, Q. Yin, R. Yang, S. Li, J. Zhou, *Analyst* **2021**, 146, 4674.
- [167] J.-A. Chen, W. Guo, Z. Wang, N. Sun, H. Pan, J. Tan, Z. Ouyang, W. Fu, Y. Wang, W. Hu, X. Gu, *Anal. Chem.* **2020**, 92, 12613.
- [168] B. Wang, F. Zhang, S. Wang, R. Yang, C. Chen, W. Zhao, *Chem. Commun.* **2020**, 56, 2598.
- [169] H. Ikeda, A. Ishii, K. Sano, H. Chihara, D. Arai, Y. Abekura, H. Nishi, M. Ono, H. Saji, S. Miyamoto, *Atherosclerosis* **2018**, 275, 1.
- [170] a) M. S. Albaghdadi, R. Ikegami, M. B. Kassab, J. A. Gardecki, M. Kunio, M. M. Chowdhury, R. Khamis, P. Libby, G. J. Tearney, F. A. Jaffer, *Arterioscler., Thromb., Vasc. Biol.* **2021**, 41, e385; b) J. Bec, D. Vela, J. E. Phipps, M. Agung, J. Unger, K. B. Margulies, J. A. Southard, L. M. Buja, L. Marcu, *JACC: Cardiovasc. Imaging* **2021**, 14, 1832; c) N. M. Htun, Y. C. Chen, B. Lim, T. Schiller, G. J. Maghazal, A. L. Huang, K. D. Elgass, J. Rivera, H. G. Schneider, B. R. Wood, R. Stocker, K. Peter, *Nat. Commun.* **2017**, 8, 75.
- [171] a) S.-A. Manea, M.-L. Vlad, D. Rebleanu, A.-G. Lazar, I. M. Fenyo, M. Calin, M. Simionescu, A. Manea, *Oxid. Med. Cell. Longevity* **2021**, 2021, 6685612; b) R. Y. Khamis, K. J. Woollard, G. D. Hyde, J. J. Boyle, C. Bicknell, S.-H. Chang, T. H. Malik, T. Hara, A. Mauskopf, D. W. Granger, J. L. Johnson, V. Ntziachristos, P. M. Matthews, F. A. Jaffer, D. O. Haskard, *Sci. Rep.* **2016**, 6, 21785; c) H. Nie, J. Jing, Y. Tian, W. Yang, R. Zhang, X. Zhang, *ACS Appl. Mater. Interfaces* **2016**, 8, 8991.
- [172] Y. Narita, K. Shimizu, K. Ikemoto, R. Uchino, M. Kosugi, M. B. Maess, Y. Magata, N. Oku, M. Ogawa, *J. Controlled Release* **2019**, 302, 105.
- [173] K. Wang, H. Q. Gao, Y. W. Zhang, H. Y. Yan, J. H. Si, X. Y. Mi, S. A. Xia, X. Q. Feng, D. B. Liu, D. L. Kong, T. Wang, D. Ding, *Adv. Mater.* **2022**, 34, 2106994.
- [174] R. Qiao, H. Qiao, Y. Zhang, Y. Wang, C. Chi, J. Tian, L. Zhang, F. Cao, M. Gao, *ACS Nano* **2017**, 11, 1816.
- [175] X. Sun, W. Li, X. Zhang, M. Qi, Z. Zhang, X.-E. Zhang, Z. Cui, *Nano Lett.* **2016**, 16, 6164.
- [176] E. C. Ximendes, U. Rocha, B. del Rosal, A. Vaquero, F. Sanz-Rodríguez, L. Monge, F. Ren, F. Vetrone, D. Ma, J. García-Solé, C. Jacinto, D. Jaque, N. Fernández, *Adv. Healthcare Mater.* **2017**, 6, 1601195.
- [177] H. P. Deng, C. J. Konopka, S. Prabhu, S. Sarkar, N. G. Medina, M. Fayyaz, O. H. Arogundade, H. E. V. Gamage, S. H. Shahoei, D. Nall, Y. Youn, I. T. Dobrucka, C. O. Audu, A. Joshi, W. J. Melvin, K. A. Gallagher, P. R. Selvin, E. R. Nelson, L. W. Dobrucki, K. S. Swanson, A. M. Smith, *ACS Nano* **2022**, 16, 1999.
- [178] L. V. Wang, S. Hu, *Science* **2012**, 335, 1458.
- [179] B. Wang, J. L. Su, J. Amiran, S. H. Litovsky, R. Smalling, S. Emelianov, *Opt. Express* **2010**, 18, 4889.
- [180] Y. Cao, A. Kole, L. Lan, P. Wang, J. Hui, M. Sturek, J.-X. Cheng, *J. Photoacoust.* **2017**, 7, 12.
- [181] B. R. Smith, E. E. B. Ghosn, H. Rallapalli, J. A. Prescher, T. Larson, L. A. Herzenberg, S. S. Gambhir, *Nat. Nanotechnol.* **2014**, 9, 481.
- [182] Z. Xie, Y. Yang, Y. He, C. Shu, D. Chen, J. Zhang, J. Chen, C. Liu, Z. Sheng, H. Liu, J. Liu, X. Gong, L. Song, S. Dong, *Theranostics* **2020**, 10, 4694.
- [183] Y. Ma, L. Xu, B. Yin, J. Shang, F. Chen, J. Xu, Z.-L. Song, B. Nan, G. Song, X.-B. Zhang, *Nano Lett.* **2021**, 21, 4484.
- [184] M. Araki, S. J. Park, H. L. Dauerman, S. Uemura, J. S. Kim, C. Di Mario, T. W. Johnson, G. Guagliumi, A. Kastrati, M. Joner, N. R. Holm, F. Alfonso, W. Wijns, T. Adriaenssens, H. Nef, G. Rioufol, N. Amabile, G. Souteyrand, N. Meneveau, E. Gerbaud, M. P. Opolski, N. Gonzalo, G. J. Tearney, B. Bouma, A. D. Aguirre, G. S. Mintz, G. W. Stone, C. V. Bourantas, L. Räber, S. Gili, et al., *Nat. Rev. Cardiol.* **2022**, 19, 684.
- [185] J. Hu, F. Rivero, R. A. Torres, H. Loro Ramírez, E. M. Rodríguez, F. Alfonso, J. García Solé, D. Jaque, *J. Biophotonics* **2017**, 10, 674.
- [186] J. Hu, F. Sanz-Rodríguez, F. Rivero, E. M. Rodríguez, R. A. Torres, D. H. Ortgies, J. G. Solé, F. Alfonso, D. Jaque, *Nano Res.* **2018**, 11, 676.
- [187] J. Hu, D. H. Ortgies, R. Aguiar Torres, N. Fernández, L. Porto, E. Martín Rodríguez, J. García Solé, D. Jaque, F. Alfonso, F. Rivero, *Adv. Funct. Mater.* **2017**, 27, 1703276.
- [188] R. Chaudhary, K. Roy, R. K. Kanwar, K. Walder, J. R. Kanwar, *J. Nanobiotechnol.* **2016**, 14, 6.
- [189] M. Larivière, C. S. Lorenzato, L. Adumeau, S. Bonnet, A. Hémadou, M.-J. Jacobin-Valat, A. Noubhani, X. Santarelli, L. Minder, C. Di Primo, S. Sanchez, S. Mornet, J. Laroche-Traineau, G. Clofent-Sanchez, *Nanomed.: Nanotechnol. Biol. Med.* **2019**, 22, 102082.
- [190] M. Wu, X. Li, Q. Guo, J. Li, G. Xu, G. Li, J. Wang, X. Zhang, *Nanomed.: Nanotechnol. Biol. Med.* **2021**, 32, 102330.

- [191] W. Tong, H. Hui, W. Shang, Y. Zhang, F. Tian, Q. Ma, X. Yang, J. Tian, Y. Chen, *Theranostics* **2021**, 11, 506.
- [192] O. Will, S. Purkayastha, C. Chan, T. Athanasiou, A. W. Darzi, W. Gedroyc, P. P. Tekkis, *Lancet Oncol.* **2006**, 7, 52.
- [193] a) S. P. Howarth, T. Y. Tang, R. Trivedi, R. Weerakkody, J. M. U-King-Im, M. E. Gaunt, J. R. Boyle, Z. Y. Li, S. R. Miller, M. J. Graves, J. H. Gillard, *Eur. J. Radiol.* **2009**, 70, 555; b) T. Y. Tang, S. P. Howarth, S. R. Miller, M. J. Graves, U. K.-I. JM, Z. Y. Li, S. R. Walsh, P. D. Hayes, K. Varty, J. H. Gillard, *Eur. J. Vasc. Endovasc. Surg.* **2008**, 35, 392.
- [194] L. P. Smits, F. Tiessens, K. H. Zheng, E. S. Stroes, A. J. Nederveen, B. F. Coolen, *Atherosclerosis* **2017**, 263, 211.
- [195] K. H. Zheng, J. Schoormans, L. C. A. Stiekema, C. Calcagno, I. Cicha, C. Alexiou, G. J. Strijkers, A. J. Nederveen, E. S. G. Stroes, B. F. Coolen, *JACC: Cardiovasc. Imaging* **2019**, 12, 2081.
- [196] A. Usman, A. J. Patterson, J. Yuan, A. Cluroe, I. Patterson, M. J. Graves, J. H. Gillard, U. Sadat, *Sci. Rep.* **2020**, 10, 1808.
- [197] a) C. G. Stirrat, S. R. Alam, T. J. MacGillivray, C. D. Gray, R. Forsythe, M. R. Dweck, J. R. Payne, S. K. Prasad, M. C. Petrie, R. S. Gardner, S. Mirsadraee, P. A. Henriksen, D. E. Newby, S. I. Semple, *J. Cardiovasc. Magn. Reson.* **2016**, 18, 46; b) J. P. Walker, E. Nosova, M. Sigovan, J. Rapp, M. S. Grenon, C. D. Owens, W. J. Gasper, D. A. Saloner, *Ann. Vasc. Surg.* **2015**, 29, 63.
- [198] a) S. Y. Chong, X. Wang, L. van Bloois, C. Huang, N. S. Syeda, S. Zhang, H. J. Ting, V. Nair, Y. Lin, C. K. L. Lou, A. A. Benetti, X. Yu, N. J. Y. Lim, M. S. Tan, H. Y. Lim, S. Y. Lim, C. H. Thiam, W. D. Looi, O. Zharkova, N. W. S. Chew, C. H. Ng, G. K. Bonney, M. Muthiah, X. Chen, G. Pastorin, A. M. Richards, V. Angeli, G. Storm, J. W. Wang, *J. Controlled Release* **2023**, 360, 344; b) K. Chen, L. Y. Cheong, Y. Gao, Y. Zhang, T. Feng, Q. Wang, L. Jin, E. Honoré, K. S. L. Lam, W. Wang, X. Hui, A. Xu, *Nat. Commun.* **2022**, 13, 7838.
- [199] a) Y. Chen, D. Qin, J. Zou, X. Li, X. D. Guo, Y. Tang, C. Liu, W. Chen, N. Kong, C. Y. Zhang, W. Tao, *Adv. Mater.* **2023**, 35, 2207787; b) Z. Li, H. Zhu, H. Liu, D. Liu, J. Liu, J. Jiang, Y. Zhang, Z. Qin, Y. Xu, Y. Peng, B. Liu, Y. Long, *J. Nanobiotechnol.* **2023**, 21, 158.
- [200] a) D. D. Chin, N. Patel, W. Lee, S. Kanaya, J. Cook, E. J. Chung, *Bioact. Mater.* **2023**, 27, 327; b) Q. Wang, Y. Duan, H. Jing, Z. Wu, Y. Tian, K. Gong, Q. Guo, J. Zhang, Y. Sun, Z. Li, Y. Duan, *J. Controlled Release* **2023**, 354, 294.
- [201] B. Boersma, K. Möller, L. Wehl, V. Puddinu, A. Huard, S. Fauteux-Daniel, C. Bourquin, G. Palmer, T. Bein, *J. Controlled Release* **2022**, 351, 989.
- [202] Y. Liu, M. He, Y. Yuan, C. Nie, K. Wei, T. Zhang, T. Chen, X. Chu, *ACS Nano* **2023**, 17, 7721.
- [203] J. Wan, J. Yang, W. R. Lei, Z. Z. Xiao, P. Y. Zhou, S. Y. Zheng, P. Zhu, *Int. J. Nanomed.* **2023**, 18, 579.
- [204] M. Rakshit, A. Darwitan, A. Muktabar, P. Das, L. T. H. Nguyen, Y. Cao, C. Vizetto-Duarte, J. K. Tang, Y. S. Wong, S. Venkatraman, K. W. Ng, *Nanomed.: Nanotechnol. Biol. Med.* **2021**, 37, 102434.
- [205] N. Benne, R. M. Cardoso, A. L. Boyle, A. Kros, W. Jiskoot, J. Kuiper, J. Bouwstra, M. Van Eck, B. Slutter, *Adv. Healthcare Mater.* **2020**, 9, 2000043.
- [206] a) X. Jia, X. Bai, X. Yang, L. Wang, Y. Lu, L. Zhu, Y. Zhao, W. Cheng, M. Shu, Q. Mei, S. Jin, *Metabolism* **2022**, 135, 155274; b) D. A. Ho, T. O. Lynd, C. R. Jun, J. Shin, R. C. Millican, B. K. Estep, J. Chen, X. X. Zhang, B. C. Brott, D. W. Kim, J. A. Sherwood, P. T. J. Hwang, *Nanoscale* **2023**, 15, 3461.
- [207] Y. Wu, Y. Zhang, L. Dai, Q. Wang, L. Xue, Z. Su, C. Zhang, *J. Controlled Release* **2019**, 316, 236.
- [208] Y. Song, Z. Huang, X. Liu, Z. Pang, J. Chen, H. Yang, N. Zhang, Z. Cao, M. Liu, J. Cao, C. Li, X. Yang, H. Gong, J. Qian, J. Ge, *Nanomedicine* **2019**, 15, 13.
- [209] Y. N. Song, N. Zhang, Q. Y. Li, J. Chen, Q. Z. Wang, H. B. Yang, H. P. Tan, J. F. Gao, Z. H. Dong, Z. Q. Pang, Z. Y. Huang, J. Y. Qian, J. B. Ge, *Chem. Eng. J.* **2021**, 408, 127296.
- [210] J. X. Liu, Y. Y. Yang, X. Liu, A. S. Widjaya, B. H. Jiang, Y. Y. Jiang, *J. Controlled Release* **2021**, 337, 224.
- [211] X. Sha, Y. Dai, L. J. Chong, M. Wei, M. Y. Xing, C. Zhang, J. J. Li, *J. Nanobiotechnol.* **2022**, 20, 506.
- [212] Y. Li, J. Che, L. Chang, M. Guo, X. Bao, D. Mu, X. Sun, X. Zhang, W. Lu, J. Xie, *Adv. Healthcare Mater.* **2022**, 11, 2101788.
- [213] M. L. Shen, S. Y. Yao, S. J. Li, X. D. Wu, S. Liu, Q. B. Yang, J. S. Du, J. Y. Wang, X. Y. Zheng, Y. P. Li, *Nanoscale* **2021**, 13, 20013.
- [214] C. Gao, C. H. Liu, Q. Chen, Y. Wang, C. H. T. Kwong, Q. F. Wang, B. B. Xie, S. M. Y. Lee, R. B. Wang, *J. Controlled Release* **2022**, 349, 2.
- [215] Z. J. Li, Q. Wang, H. S. Jing, X. H. Luo, L. F. Du, Y. R. Duan, *ACS Appl. Nano Mater.* **2021**, 4, 11554.
- [216] a) R. Zhao, X. Ning, M. Wang, H. Wang, G. Xing, L. Wang, C. Lu, A. Yu, Y. Wang, *ACS Appl. Mater. Interfaces* **2022**, 14, 25080; b) X. Hou, H. Lin, X. Zhou, Z. Cheng, Y. Li, X. Liu, F. Zhao, Y. Zhu, P. Zhang, D. Chen, *Carbohydr. Polym.* **2020**, 232, 115787.
- [217] M. R. Guo, Z. S. He, Z. H. Jin, L. J. Huang, J. M. Yuan, S. G. Qin, X. C. Wang, L. L. Cao, X. R. Song, *Nano Res.* **2022**, 16, 925.
- [218] a) X. Y. Li, R. Wu, H. Chen, T. Li, H. M. Jiang, X. Q. Xu, X. T. Tang, M. Wan, C. Mao, D. Q. Shi, *ACS Appl. Mater. Interfaces* **2021**, 13, 30930; b) H. Yang, C. Liu, Y. J. Wu, M. Yuan, J. R. Huang, Y. H. Xia, Q. J. Ling, P. R. Hoffmann, Z. Huang, T. F. Chen, *Nano Today* **2022**, 48, 101736; c) Q. Q. Bai, Y. Xiao, H. L. Hong, X. Y. Cao, L. Zhang, R. F. Han, L. K. C. Lee, E. Y. Xue, X. Y. Tian, C. H. J. Choi, *Proc. Natl. Acad. Sci. USA* **2022**, 119, e2201443119.
- [219] H. J. Pu, M. H. Yao, Z. Y. Wu, Z. J. Xu, C. Y. Cui, R. H. Huang, M. Shafiq, W. M. Li, X. W. Lu, B. Li, *Nano Res.* **2022**, 15, 7342.
- [220] W. D. Sun, Y. Y. Xu, Y. Yao, J. Yue, Z. Wu, H. C. Li, G. H. Shen, Y. Liao, H. Y. Wang, W. H. Zhou, *J. Nanobiotechnol.* **2022**, 20, 88.
- [221] Z. J. Xu, Z. Y. Wu, S. Huang, K. C. Ye, Y. H. Jiang, J. Q. Liu, J. C. Liu, X. W. Lu, B. Li, *J. Controlled Release* **2023**, 354, 615.
- [222] X. Zhu, H. Wang, L. Zheng, Z. Zhong, X. Li, J. Zhao, J. Kou, Y. Jiang, X. Zheng, Z. Liu, H. Li, W. Cao, Y. Tian, Y. Wang, L. Yang, *Int. J. Nanomed.* **2015**, 10, 3719.
- [223] L. Zou, Y. Zhang, N. Cheraga, O. D. Abodunrin, K.-Y. Qu, L. Qiao, Y.-Q. Ma, L.-J. Chen, N.-P. Huang, *Talanta* **2023**, 265, 124772.
- [224] M. Xu, C. Mao, H. Chen, L. Liu, Y. Wang, A. Hussain, S. Li, X. Zhang, R. G. Tuguntaev, X.-J. Liang, W. Guo, F. Cao, *Acta Pharm. Sin. B* **2022**, 12, 2014.
- [225] G. Wang, Y. Zhu, K. Li, B. Liao, F. Wang, L. Shao, L. Huang, D. Bai, *J. Cardiovasc. Pharmacol.* **2021**, 79, 390.
- [226] Y. Ma, Y. Ma, M. Gao, Z. Han, W. Jiang, Y. Gu, Y. Liu, *Adv. Sci.* **2021**, 8, 2004128.
- [227] X. Zhang, J. Liu, X. Yang, G. He, B. Li, J. Qin, P. R. Shearing, D. J. L. Brett, J. Hu, X. Lu, *Nanoscale* **2019**, 11, 9733.
- [228] X. Wang, X. Wu, J. Qin, K. Ye, F. Lai, B. Li, G. He, X. Lu, D. J. L. Brett, I. P. Parkin, *ACS Appl. Mater. Interfaces* **2019**, 11, 41009.
- [229] X. Peng, J. Liu, C. Ming, B. Li, Z. Zhao, K. Ye, M. Zeng, R. Zou, X. Lu, J. Hu, *Nanoscale* **2020**, 12, 11288.
- [230] R. Lu, W. Wang, B. Dong, C. Xu, B. Li, Y. Sun, J. Liu, B. Hong, *Molecules* **2022**, 27, 8134.
- [231] a) J. Ouyang, X. Ji, X. Zhang, C. Feng, Z. Tang, N. Kong, A. Xie, J. Wang, X. Sui, L. Deng, Y. Liu, J. S. Kim, Y. Cao, W. Tao, *Proc. Natl. Acad. Sci. USA* **2020**, 117, 28667; b) X. Zhang, Q. Li, L. Li, J. Ouyang, T. Wang, J. Chen, X. Hu, Y. Ao, D. Qin, L. Zhang, J. Xue, J. Cheng, W. Tao, *ACS Nano* **2023**, 17, 6466; c) S. Tu, W. Ren, J. Han, H. Cui, T. Dai, H. Lu, Y. Xie, W. He, A. Wu, *Regener. Biomater.* **2023**, 10, rbad031.
- [232] T. Dai, W. He, S. Tu, J. Han, B. Yuan, C. Yao, W. Ren, A. Wu, *Bioact. Mater.* **2022**, 17, 18.
- [233] J. Ouyang, Z. Tang, N. Farokhzad, N. Kong, N. Y. Kim, C. Feng, S. Blake, Y. Xiao, C. Liu, T. Xie, W. Tao, *Nano Today* **2020**, 35, 100949.
- [234] Z. Li, X. Sun, S. Guo, L. Wang, T. Wang, C. Peng, W. Wang, Z. Tian, R. Zhao, W. Cao, Y. Tian, *Thromb. Haemostasis* **2015**, 114, 793.

- [235] a) H. Wang, Y. Yang, X. Sun, F. Tian, S. Guo, W. Wang, Z. Tian, H. Jin, Z. Zhang, Y. Tian, *Theranostics* **2018**, *8*, 4969; b) X. Sun, S. Guo, J. Yao, H. Wang, C. Peng, B. Li, Y. Wang, Y. Jiang, T. Wang, Y. Yang, J. Cheng, W. Wang, Z. Cao, X. Zhao, X. Li, J. Sun, J. Yang, F. Tian, X. Chen, Q. Li, W. Gao, J. Shen, Q. Zhou, P. Wang, Z. Li, Z. Tian, Z. Zhang, W. Cao, M. Li, Y. Tian, *Cardiovasc. Res.* **2019**, *115*, 190.
- [236] J. Yao, W. Gao, Y. Wang, L. Wang, K. Diabakte, J. Li, J. Yang, Y. Jiang, Y. Liu, S. Guo, X. Zhao, Z. Cao, X. Chen, Q. Li, H. Zhang, W. Wang, Z. Tian, B. Li, F. Tian, G. Wu, S. Pourteymour, X. Huang, F. Tan, X. Cao, Z. Yang, K. Li, Y. Zhang, Y. Li, Z. Zhang, H. Jin, et al., *JACC: Basic Transl. Sci.* **2020**, *5*, 53.
- [237] B. Li, J. Gong, S. Sheng, M. Lu, S. Guo, J. Yao, H. Zhang, X. Zhao, Z. Cao, X. Sun, H. Wang, Y. Cao, Y. Jiang, Z. Tian, B. Liu, H. Zhao, Z. Zhang, H. Jin, Y. Tian, *Bioeng. Transl. Med.* **2021**, *6*, e10193.
- [238] Y. Jiang, J. Kou, X. Han, X. Li, Z. Zhong, Z. Liu, Y. Zheng, Y. Tian, L. Yang, *Oxid. Med. Cell. Longevity* **2017**, *2017*, 8519169.
- [239] F. Wang, Q. Gao, S. Guo, J. Cheng, X. Sun, Q. Li, T. Wang, Z. Zhang, W. Cao, Y. Tian, *Biomed. Res. Int.* **2013**, *2013*, 737264.
- [240] L. Jiang, J. Wang, J. Jiang, C. Zhang, M. Zhao, Z. Chen, N. Wang, D. Hu, X. Liu, H. Peng, M. Lian, *Eur. J. Pharm. Biopharm.* **2020**, *146*, 101.
- [241] Z. Cao, G. Yuan, L. Zeng, L. Bai, X. Liu, M. Wu, R. Sun, Z. Chen, Y. Jiang, Q. Gao, Y. Chen, Y. Zhang, Y. Pan, J. Wang, *ACS Nano* **2022**, *16*, 10608.
- [242] a) O. Bornachea, A. Benitez-Amaro, A. Veá, L. Nasarre, D. de Gonzalo-Calvo, J. C. Escola-Gil, L. Cedó, A. Iborra, L. Martínez-Martínez, C. Juárez, J. A. Camara, C. Espinet, M. Borrell-Pages, L. Badimon, J. Castell, V. Llorente-Cortés, *Theranostics* **2020**, *10*, 3263; b) T. T. Wang, Y. Dong, L. Yao, F. Lu, C. X. Wen, Z. Wan, L. Fan, Z. L. Li, T. u, M. Y. Wei, X. K. Yang, Y. Zhang, *Bioact. Mater.* **2022**, *16*, 82.
- [243] M. Lameijer, T. Binderup, M. M. T. van Leent, M. L. Senders, F. Fay, J. Malkus, B. L. Sanchez-Gaytan, A. J. P. Teunissen, N. Karakatsanis, P. Robson, X. Zhou, Y. Ye, G. Wojtkiewicz, J. Tang, T. T. P. Seijkens, J. Kroon, E. S. G. Stroes, A. Kjaer, J. Ochando, T. Reiner, C. Pérez-Medina, C. Calcagno, E. A. Fisher, B. Zhang, R. E. Temel, F. K. Swirski, M. Nahrendorf, Z. A. Fayad, E. Lutgens, W. J. M. Mulder, et al., *Nat. Biomed. Eng.* **2018**, *2*, 279.
- [244] Y. Zhou, S. Y. Wang, X. Y. Liang, Z. Heger, M. Xu, Q. Lu, M. Yu, V. Adam, N. Li, *ACS Nano* **2022**, *16*, 10517.
- [245] T. Binderup, R. Duivenvoorden, F. Fay, M. M. T. van Leent, J. Malkus, S. Baxter, S. Ishino, Y. Zhao, B. Sanchez-Gaytan, A. J. P. Teunissen, Y. C. A. Frederico, J. Tang, G. Carlucci, S. Lyashchenko, C. Calcagno, N. Karakatsanis, G. Soultanidis, M. L. Senders, P. M. Robson, V. Mani, S. Ramachandran, M. E. Lobatto, B. A. Hutten, J. F. Granada, T. Reiner, F. K. Swirski, M. Nahrendorf, A. Kjaer, E. A. Fisher, Z. A. Fayad, et al., *Sci. Transl. Med.* **2019**, *11*, eaaw7736.
- [246] a) T. Y. Wang, X. Y. Zhu, F. G. Wu, *Bioact. Mater.* **2023**, *23*, 129; b) Z. Yang, H. Chen, *Nano Res.* **2023**, *16*, 3924.
- [247] J. S. Rink, W. Sun, S. Misener, J.-J. Wang, Z. J. Zhang, M. R. Kibbe, V. P. Dravid, S. Venkatraman, C. S. Thaxton, *ACS Appl. Mater. Interfaces* **2018**, *10*, 6904.
- [248] A. M. Garzón-Porras, D. L. Bertuzzi, K. Lucas, L. C. E. da Silva, M. G. de Oliveira, C. Ornelas, *ACS Appl. Polym. Mater.* **2020**, *2*, 2027.
- [249] a) A. Wijaya, Y. Wang, D. Tang, Y. Zhong, B. Y. Liu, M. Yan, Q. H. Jiu, W. Wu, G. X. Wang, *J. Mater. Chem. B* **2022**, *10*, 607; b) M. Li, J. Li, J. Chen, Y. Liu, X. Cheng, F. Yang, N. Gu, *ACS Nano* **2020**, *14*, 2024; c) X. Tang, L. Chen, Z. Wu, Y. Li, J. Zeng, W. Jiang, W. Lv, M. Wan, C. Mao, M. Zhou, *Small* **2022**, *19*, e2203238.
- [250] Z. Wu, M. Zhou, X. Tang, J. Zeng, Y. Li, Y. Sun, J. Huang, L. Chen, M. Wan, C. Mao, *ACS Nano* **2022**, *16*, 3808.
- [251] M. Xu, Y. Zhou, C. Ren, X. Liang, N. Li, *Adv. Funct. Mater.* **2021**, *31*, 2104892.
- [252] R. Hu, C. Dai, C. Dong, L. Ding, H. Huang, Y. Chen, B. Zhang, *ACS Nano* **2022**, *16*, 15959.
- [253] M. E. Lobatto, Z. A. Fayad, S. Silvera, E. Vucic, C. Calcagno, V. Mani, S. D. Dickson, K. Nicolay, M. Banciu, R. M. Schifferers, J. M. Metselaar, L. van Bloois, H.-S. Wu, J. T. Fallon, J. H. Rudd, V. Fuster, E. A. Fisher, G. Storm, W. J. M. Mulder, *Mol. Pharmaceutics* **2010**, *7*, 2020.
- [254] F. M. van der Valk, D. F. van Wijk, M. E. Lobatto, H. J. Verberne, G. Storm, M. C. Willems, D. A. Legemate, A. J. Nederveen, C. Calcagno, V. Mani, S. Ramachandran, M. P. Paridaans, M. J. Otten, G. M. Dallinga-Thie, Z. A. Fayad, M. Nieuwdorp, D. M. Schulte, J. M. Metselaar, W. J. Mulder, E. S. Stroes, *Nanomedicine* **2015**, *11*, 1039.
- [255] A. A. Shiozaki, T. Senra, A. T. Morikawa, D. F. Deus, A. T. Paladino-Filho, I. M. Pinto, R. C. Maranhão, *Clinics* **2016**, *71*, 435.
- [256] S. E. Nissen, T. Tsunoda, E. M. Tuzcu, P. Schoenhagen, C. J. Cooper, M. Yasin, G. M. Eaton, M. A. Lauer, W. S. Sheldon, C. L. Grines, S. Halpern, T. Crowe, J. C. Blankenship, R. Kerensky, *JAMA, J. Am. Med. Assoc.* **2003**, *290*, 2292.
- [257] D. G. Kallend, J. A. A. Reijers, S. E. Bellibas, A. Bobillier, H. Kempen, J. Burggraaf, M. Moerland, P. L. J. Wijngaard, *Eur. Heart J.: Cardiovasc. Pharmacother.* **2016**, *2*, 23.
- [258] S. J. Nicholls, R. Puri, C. M. Ballantyne, J. W. Jukema, J. J. P. Kastelein, W. Koenig, R. S. Wright, D. Kallend, P. Wijngaard, M. Borgman, K. Wolski, S. E. Nissen, *JAMA Cardiol.* **2018**, *3*, 806.
- [259] a) J.-C. Tardif, C. M. Ballantyne, P. Barter, J.-L. Dasseux, Z. A. Fayad, M.-C. Guertin, J. J. P. Kastelein, C. Keyserling, H. Klepp, W. Koenig, P. L. L'Allier, J. Lespérance, T. F. Lüscher, J. F. Paolini, A. Tawakol, D. D. Waters, M. Pfeffer, V. Brown, J. Rouleau, P. Watkins, L. J. Wei, G. Gosselin, C. Chayer, S. Lanthier, G. B. Pelletier, N. Racine, H. Agarwal, E. Brilakis, L. Cannon, D. Carrié, et al., *Eur. Heart J.* **2014**, *35*, 3277; b) S. J. Nicholls, J. Andrews, J. J. P. Kastelein, B. Merkely, S. E. Nissen, K. K. Ray, G. G. Schwartz, S. G. Worthley, C. Keyserling, J.-L. Dasseux, L. Griffith, S. W. Kim, A. Janssan, G. Di Giovanni, A. D. Pisanelli, D. J. Scherer, P. J. Psaltis, J. Butters, *JAMA Cardiol.* **2018**, *3*, 815.
- [260] J.-C. Tardif, J. Grégoire, P. L. L'Allier, R. Ibrahim, J. Lespérance, T. M. Heinonen, S. Kouz, C. Berry, R. Basser, M.-A. Lavoie, M.-C. Guertin, J. Rodés-Cabau, Effect of rHDL on Atherosclerosis-Safety and Efficacy (ERASE) Investigators, *JAMA, J. Am. Med. Assoc.* **2007**, *297*, 1675.
- [261] C. Michael Gibson, S. Korjian, P. Tricoci, Y. Daaboul, M. Yee, P. Jain, J. H. Alexander, P. G. Steg, A. M. Lincoff, J. J. Kastelein, R. Mehran, D. M. D'Andrea, L. I. Deckelbaum, B. Merkely, M. Zarebinski, T. O. Ophuis, R. A. Harrington, *Circulation* **2016**, *134*, 1918.
- [262] a) B. Zheng, D. Duffy, P. Tricoci, H. Kastrissios, M. Pfister, S. D. Wright, A. Gille, M. A. Tortorici, *Br. J. Clin. Pharmacol.* **2021**, *87*, 2558; b) R. Easton, A. Gille, D. D'Andrea, R. Davis, S. D. Wright, C. Shear, *J. Clin. Pharmacol.* **2014**, *54*, 301.
- [263] S. Korjian, S. H. A. Kazmi, G. Chi, A. Kalayci, J. J. Lee, U. Talib, S. D. Wright, D. Duffy, B. A. Kingwell, R. Mehran, P. M. Ridker, C. M. Gibson, *Eur. Heart J.: Cardiovasc. Pharmacother.* **2023**, *9*, 387.
- [264] P. Tricoci, D. M. D'Andrea, P. A. Gurbel, Z. Yao, M. Cuchel, B. Winston, R. Schott, R. Weiss, M. A. Blazing, L. Cannon, A. Bailey, D. J. Angiolillo, A. Gille, C. L. Shear, S. D. Wright, J. H. Alexander, *J. Am. Heart Assoc.* **2015**, *4*, e002171.
- [265] C. M. Gibson, M. Kerneis, M. K. Yee, Y. Daaboul, S. Korjian, A. P. Mehr, P. Tricoci, J. H. Alexander, J. J. P. Kastelein, R. Mehran, C. Bode, B. S. Lewis, R. Mehta, D. Duffy, J. Feaster, M. Halabi, D. J. Angiolillo, D. Dierschmied, T. O. Ophuis, B. Merkely, *Am. Heart J.* **2019**, *208*, 81.
- [266] C. M. Gibson, S. H. A. Kazmi, S. Korjian, G. Chi, A. T. Phillips, S. M. Montazerin, D. Duffy, B. Zheng, M. Heise, C. Liss, L. I. Deckelbaum, S. D. Wright, A. Gille, *J. Cardiovasc. Pharmacol. Ther.* **2022**, *27*, 10742484221121507.
- [267] M. Dastani, H. R. Rahimi, V. R. Askari, M. R. Jaafari, L. Jarahi, A. Yadollahi, V. B. Rahimi, *BioFactors* **2023**, *49*, 108.

- [268] A. N. Kharlamov, A. E. Tyurnina, V. S. Veselova, O. P. Kovtun, V. Y. Shur, J. L. Gabinsky, *Nanoscale* **2015**, 7, 8003.
- [269] A. N. Kharlamov, J. A. Feinstein, J. A. Cramer, J. A. Boothroyd, E. V. Shishkina, V. Shur, *Future Cardiol.* **2017**, 13, 345.
- [270] A. Kharlamov, *Atherosclerosis* **2019**, 287, E34.
- [271] L. Maillard, A. Tavildari, N. Barra, J. Billé, P. Joly, P. Peycher, M. Silvestri, F. Vochelet, *Arch. Cardiovasc. Dis.* **2017**, 110, 682.
- [272] L. Maillard, A. de Labriolle, C. Brasselet, B. Faurie, N. Durel, F. de Poli, S. Bosle, H. Madiot, J. Berland, L. Belle, *Catheter. Cardiovasc. Interventions* **2021**, 98, 45.
- [273] R. Collieran, M. Joner, D. Cutlip, P. Urban, M. Maeng, R. Jauhar, M. Barakat, J. M. Michel, R. Mehran, A. J. Kirtane, L. Maillard, A. Kastrati, R. A. Byrne, *Cardiovasc. Revasc. Med.* **2022**, 34, 17.
- [274] a) Q. Ma, S. J. Wu, L. Yang, Y. H. Wei, C. Y. He, W. S. Wang, Y. X. Zhao, Z. J. Wang, S. W. Yang, D. M. Shi, Y. Y. Liu, Z. M. Zhou, J. F. Sun, Y. J. Zhou, *Adv. Sci.* **2022**, 10, 5; b) A. Maisseyu, L. Di, A. Ravodina, A. Barajas-Espinosa, A. Sakamoto, A. Chaplin, J. X. Zhong, H. Y. Gao, M. Mignery, N. Narula, A. V. Finn, S. Rajagopalan, *Theranostics* **2022**, 12, 2741.
- [275] B. Banik, B. Surnar, B. W. Askins, M. Banerjee, S. Dhar, *ACS Appl. Mater. Interfaces* **2020**, 12, 6852.
- [276] a) Y. Yang, X. Fan, L. Li, Y. Yang, A. Nuernisha, D. Xue, C. He, J. Qian, Q. Hu, H. Chen, J. Liu, W. Huang, *ACS Nano* **2020**, 14, 2509; b) J. W. Song, H. S. Nam, J. W. Ahn, H.-S. Park, D. O. Kang, H. J. Kim, Y. H. Kim, J. Han, J. Y. Choi, S.-Y. Lee, S. Kim, W.-Y. Oh, H. Yoo, K. Park, J. W. Kim, *Theranostics* **2021**, 11, 8874; c) B. Ma, H. Xu, W. Zhuang, Y. Wang, G. Li, Y. Wang, *ACS Nano* **2020**, 14, 5862.
- [277] Q. Wang, Y. Wang, S. Liu, X. Sha, X. Song, Y. Dai, M. Zhao, L. Cai, K. Xu, J. Li, *J. Nanobiotechnol.* **2021**, 19, 222.
- [278] W.-L. Wan, B. Tian, Y.-J. Lin, C. Korupalli, M.-Y. Lu, Q. Cui, D. Wan, Y. Chang, H.-W. Sung, *Nat. Commun.* **2020**, 11, 534.
- [279] G. Wu, J. Zhang, Q. Zhao, W. Zhuang, J. Ding, C. Zhang, H. Gao, D.-W. Pang, K. Pu, H.-Y. Xie, *Angew. Chem., Int. Ed.* **2020**, 59, 4068.
- [280] J. Hou, J. Zhou, M. Chang, G. Bao, J. Xu, M. Ye, Y. Zhong, S. Liu, J. Wang, W. Zhang, H. Ran, Z. Wang, Y. Chen, D. Guo, *Bioact. Mater.* **2022**, 16, 120.
- [281] M. Ye, J. Zhou, Y. Zhong, J. Xu, J. Hou, X. Wang, Z. Wang, D. Guo, *ACS Appl. Mater. Interfaces* **2019**, 11, 9702.
- [282] H. Xu, P. She, Z. Zhao, B. Ma, G. Li, Y. Wang, *Adv. Mater.* **2023**, 35, 2300439.
- [283] R. J. Zotz, U. Dietz, S. Lindemann, S. Genth-Zotz, *Herz* **2019**, 44, 35.
- [284] N. S. Vos, N. D. Fagel, G. Amoroso, J. R. Herrman, M. S. Patterson, L. H. Piers, R. J. van der Schaaf, T. Slagboom, M. A. Vink, *JACC: Cardiovasc. Interventions* **2019**, 12, 1691.
- [285] K. Lee, S. G. Lee, I. Jang, S. H. Park, D. Yang, I. H. Seo, S. K. Bong, D. H. An, M. K. Lee, I. K. Jung, Y. H. Jang, J. S. Kim, W. Ryu, *Sci. Rep.* **2018**, 8, 3666.
- [286] a) W. C. Xu, X. Dong, J. L. Ding, J. C. Liu, J. J. Xu, Y. H. Tang, Y. P. Yi, C. Lu, W. Yang, J. S. Yang, Y. Gong, J. L. Zhou, *Int. J. Nanomed.* **2019**, 14, 441; b) L. Mao, L. Shen, J. Chen, Y. Wu, M. Kwak, Y. Lu, Q. Xue, J. Pei, L. Zhang, G. Yuan, R. Fan, J. Ge, W. Ding, *ACS Appl. Mater. Interfaces* **2015**, 7, 5320.
- [287] a) N. Bricout, F. Chai, J. Sobocinski, A. Hertault, W. Laure, A. Ung, P. Woisel, J. Lyskawa, N. Blanchemain, *Mater. Sci. Eng.: C* **2020**, 113, 110967; b) J.-a. Li, L. Chen, X.-q. Zhang, S.-k. Guan, *Mater. Sci. Eng.: C* **2020**, 109, 110607.
- [288] a) C. H. Lee, M. J. Hsieh, K. S. Liu, C. W. Cheng, S. H. Chang, S. J. Liu, C. J. Wang, M. Y. Hsu, K. C. Hung, Y. H. Yeh, W. J. Chen, I. C. Hsieh, J. H. Juang, M. S. Wen, *Int. J. Nanomed.* **2018**, 13, 6039; b) C. H. Lee, M. J. Hsieh, S. H. Chang, K. C. Hung, C. J. Wang, M. Y. Hsu, J. H. Juang, I. C. Hsieh, M. S. Wen, S. J. Liu, *Int. J. Nanomed.* **2019**, 14, 7503.
- [289] L. Huang, H. Fang, T. Zhang, B. Hu, S. Liu, F. Lv, Z. Zeng, H. Liu, W. Zhou, X. Wang, *Bioact. Mater.* **2023**, 23, 526.
- [290] M. R. Moradi, E. Salahinejad, E. Sharifi, L. Tayebi, *Carbohydr. Polym.* **2023**, 314, 120961.
- [291] D. Kersani, J. Mougin, M. Lopez, S. Degoutin, N. Tabary, F. Cazaux, L. Janus, M. Maton, F. Chai, J. Sobocinski, N. Blanchemain, B. Martel, *Eur. J. Pharm. Biopharm.* **2020**, 150, 156.
- [292] A. Gossart, D. Letourneur, A. Gand, V. Regnault, M. A. Ben Mlouka, P. Cosette, E. Pauthe, V. Ollivier, J. P. Santerre, *Biomaterials* **2019**, 217, 119306.
- [293] H. Mo, C. Fu, Z. Wu, P. Liu, Z. Wen, Q. Hong, Y. Cai, G. Li, *RSC Adv.* **2020**, 10, 15346.
- [294] a) X. Qi, C. Pan, L. Zhang, D. Yue, *ACS Appl. Mater. Interfaces* **2023**, 15, 3497; b) M. Janjic, F. Pappa, V. Karagkiozaki, C. Gitas, K. Ktenidis, S. Logothetidis, *Int. J. Nanomed.* **2017**, 12, 6343; c) A. M. ElSawy, N. F. Attia, H. I. Mohamed, M. Mohsen, M. H. Talaat, *Mater. Sci. Eng.: C* **2019**, 96, 708.
- [295] Y. Wang, H. Lan, T. Yin, X. Zhang, J. Huang, H. Fu, J. Huang, S. McGinty, H. Gao, G. Wang, Z. Wang, *Mater. Sci. Eng.: C* **2020**, 106, 110187.
- [296] a) B. Zhang, Y. Qin, Y. Wang, *Biomaterials* **2022**, 284, 121478; b) Q. Ma, X. Shi, X. Tan, R. Wang, K. Xiong, M. F. Maiz, Y. Cui, Z. Hu, Q. Tu, N. Huang, L. Shen, Z. Yang, *Bioact. Mater.* **2021**, 6, 4786.
- [297] a) T. J. Beldman, M. L. Senders, A. Alaarg, C. Pérez-Medina, J. Tang, Y. Zhao, F. Fay, J. Deichmüller, B. Born, E. Desclos, N. N. van der Wel, R. A. Hoebe, F. Kohen, E. Kartvelishvili, M. Neeman, T. Reiner, C. Calcagno, Z. A. Fayad, M. P. J. de Winther, E. Lutgens, W. J. M. Mulder, E. Kluza, *ACS Nano* **2017**, 11, 5785; b) E. Jung, J. Lee, L. Jeong, S. Park, M. Lee, C. Song, D. Lee, *Biomaterials* **2019**, 192, 282.
- [298] J. Qin, Z. Peng, B. Li, K. Ye, Y. Zhang, F. Yuan, X. Yang, L. Huang, J. Hu, X. Lu, *Nanoscale* **2015**, 7, 13991.
- [299] a) W. Najahi-Missaoui, R. D. Arnold, B. S. Cummings, *Int. J. Mol. Sci.* **2020**, 22, 385; b) W. N. Misaoui, R. D. Arnold, B. S. Cummings, *Chem.-Biol. Interact.* **2018**, 295, 1.
- [300] T. Skotland, T. G. Iversen, A. Llorente, K. Sandvig, *Adv. Drug Delivery Rev.* **2022**, 186, 114326.
- [301] a) K. S. Kim, K. Suzuki, H. Cho, Y. S. Youn, Y. H. Bae, *ACS Nano* **2018**, 12, 8893; b) R. Mohammadpour, M. Yazdimamaghani, D. L. Cheney, J. Jedrkiewicz, H. Ghandehari, *J. Controlled Release* **2019**, 304, 216; c) S. M. Kong, D. F. Costa, A. Jagielska, K. J. Van Vliet, P. T. Hammond, *Proc. Natl. Acad. Sci. USA* **2021**, 118, e2104826118.
- [302] Z. Zhang, J. Guan, Z. Jiang, Y. Yang, J. Liu, W. Hua, Y. Mao, C. Li, W. Lu, J. Qian, C. Zhan, *Nat. Commun.* **2019**, 10, 3561.
- [303] a) C. Ghimire, H. Wang, H. Li, M. Vieweger, C. Xu, P. Guo, *ACS Nano* **2020**, 14, 13180; b) E. M. Higbee-Dempsey, A. Amirshaghagh, M. J. Case, M. Bouché, J. Kim, D. P. Cormode, A. Tsourkas, *J. Am. Chem. Soc.* **2020**, 142, 7783; c) H. Kang, M. Han, J. Xue, Y. Baek, J. Chang, S. Hu, H. Nam, M. J. Jo, G. El Fakhri, M. P. Hutchens, H. S. Choi, J. Kim, *Nat. Commun.* **2019**, 10, 5134.
- [304] a) E. P. Stater, A. Y. Sonay, C. Hart, J. Grimm, *Nat. Nanotechnol.* **2021**, 16, 1180; b) S. P. Hadipour Moghaddam, R. Mohammadpour, H. Ghandehari, *J. Controlled Release* **2019**, 311, 1.
- [305] M. A. Dobrovolskaia, S. E. McNeil, *J. Controlled Release* **2013**, 172, 456.
- [306] R. Mohammadpour, M. A. Dobrovolskaia, D. L. Cheney, K. F. Greish, H. Ghandehari, *Adv. Drug Delivery Rev.* **2019**, 144, 112.
- [307] E. B. Ehlerding, P. Grodzinski, W. Cai, C. H. Liu, *ACS Nano* **2018**, 12, 2106.



Yu Chen received Ph.D. degree at the Shanghai Institute of Ceramics, Chinese Academy of Sciences (SICCAS). He is a full professor in Shanghai University. His research focuses on materdicine, nanomedicine, and nanobiotechnology, involving the design, fabrication and biomedical applications of mesoporous nanoparticles, 2D nanosheets and 3D-printing bioscaffolds. The focused biomedical applications include drug/gene delivery, molecular imaging, chemoreactive nanomedicine, energetic nanomedicine and the regenerative biomaterials. He has published more than 300 scientific papers in nanomedicine field with a total citation of more than 37000 times (h-index: 106). He is 2018–2022 Highly Cited Researcher by Clarivate Analytics, Web of Science.



Rong Wu received her Ph.D. degree at Shanghai Jiao Tong University School of Medicine. She currently works as the director of the Department of Ultrasound, Shanghai General Hospital, Shanghai Jiao Tong University School of Medicine. She specializes in cardiovascular diseases ultrasound diagnosis, artery photoacoustic molecular imaging, and the non-invasive intelligent precision theranostic systems for vulnerable plaque based on multiparameter ultrasound and artificial intelligence. She has presided several national, provincial, and ministerial projects, including one Key Program and three General Programs of the National Natural Science Foundation of China. She has published more than 70 scientific papers as the first or corresponding author.